ProQuest LLC.
789 East Eisenhower Parkway
P.O. Box 1346
Ann Arbor, MI 48106 – 1346

SOLID INTERCALATION TO PRODUCE POLYMER/CLAY NANOCOMPOSITES

Shuaijin Chen Carreyette

A thesis submitted in partial fulfilment of the
requirements of The Nottingham Trent University
for the degree of

Doctor of Philosophy

This research project was carried out in the
Polymer Engineering Centre
School of Engineering
Faculty of Construction, Computing and Technology
The Nottingham Trent University
Burton Street, Nottingham NG1 4BU, UK

October 2003

ABSTRACT

A review of recent literature and current knowledge relating to the development in polymer/clay nanocomposites has been presented.

A novel method, solid intercalation, to produce polymer/clay nanocomposites is described based on two polymers, polyethylene oxide and polystyrene with two clays, hydrophilic clay G105 and organoclay I.28. The clays used in the solid intercalation are selected based on the nanostructure, microstructure and thermal stability results. The polymers are selected based on their potential applications. The structures of the resultant materials are analysed and the possible mechanisms of the solid intercalation in different polymer/clay systems are presented.

The experiment results show that the organoclay is more promising in obtaining a good dispersion and expansion of the clay layers in polymer matrices, especially at high clay loading. Hydrophilic clay can be well dispersed and expanded in the polyethylene oxide/clay system for clay contents below 10 wt%.

A comparison between solid intercalation and solution synthesis is made for the polyethylene oxide/clay system. The structure diagrams for the corresponding method are illustrated. The nanocomposites produced by solid intercalation are composed of isolated polymer and intercalated/exfoliated polymer/clay structures, while those produced by solution synthesis are mainly composed of intercalated structures.

Studies of the processing conditions of solid intercalation of the PEO/G105 clay system were carried out. The results show that the moisture level is critical in producing the composites by solid intercalation. There are two possible mechanisms for producing the composites – the melt and flow of the polymer into the clay galleries or the formation of the polymer solution and flow into the clay galleries. The results also show that high pressure and temperature improve the melt and flow of the polymer in solid intercalation which encourages more intercalation to take place.

The mechanical properties and thermal stability of the composites were investigated using nanoindentation test and thermo-gravimetric analysis to explore the potential

of solid intercalation in commercial applications. Comparing the nanoindentation results of the polymer/clay nanocomposites produced by solid intercalation with those produced by solution synthesis, the composites produced by solid intercalation have higher hardness and reduced modulus which offer the potential for the direct application of solid intercalated products. The results from TGA show the thermal properties of the polymer/clay nanocomposite produced by solid intercalation are significantly improved which offers the opportunity to use the existing available organoclays to produce high quality nanocomposites by using a combined approach involving both solid intercalation and melt processing.

ACKNOWLEDGEMENTS

I would initially like to acknowledge the financial assistance of Nottingham Trent University and my family for supporting my studies over these years.

I would like to give my warmest thanks to my supervisor, Dr. F. Gao for his guidance and encouragement during both the research and writing process of this thesis. This work would not have been possible without the mentoring he provided to me during my time at Nottingham Trent University.

I am very grateful to Professor J. L. Henshall for his help during the writing up period of this thesis.

I would like to thank all the technical staff who have contributed to the experiments carried out in the Polymer Engineering Centre and my friends in the Faculty Research Institute who made my life in University enjoyable and rich in experience. My special thanks go to Judith Kipling for her personal help and support in both research and improving my English language.

I am forever indebted to my parents, whose unwavering support and encouragement give me an opportunity to pursue my dream.

Last, but by no means least, I am greatly indebted to David, my husband, for his love, patience and encouragement.

CONTENTS

LIST OF FIGURES

LIST OF TABLES

LIST OF SYMBOLS AND ABBREVIATIONS

PEO	Poly(ethylene oxide)
PS	Polystyrene
PA	Polyamide
PP	Polypropylene
PMMA	Poly(methyl methacrylate)
SIS	Styrene-isoprene-styrene
SBS	Styrene-butadiene-styrene
PE	Polyethylene
EVA	Ethylene vinyl acetate copolymer
PCL	Poly(ε-caprolactone)
PET	Poly(ethylene terephthalate)
PDMS	Polydimethyl-siloxane
PU	Polyurethane
SAN	Styrene-acylonitrile
PI	Poly(imide)
$\overline{M}_n$	Average numerical molecular weight
XRD	X-ray diffractometry
SEM	Scanning electron microscopy
NMR	Nuclear magnetic resonance
DSC	Differential scanning calorimetry
TGA	Thermogravimetric or thermogravimetrical analysis
D	Diffusion coefficient
S	Solubility coefficient
W	Water permeability
P	Vapour or gas permeability
HDT	Heat distortion temperature
HRR	Heat release rate
SEA	Specific extinction area
CEC	Cation exchange capacity

meq/g	Milliequivalents per gram
Tg	Glass transition temperature
d	Interlayer spacing
λ	Wavelength of X-ray
θ	The Bragg angle
K	Scherrer parameter
β	Half peak height
L	The average dimension along a line normal to the reflecting plane
(Lc/La)e	Apparent aspect ratio
H	Hardness
Er	Reduced modulus
P_{max}	The maximum load
A	The projected contact area of the indentor during maximum loading
E	Young's modulus
ν	Poisson's ratio

GLOSSARY

CEC: cation exchange capacity, the maximum amount of exchangeable cations, the quantity of positively charged ions (cations) that a clay mineral or similar material can accommodate on its negatively charged surface, commonly expressed as milliequivalent (meq) per gram or per 100 gram.

Clay: aluminosilicates in which some of the aluminum and silicon ions have been replaced by elements with different valence, or charge. Also know as **layered silicate** due to its layered structure.

Clay modification: the process of an organoclay using a clay modifier which normally containing an ammonium or phosphonium functional group. The groups modify a hydrophilic clay surface by ionically bonding to it, converting the surface from a hydrophilic to an organophilic species.

Exfoliated structure: refers to the composite structure in which the individual clay layers are completely dispersed in a continuous polymer matrix.

Exfoliation: a process wherein the clay layers separate from one another in a polymer matrix.

Hydrophilic: a chemical environment favouring the attraction of water or materials which are miscible in water. Hydrophilic materials are characterized by strong dipole moments.

Master batch: A convenient way for handling small amounts of critical ingredients in higher concentrations than those occurring in a normal mixture for subsequent dilution with the remainder of the ingredients. In the case of polymer/clay nanocomposite, the polymer pellets which contain high concentrations (> 40-50%) of nanoclay in partially dispersed form. Master batch can be diluted with additional polymer to form nanocomposites with nanoclay loadings of 4-6%.

Montmorillonite: the most common member of the smectite clay family. Montmorillonite is generally referred to as "nanoclay". It is also the most common material used in polymer/clay nanocomposites.

In-situ polymerisation: the first method used to synthesise polymer/clay nanocomposites. The process comprises the intercalation of monomers or oligomers into clay galleries and the polymerisation of the intercalated monomers or oligomers. The reactions cause the clay layers to expand, forming polymer/clay nanocomposite.

Intercalated structure: refers to the composite structure containing the expanded clay layers which are inserted with polymers

Intercalation: a process wherein the clay layers are expanded in a polymer matrix.

Interlayer space: the gap between two adjacent clay layers. Also known as 'd-spacing', 'basal spacing' or 'clay gallery'.

Melt synthesis: in which mainly organoclays are mixed with a polymer matrix in the melt phase. Where the surfaces of clay layers are compatible with the chosen

polymer, the polymer can flow into the interlayer space and form either intercalated or exfoliated nanocomposites.

Nanoclay: a clay from the smectite family. Smectites have a unique morphology, featuring one dimension in the nanometer range.

Nanocomposite technology: the materials and processes required to disperse nanoscale particles in plastics, metals, or ceramics.

Nanoindentation: Nanoindentation is similar to conventional hardness testing performed on a much smaller scale. The force required to press a sharp diamond indenter into a material is measured as a function of indentation depth. As depth resolution is on the scale of nanometers (hence the name of the instrument), it is possible to conduct indentation experiments even on thin films. Two quantities which can be readily extracted from nanoindentation experiments are the material's modulus, or stiffness, and its hardness, which can be correlated to yield strength. Investegators have also used nanoindentation to study creep, plastic flow, and fracture of materials.

Nanomaterials: can be subdivided into nanoparticles, nanofilms and nanocomposites. The focus of nanomaterials is a bottom up approach to structures and functional effects whereby the building blocks of materials are designed and assembled in controlled ways.

Nanostructure: structure at the nanometer scale.

Nanotechnology: The creation and use of objects at the nanoscale, up to 100 nanometers in size; a manufacturing technology able to inexpensively fabricate most structures consistent with natural law, and to do so with molecular precision.

Organoclay: clay whose surface has been modified by organic salt. This type of clay is normally compatible with organic polymers.

Phyllosilicate: mineral with crystal structure containing silicon-oxygen tetrahedra arranged as sheets.

Polymer/clay nanocomposite: comprises organic polymers and inorganic clays that have at least one dimension in the nanometer size range.

Solution synthesis: in which unmodified or modified clays are dispersed in a solvent in which the polymer is soluble. The polymer is then dissolved in a solvent and added to the clay suspension where it will intercalate between the clay layers. When the solvent is evaporated (or the mixture precipitated), the clay layers sandwiches the polymer to form polymer/clay nanocomposite.

Solid intercalation: in which polymers and clays are blended in solid phase, followed by compressing the mixture under high pressure to form polymer/clay nanocomposites.

Zwitter ion: the dipolar form of an amino acid which occurs when H^+ ion is transferred from an acid group to an amine group, i.e., ion contains both positive and negative charges.

Chapter 1 INTRODUCTION

Polymer/clay nanocomposites comprise organic polymers and inorganic layered silicates (or clays) that have at least one dimension in the nanometer size range. They are a new class of materials offering great opportunities in a broad range of markets through extraordinary enhancement of major engineering properties, pushing the performance envelope well beyond the domain of known polymer technologies.

The excellent mechanical properties of polymer/clay nanocomposites are achieved by the reinforcement of individual silicate layers, which behave in a similar way to chopped fibres in conventional fibre reinforced composites. This improves not only the mechanical properties of the nanocomposites but also their barrier resistance, fire retardancy and chemical resistance [1-4]. In addition, polymer/clay nanocomposites have become an environmental-friendly approach to achieve fire retardancy because clays do not produce toxic species during burning. The emerging nanocomposite technologies have been regarded as the "superstars" of the plastics industry and this will continue through the next few decades [5].

The history of polymer/clay nanocomposites can be traced back to the 1950's when Carter et al. found that onium based organoclays could be used to reinforce natural and synthetic elastomers [6-7]. In the subsequent two decades, several researchers have reported the intercalation between different clays and polymers [8-13]. However these activities did not receive much attention until the early 1990's, when the Toyota group demonstrated that exfoliation of a clay in polyamide 6, using an in-situ polymerisation method, can improve a wide range of physical and engineering properties of polymers [1-2]. Since then, the group has also reported the development of several other types of polymer/clay nanocomposite based on polyimide [14], rubber [15] and acrylic resin [16] using similar methods. These developments have brought about extensive global research in this field and nanocomposite manufacturing techniques have been applied to almost every engineering polymer.

The majority of the research work over the past decade has been focused on three synthetic methods. The first method is in-situ polymerisation [17-20], which involves insertion of a monomer between clay layers and polymerisation of the

inserted monomer. In the polymerisation process, the individual clay layers are expanded and dispersed into the polymer matrix to form polymer/clay nanocomposite. This approach can be applied to both thermoplastic and thermosetting polymers and is suitable for polymer manufacturers to produce nanocomposite materials in bulk production scale. Polyamide 6/clay nanocomposites have been commercialised using this method. The second method is solution synthesis [8, 10, 21-22], which uses solvents to swell and disperse clays into a polymer solution. This technique has difficulties in commercial production of nanocomposites for most engineering polymers due to the high costs of solvents and the phase separation of the synthesised products from the solvents. Health and safety issues are also a concern in the application of the solution method. However the solution method may be applicable to water soluble polymers in the commercial production of nanocomposites because of the low cost of using water as a solvent and it is risk-free in terms of health and safety. The third method, melt synthesis [23-24] introduces the intercalation between clays and polymers in the melt phase. This technique can be used by the plastic processing industry to produce nanocomposites as it uses traditional plastic processing techniques such as extrusion and injection moulding. At present, the degradation of organoclays during processing makes this technique less efficient compared to the in-situ polymerisation method [25].

In this study, a novel synthetic method, namely solid intercalation, has been developed. In this method, polymer/clay nanocomposites were formed by the blending and compressing of a solid mixture of polymer and clay at room temperature. As no polymerisation process is involved in the solid intercalation approach, the nanocomposite can be prepared using traditional compression equipment. Compared to other synthetic methods this technique has the potential to overcome the problems associated with the melt synthesis method.

The overall aims of this study are to develop solid intercalation technology and to provide an understanding of the mechanism of solid intercalation via a parallel investigation of this technique with other synthetic methods. Investigations include the development of solid intercalation methodology, the understanding of the mechanisms of solid intercalation, a preliminary study of the effect of processing conditions on solid intercalation, the mechanical properties of solid intercalated

nanocomposites and a preliminary exploration of the possible commercial application of solid intercalation technology.

Chapter 2 LITERATURE REVIEW

This chapter will give an overview of the development of polymer/clay nanocomposites and cover the definition and the structure of polymer/clay nanocomposites, the fundamental knowledge on clays, the compatibility between polymers and clays, the characterisation of polymer/clay nanocomposites, the synthetic methods and the major physical and engineering properties of polymer/clay nanocomposites.

2.1 The definition and structure of polymer/clay nanocomposites

The term "nanocomposite" refers to a type of material containing at least two components for which at least one dimension of one component is in the nanometre range. In the case of polymer/clay nanocomposites, the two components are polymers and layered silicates (clays).

Depending on the nature of polymers and clays used and the fabrication methods applied, four types of possible structures can be formed when clays are added into a polymer. These include a conventional micro-composite structure and three nanocomposite structures as shown in Figure 2-1. [4]

In a *conventional composite* in Figure 2-1 A, the distance between clay layers is not changed. No polymer is present between clay layers even though clay particles can be well dispersed in the polymer matrix. The three types of nanocomposite structures which can be formed are intercalated, ordered exfoliated and disordered exfoliated structures. *An intercalated structure*, as shown in Figure 2-1 B, refers to the composite containing expanded clay layers which are inserted with polymers. *An ordered exfoliated or delaminated structure*, in Figure 2-1 C, has completely separated clay layers in a polymer matrix, but these layers are more or less oriented in one direction. When the individual clay layers are completely and uniformly dispersed in a continuous polymer matrix in a random order, a *disordered exfoliated or delaminated structure* is obtained, as illustrated in Figure 2-1 D.

The reinforcement of clay in a polymer in different dimensions results in different degrees of enhancement of the physical and engineering properties of polymer/clay composites. This will be discussed in Section 2.6 in this chapter.

2.2 Clay

Clay minerals comprise primarily magnesium and hydrous aluminium silicates [27]. Typical layered silicates used in nanocomposite application are 2:1 type phyllosilicates. Such a structure contains two tetrahedral layers sandwiching an edge-shared octahedral layer of either aluminium hydroxide (dioctahedral) or magnesium hydroxide (trioctahedral) as shown in Figure 2-2 [26-27]. The thickness of an individual layer is approximately 1 nanometer (nm) while the lateral dimensions of these layers may vary from 30 nm to several microns (μm). The layers form stacking tactoids with a regular gap between the layers. These gaps are called interlayer space, sometimes *d*-spacing or basal spacing. The extent of the interlayer space can be calculated using the angle of the (001) peak in the X-ray diffraction pattern of the clay.

Between the clay layers, different compensating cations can be present depending on the origin of particular clay minerals. These cations can be exchanged with other cations during clay modification. Cations in some locations can be replaced by a variety of other cations having similar ionic radii, without greatly altering the dimension and arrangement of the layer structure. Such isomorphous substitution, such as Al^{3+} for Si^{4+} in tetrahedral lattices and Mg^{2+} for Al^{3+} in the octahedral layers of clays, causes an excess of negative charges within the layers. These negative charges are counterbalanced by matched isomorphous substitutions elsewhere in the structure or by compensating cations such as Li^{+}, Na^{+}, Ca^{2+}, Mg^{2+} and Al^{3+} ions located between the clay layers.

The classification and the nominal chemical formula of various 2:1-layered silicates are summarized in Table 2-1 [27]. All 2:1-layered silicates can be classified into four groups using the layer charge or charge per formula unit as the criterion and then divided into two subgroups based on whether the octahedral sheets are dioctahedral or trioctahedral in clay minerals. With the layer charge $x \sim 0$, the Pyrophyllite-Talc

group contains little isomorphous substitution in its layers, which results in the clay layers being ionically neutral. In other words, the clay lacks of any equivalent compensating cations between the layers. Other groups, Smectite ($0.2 < x < 0.6$), Vermiculite ($0.6 < x < 0.9$) and Mica ($x \sim 1$), exhibit negative charges on the clay layers due to isomorphous substitution. These anionic charges are counterbalanced by the exchangeable compensating cations. However, for the clays with higher layer charge, the process of ion exchange becomes difficult due to the strong interaction between the layer surface and compensating cations. Hence, the most commonly used clays in nanocomposites are montmorillonite, hectorite and synthetic mica due to the availability, aspect ratios and the potential for layer expansion. Among these three types of clays, the hectorite has the highest aspect ratio and the synthetic mica has the lowest aspect ratio.

A typical character of these selected layered clays is their ability to absorb interlayer compensating cations. These cations can be exchanged, in a reversible process, using solutions of other cations. The exchangeable cations are normally quantified by a parameter called the cation exchange capacity (CEC) which is the maximum amount of exchangeable cations. This parameter is very important to hydrophilic clays in the research of polymer/clay nanocomposites. The unit of CEC is milliequivalents per gram (meq/g) or often milliequivalents per 100 gram (meq/100g). The CEC measurements are performed in neutral conditions, that is at PH = 7. The CEC of mortmorillonites varies between 80 – 150 meq/100g.

The exchangeable cations can be either inorganic or organic. When an inorganic ion exchange process occurs, the exchange rate mainly depends on the accessibility of the interlayer cations, the valence electrons and the size of the cations. When an exchange cation is organic, such as an aliphatic ammonium cation, the reaction normally occurs in the following way between the cations in the clay (A^+) and the organic cation (B^+):

$$\text{Clay} \cdot A^+ + B^+ \Leftrightarrow \text{Clay} \cdot B^+ + A^+$$

The extent of the reaction depends on the nature of the cation A^+ originally in the clay, the nature of the organic cation B^+ and their relative concentrations. During this ion exchange process, the diffusion of the cations also plays an important role. In the case of short-chain ammonium or phosphonium (onium) salts such as methyl-, ethyl-

, propyl-, allyl-, or butyl- salts, the exchanged clays may remain sufficiently hydrophilic to form stable aqueous dispersions [27]. However, when longer-chain alkylammonium or phosphonium (onium) salts such as an octadecylammonium salt are used, the resultant clay will become increasingly hydrophobic and can be dispersed in organic media, forming gel structures with high liquid contents. This phenomenon was first discovered by Jordan [28] and summarised later on by Weiss [29].

The thermodynamic stability of an ion exchanged clay increases with the increase in the alkyl chain length and the extent of substitution of the cation due to the Van der Waals force between the chains in the clay layers, while the thermodynamic stability of the cations between the layers depends on the magnitude of the layer charge, the type of cation and the distribution of the cations [30-31]. X-ray diffraction data indicates that the organic chains of the inserted cations conceptually lie between the clay layers in four states depending on the packing density and the alkyl chain length as shown in Figure 2-3. This includes the chains being parallel to the clay layers in monolayers or bilayers, alternatively these chains can radiate away from the surface in inclined, closely packed arrays in monolayers or bilayers [27].

2.3 The compatibility between clay and polymer

In order to achieve nano-scale interactions between polymers and clays, a good dispersion of a clay into a polymer matrix is essential. However, polymers and clays are normally not compatible since most polymers are hydrophobic while clays are hydrophilic. To make polymers and clays compatible, one of the components has to be modified.

2.3.1 Organoclay Approach

The use of organoclays is the most popular ways to improve the compatibility between polymers and clays. Organoclays are made by converting hydrophilic clays into organophilic ones. Numerous modifiers have been used in the synthesis of nanocomposites. The commonly used modifiers are alkylammonium ions because these substances can be exchanged easily with the cations situated between the

layers. The organoclays can be also obtained through covalent bond formation using reactive silanes. Other modifiers will be also reviewed.

2.3.1.1 Amino Acids

Amino acids have a basic amino group ($-NH_2$) and an acidic carboxyl group (-COOH). A proton can be transferred from the -COOH group to the intramolecular - NH_2 group. This type of acid forms a zwitter ion structure in neutral conditions. In an acidic medium, the structure changes to $H_3N^+(CH_2)_{n-1}COOH$ and in an alkaline environment, the amino acids are present in the form of $H_2N\ (CH_2)_{n-1}COO^-$.

$$H_3N^+(CH_2)_{n-1}COOH \xleftarrow{H^+} H_3N^+(CH_2)_{n-1}COO^- \xrightarrow{OH^-} H_2N(CH_2)_{n-1}COO^-$$

Hence, an ion exchange is then possible between the $-NH_3^+$ functional group formed and cations (i.e. Na^+, K^+...) in the clay layers to make the clay organophilic. A wide range of ω-amino acids ($H_3N^+(CH_2)_{n-1}COOH$) have been investigated for using ion exchange reactions in montmorillonites [18]. This method has been successfully used in the synthesis of polyamide 6 (PA 6)/clay nanocomposites because their acid function groups have the ability to polymerise with ε-caprolactam which has been intercalated between the clay layers, resulting in an exfoliated nanocomposite structure [19].

2.3.1.2 Alkylammonium Ions

As described in Section 2.2 of this Chapter, the hydrophilic clays can be modified into organoclays through an ion exchange process with long-chain alkylammonium or phosphonium (onium) salts such as an octadecylammonium salt. Alkylammonium cations offer a good alternative to amino acids for the synthesis of polymer/clay nanocomposites since these cations can be intercalated into the clay layers easily. Alkylammonium cations between clay layers are able to reduce the surface energy of the clay so that organic species with different polarities can be intercalated.

The most widely used alkylammonium cations are based on primary alkylamines in an acidic medium to protonate the amine function. Their generic formula is $CH_3(CH_2)_nNH_3^+$, where n varies between 1 and 18. The chain length of the ammonium cations has a strong impact on the resulting structure of the nanocomposites. Lan et al. [32] showed that alkylammonium cations with chain lengths larger than eight carbon atoms were favouring the synthesis of exfoliated nanocomposites whereas alkylammonium ions with shorter chains led to the

formation of intercalated nanocomposites. Quaternary ammonium cations and alkylammonium cations based on secondary amines have also been used successfully to produce organoclays [33-34].

2.3.1.3 Silanes

Organoclays are also synthesised by the reaction of silanes with the hydroxyl groups situated on the surface and at the edges of the clay layers.

Silane coupling agents are a family of organo-silicone monomers which are characterised by the formula R–SiX_3, where R is an organic functional group attached to silicon in a hydrolytically stable manner and X designates hydrolyzable groups which are converted to silanol groups on hydrolysis. In principle, silane coupling agents interact with "receptive" inorganic surfaces forming covalent bonds at the interface. These receptive inorganic surfaces are characterised by the presence of hydroxyl groups (-OH) attached principally to silicon and aluminium which particularly favourable for bonding with silanes. In a clay, hydroxyl groups are not only present on the surface of the layers, but also predominantly on their edges. The silane coupling agent is first physically adsorbed on the surfaces or edges, and then converted into the reactive silanol form by hydrolysis (Figure 2-4 a) in the presence of water. The silanol then reacts with the hydroxyl groups present on the inorganic clay surface (Figure 2-4 b).

Silanes have been used in the synthesis of unsaturated polyester-clay nanocomposites by Kornmann et al. [35]. Since then, more research using silanes to modify clays has been carried out. For example, an octadecylammonium salt modified clay with about 60% semifluorinated alkyltrichlorosilane [$CF_3(CF_2)_5(CH_2)_2SiCl_3$] bonded to the surface was synthesised and used to produce PP/clay nanocomposites by melt intercalation [36-40].

2.3.1.4 Other clay modifiers

Other clay modifiers have also been used in the synthesis of polymer/clay nanocomposites because they can directly assist in the nanocomposite formation. These modifiers can initiate polymerisation or increase the compatibility between the polymer and the clay significantly. In the case of polystyrene/clay nanocomposites, aminomethylstyrene, 2-phenylethylamine, amine-terminated polystyrene [41-42] and living free radical polymerisation initiator [43] have all been used successfully for

clay modification. Ogawa et al. [44] reviewed other suitable agents for clay modification in nanocomposite applications.

2.3.2 Polymer Modification Approach

Another method to improve the compatibility of polymers with clays is the modification of polymers, by introducing polar groups into the polymer by grafting and other co-polymerisation methods.

The manufacture of copolymers with polar groups has been actively studied. Polar functional groups can be introduced into polymers by random co-polymerisation or block copolymerisation. For example, polar polypropylenes (PP) were synthesised by random copolymerisation of PP and a small amount of *p*-methylstyrene comonomers using a metallocene catalyst. The *p*-methylstyrene was converted to the substances with functional groups such as hydroxyl and maleic anhydride by lithiation and free radical reactions, respectively [40]. Poly(styrene-maleic anhydride) [47], poly(styrene-co-acrylonitrile) [48-50], nitrile based copolymer (Barex 210 E) [51] and poly(ethylene terephthalate-co-ethylene naphthalate) [52] were also produced for polymer/clay nanocomposite application.

Block copolymers are more commonly used due to their availability. Chung et al synthesised polypropylene based diblock copolymers with poly(methyl methacrylate) (PP-b-PMMA) containing 1 and 5 mol% PMMA. The syntheses involved PP synthesised by metallocene catalysis, hydroboranation of the olefin chain end and free radical polymerization of the PMMA block [40, 53]. Both diblock copolymers (e.g. polystyrene-b-PMMA and polystyrene-b-1,4-polyisoprene) and triblock copolymers (e.g. styrene-isoprene-styrene (SIS) and styrene-butadiene-styrene (SBS)) with different ratios were synthesised. [54-59]

Grafting is another way to modify polymers by introducing polar groups. Although a lot of work was carried out in polymer grafting, only limited grafted polymers have been used to produce polymer/clay nanocomposites. Research in this area is still in progress. Presently, maleic anhydride grafted PP, PE and EVA are common in nanocomposite applications [60-64].

2.4 Characterisation of polymer/clay nanocomposites

The commonly used methods for characterising the nano-structure of polymer/clay nanocomposites are X-ray diffraction analysis (XRD) and transmission electron microscopy (TEM). X-ray diffraction analysis can be used to measure interlayer spacing between the clay layers while TEM can be applied to characterize not only the layer separation but also the dispersion of the clay layers in a polymer. This section will give a brief introduction of these two techniques together with the recent progress in other characterisation techniques

2.4.1 X-Ray Diffraction Analysis

2.4.1.1 Principle

When X-rays strike a sample, if constructive interference of the waves occurs, a diffracted beam is formed due to these waves mutually reinforcing one another. Figure 2-5 shows an X-ray beam with a wavelength λ striking a sample of two clay layers with a distance *d* apart, of an angle θ. The experimental 2θ value is the angle between the diffracted and incident X-ray waves. In order to form a diffracted beam, the rays at the wave front, Y-Y', must be in phase precisely. Some rays travel further than others to reach Y-Y'. For example, Ray 2-2' travelled further than Ray 1-1', the additional distance, EG+GF, must equal the whole number of wavelength (i.e. $n\lambda$, where n is integer) for reinforcement. Since the direction of *d* is normal to the planes and the wave normal is normal to the wavelets, according to the geometry in the diagram, the following equations are obtained if a diffracted beam is formed:

$2\ AG \sin\theta = EG + GF = n\lambda,\ AG = d$

This can be rewritten as

$2d \sin\theta = n\lambda$, namely the Bragg equation. The integer n refers to the degree of the diffraction.

For powder X-ray diffraction, Bragg-Brentano reflection geometry is used, in which the normal of the sample surface bisects the angle (2θ) between the incident and reflected beam. The detector converts individual X-ray photon counts into a signal which can be recorded by a computer. The XRD pattern, i.e. the graph of intensity versus 2θ, can then be generated.

2.4.1.2 Analysis

From a typical XRD pattern (intensity versus 2θ), the interlayer spacing can be calculated according to the Bragg equation. By using the interlayer distance d_{001}, the distance d_{002} and d_{003} ... which are based on subsequent diffracting planes can also be calculated. Since a clay is normally imperfect in crystal order, broad peaks in the corresponding XRD patterns are often observed. The width at half-maximum of the XRD diffraction peak can be used to estimate the particle size and the distribution of the particle sizes. This is useful for assessing the changing of particle size in nanocomposite formation.

Although XRD technology provides informative data on the periodic structure in polymer/clay systems, the technique is not sufficient to detect very thin clay tactoids [65]. Therefore the TEM technique is required to overcome this problem.

2.4.2 Transmission Electron Microscopy

2.4.2.1 Principle

In TEM, images are formed by the scattering of electrons as the electron beam passes through a sample. A transmission electron microscope, as shown in Figure 2-6, can be divided into three components: the illumination system, the objective lens and stage, and the imaging system. The illumination system comprises an electron gun to produce electrons and condenser lenses equipped with a diaphragm to provide the electron beam which passes through the specimen. The lenses use an electromagnetic field to focus the beam. The electrons are scattered as they pass through the specimen and are transferred to the objective lens. The first image of the specimen is formed by the objective lens. The objective aperture controls the spread of the electron beam and gives contrast to the image. The imaging system contains several lenses to magnify the image and focus the image onto a viewing screen where the operator can observe the magnified image of the specimen.

The standard imaging method on the TEM is bright-field imaging method in which the images are normally bright. The method works as shown in Figure 2-7. When the primary electron beam travels through the electromagnetic field and hits a specimen, some of the electrons are scattered by the specimen. The number of electrons passing through the objective aperture will depend on the aperture size. If the objective aperture is centred with the optical axis, a bright background can be seen in the

absence of a specimen. Regions with greater thickness or higher density in a specimen will result in scattering the electron beam more strongly and appear darker in the image since less electrons transmitted. A clay layer has a higher density than the polymer and will appear darker than the polymer.

2.4.2.2 Analysis

From TEM images of polymer/clay nanocomposites, different structures can be identified. For an intercalated structure, the morphology can be a uniform expansion of the clay layers. The image will show dark and bright lines with increased distance between these lines. The parallel dark lines represent individual clay sheets while the bright lines represent the polymer matrix. In many cases, the image may comprise of dispersed primary particles together with expanded layers surrounding the particles. Smaller expansion predominately occurs in the interior of the samples, while layer expansion and individual layers are observed near the edges. Sometimes micro-scale clay aggregates can also be seen in some intercalated polymer/clay nanocomposites. For an exfoliated structure, the individual layers are randomly distributed in the polymer matrix.

To optimise the TEM image, specimens have to be sufficiently thin because of the phenomenon known as the 'mass-thickness contrast'. If the specimens are too thick, the polymer would appear dark so it is difficult to distinguish between the clay and polymer. [193]

2.4.3 Other characterisation techniques

Other characterisation techniques have been recently developed including solid-state NMR [66-68] and atomic force microscopy [69].

Gilman et al used solid-state NMR along with DSC to investigate the influence of clay on the crystalline development of a PA 6. It was reported that the longitudinal relaxation times of the PA 6 protons can be used as a relative measurement of the extent of clay dispersion in PA 6/clay systems, PA 6/clay stoichiometry, state of dryness and thermal history. They also reported that a ^{13}C NMR morphological tool has been developed for investigating the stratification morphology with respect to the clay surfaces, starting at distances of ~2 nm from the clay surfaces [67-68].

2.5 The synthesis of polymer/clay nanocomposites

Several strategies have been used to produce polymer/clay nanocomposites. These include in-situ polymerisation, solution synthesis and melt processing techniques.

2.5.1 In-situ polymerisation

In-situ polymerisation was the first method used to synthesise polymer/clay nanocomposites. The Toyota research team initiated this method to produce PA 6/clay nanocomposites [17, 19]. Since then, this method has been applied to nearly all polymers.

2.5.1.1 Thermoplastic polymers

The typical method used to produce thermoplastic polymer based nanocomposites is schematically illustrated in Figure 2-8. The process consists of two stages. One is the swelling of the clay in a monomer to insert the monomer into clay layers. For some systems, clay modifiers, protonate acids and solvent/co-solvent have to be used. The second stage is the polymerisation of the intercalated monomers to form nanocomposites. The final product is normally obtained following separation, washing and drying. In the following description, the influence of various factors on nanocomposite formation will be discussed.

Swelling

The purpose of the swelling treatment is to intercalate the monomers into the clay layers. The factors involved in this treatment include clay type, clay modifier, acid, solvent, processing conditions and monomer type.

Clay is one of the most important factors. The clay used in in-situ polymerisation can be either hydrophilic or organiphilic. Organoclays are synthesised by the methods described in Section 3.1. When an organoclay is used, the clay is usually dispersed in a solvent/co-solvent, followed by the intercalation between the clay and the monomer. When a hydrophilic clay is used, modifiers, acids and solvent/co-solvent are normally required. For example, in the synthesis of PA 6/clay nanocomposites [18], ω-amino acids ($H_3N^+(CH_2)_{n-1}COOH$, n=2, 3, 4, 5, 6, 8, 11, 12 and 18) were used to modify a Na^+-montmorillonite in the presence of hydrochloric acid and water. Subsequently the modified montmorillonites were used to intercalate ε-

caprolactam monomer at both 25 °C and 100 °C. It was found that different lengths of alkyl chain in the ω-amino acids resulted in different degrees of layer expansions. Longer alkyl chains (n≥11) led to larger interlayer spacing. However, if the monomer itself is compatible to clay, no modifier is required. In the case of PA 6/clay systems, Na^+-montmorillonite could be directly intercalated with the monomer, ε-caprolactam, in the presence of hydrochloric acid and water [20]. This technique has been named as "one-pot" synthesis. Additionally, the results obtained from a PA 12/clay system showed that the swelling treatment of clays was affected by the concentration of the modifier, 12-aminolauric acid. When the concentration of the 12-aminolauric acid was low, the exchange of inorganic cations in a synthetic mica by the acid resulted in an increase in the interlayer distance from 0.95 nm to 1.7 nm. In a much higher concentration, further diffusion of the zwitterionic 12-aminolauric acid caused the interlayer distance to exceed 2 nm. Therefore high concentrations of modifier may be of benefit to nanocomposite formation [70].

However, not all hydrophilic clays can be used successfully for direct intercalation using in-situ polymerisation. It was reported that this technique was not effective when applied to ε-caprolactone (ε-CL) in Cr^+ fluorohectorite for producing poly(ε-caprolactone) (PCL)/clay nanocomposites. Only a limited amount of polymer was intercalated into the clay layers with the interlayer spacing increasing from 1.28nm to 1.37nm [71].

Other organoclay modifiers, especially ammonium salts have been extensively used in the modification of hydrophilic clays according to the potential formation of polymer/clay nanocomposites. Table 2-2 [72] lists the interlayer spacing of the clays modified by different ammonium salts and the corresponding PS based composites together with an evaluation of the clay dispersibility within styrene during the polymerisation reaction. The organoclays in the table were modified by ammonium cations with representative structure $(CH_3)_2N^+$(hydrogenated tallow alkyl)R. In the structure, hydrogenated tallow alkyl is composed of mainly octadecyl chains together with small amounts of lower linear homologues while R is another hydrogenated tallow hydrocarbon group. This hydrocarbon group was alkyl for Ta-montmorillonite (Ta-MMT), 2-ethyl hexyl for Eh-montmorillonite (Eh-MMT) and benzyl for Bz-montmorillonite (Bz-MMT). The results obtained indicated that structural affinity between styrene monomer and the organic group in the modified

montmorillonite is one of the most important factors. Another important factor is the dispersibility of organoclays in styrene. Since this work, the studies in synthesising the modifiers have progressed significantly using structural affinity and the quality of nanocomposites as guidelines.

The reason using *protonate acid* is to provide an acidic medium for the clay modifier so that cation exchange in the clay layers becomes possible. Hydrochloric acid is the first acid used for this purpose. In the one-pot synthesis of PA 6/clay nanocomposites, various acids were studied [20]. The XRD results of the final nanocomposites are listed in Table 2-3. It can be observed that exfoliated nanocomposite was obtained when using phosphoric acid, while partially exfoliated partially intercalated structures were formed when other acids were used (interlayer spacing ~ 2 nm). Hydrochloric acid is one of the effective acids among the acids studied. When no more cation exchange occurs between the clay layers, the type of protonate acid will not affect the swelling treatment. Reichert et al found that the swelling behaviour of a synthetic mica in 12-aminolauric acid was independent of the protonate acids (HCl, H_2SO_4, H_3PO_4) used [70]. The swelling process was also independent of swelling temperature, but was affected by the concentration of the clay modifier.

If the monomer used in in-situ polymerisation is a liquid, clay will be able to disperse in the monomer, allowing the monomer to intercalate between the clay layers. Otherwise, a solvent/co-solvent should be used to prepare both the clay and the monomer solutions. When a hydrophilic clay, such as Na^+-montmorillonite is used, water or alcohol could be applied. In the case of organoclays, organic solvents/co-solvents need to be considered. The information on the dispersion behaviour of clays in different solvents is normally supplied by the clay manufacturers. The solubility of a monomer in a solvent is usually predicted using the difference in solubility parameter between the monomer and the solvent. Toluene, n-heptane and methylene chloride are generally used as solvents for the intercalation of the monomers of thermoplastic polymers. Only limited work has been carried out to investigate the effect of solvent on nanocomposite structure. Akelah and Moet [73] used three solvents/co-solvents, acetonitrile, acetonitrile/toluene and acetonitrile/THF and obtained a good dispersion of organoclays in polystyrene based nanocomposites. It was found that a suitable

solvent could promote the expansion of the clay layers. The interlayer spacing of the resultant intercalated nanocomposites varied between 1.72 and 2.45nm depending on the type of solvent used. In the case of acetonitrile, an interlayer spacing of 2.45 nm was obtained in the resultant nanocomposite.

The swelling *time* is important in the swelling treatment depending on the polarity of the monomer molecules, the surface treatment of the organoclay, solvent and *temperature.* The time taken to swell the clay can vary from 30 minutes to more than 24 hours depending on the clay used [18-19, 70, 74-76]. The effect of swelling temperature on the swelling process is a function of the clay and monomer used. Usuki A. et al [18] found that the swelling of ε-caprolactam monomer in a series of organoclays was affected by temperature (25 °C & 100 °C). The interlayer spacing of the clays increased as the temperature rose. At the higher temperature, the interlayer spacing is determined by the lengths of the organic chains in the ammonium cations. The longer the chain is, the wider the interlayer spacing. However, different results were obtained by Reichert et al in the swelling of a synthetic mica in 12-aminolauric acid. In their study, the swelling behaviour was found to be independent of temperature [70].

Polymerisation Treatment

The purpose of polymerisation treatment is to polymerise the inserted monomers between clay layers to form nanocomposite structures. Different polymerisation approaches have been applied depending on the nature of polymer matrix.

Ring-open polymerisation was used in producing PA 6 and poly(ε-caprolactone) based nanocomposites. Kojima et al. [20] polymerised ε-caprolactam with an organoclay at 250 °C for 6 hours in a nitrogen atmosphere using 6-aminocaproic acid as a polymerisation accelerator.

Depending on clay loading, either exfoliated (for less than 7 wt% clay loading) or intercalated structures (from 7 to 70 wt% clay loading) were obtained. Comparison of the amount of -COOH and $-NH_2$ end groups before and after the ring-opening polymerisation showed that the COOH end groups on the surface of the organoclay were responsible for the polymerisation initiation. Approximately all of the NH_3^+ end groups in the matrix were intercalated with the clay. The ratio of bonded to non-bonded polymer chains increased as the clay content rose [17-18].

Condensation and addition polymerisation methods by free radical, ionic or coordination reactions have also been widely used for various polymer systems for nanocomposite applications.

The polymer systems attempted using the condensation polymerisation method included PA 12 [70], PA 1012 [77] and poly(ethylene terephthalate) [78]. For PA 12 based nanocomposites, a self condensation polymerisation of 12-aminolauric acid was carried out at 280 °C in an autoclave in the presence of swollen clay under pressure for 9.5 hours. X-ray diffraction and TEM investigations showed that only partially exfoliated structures were formed. When the condensation polymerisation involves two substances, the sequence of adding the reagents should be considered. For example, in the case of producing PA 1012 based nanocomposites, a diamine was mixed with an organoclay solution first. The mixture was then added to the solution of diacid to obtain diaminodecane-decanedicarboxylic acid salt. The resultant salt with a slight excess of diamine (1 mol% more) was then further reacted. X-ray diffraction and TEM showed that exfoliated structure was formed.

Addition polymerisation was used in producing polystyrene, poly(methyl methacrylate), polypropylene, polyethylene and other thermoplastic polymer based nanocomposites [43, 72-76, 79-95]. This type of polymerisation is very important in obtaining non-polar polymer based nanocomposites.

For a free radical reaction, a source of free radicals is required. In most cases, an initiator such as N,N-azobis(isobutyronitrile) (AIBN), benzoyl peroxide (BPO) or other peroxides are used, for example, a styrene polymerisation was carried out using N,N-azobis(isobutyronitrile) (AIBN) as initiator [73].

In ionic reactions, an initiator precursor is normally directly bound onto the clay surfaces and then activated for polymerisation. For example in the synthesis of PS/clay nanocomposites [79], a 1,1-diphenylethylene derivative with a triethyl-ammonium bromide group was inserted between the clay layers and the polymerisation was initiated by the 1,1-diphenylethylene on the clay surfaces reacting with *n*-BuLi. X-ray diffraction results indicate that an intercalated structure was formed. The clay layers were expanded to 2.34nm.

Coordination reactions are usually used for obtaining polyolefin based nanocomposites [88-95]. Exfoliated polyethylene (PE)/clay nanocomposites have

been obtained by Ti-based Ziegler-Natta polymerisation of ethylene using montmorillonite (MMT-OH) modified with intercalation agents containing hydroxyl groups [92].

Commercial polymerisation systems including bulk, emulsion, suspension and solution systems have also been reported for the synthesis of polymer/clay nanocomposites [79-80, 85, 96-101]. Bulk polymerisation, for example, has been used to produce PMMA/clay nanocomposites using methyl methacrylate as monomer, organoclay and BPO as initiator. An exfoliated structure was formed according to the XRD results. TEM results further confirmed that the resultant nanocomposite had an ordered exfoliated structure. The clay layers were dispersed in the nanocomposite homogeneously, with the interlayer spacing of more than 50 nm. [96]

In *emulsion polymerisation*, clay modifiers were used as surfactants for forming the emulsion. An example of this is the use of 2-acrylamido-2-methyl-1-propanesulfonic acid as a reactive surfactant in the production of an exfoliated PMMA/clay nanocomposite [97].

In suspension polymerisation of PMMA based nanocomposite, organoclays have been used as suspension stabilizers. [87].

Solution polymerisation was studied by Tabtiang et al [101]. In this work, methyl methacrylate in the presence of an alkylammonium-modified clay was used to prepare PMMA/clay nanocomposites. The interlayer spacing of the clay layers in the nanocomposite were expanded to > 8 nm. Compared to the polymer synthesised in the same condition without clay, the presence of the clay led to chain branching, reduction of the average molecular weight and an increase in the polydispersity of the polymer.

2.5.1.2 Elastomeric and Thermoset Polymers

Elastomeric and thermoset polymers based nanocomposites are formed in a similar way to the synthesis of thermoplastic polymers based ones, as illustrated in Figure 2-9. Two processes are involved: one is the swelling of the clay in monomers or pre-polymers with or without solvent/co-solvent and other reaction media; the other process is the curing of the intercalated monomers to form nanocomposites. This method has been used for the production of both intercalated and exfoliated

nanocomposites. The elastomeric or thermoset polymers attempted include epoxy resins [103-110], polyurethanes [111-117], unsaturated polyesters [118-119] and phenolic resins [102, 120-121].

Swelling

The purpose of the swelling the clay before producing either an elastermeric or thermoset polymer based nanocomposite is to intercalate the polymers into the clay layers. For this type of nanocomposite, organoclays are usually used. The factors such as clay type, solvent, processing conditions and monomer type also affect the degree of swelling of the clays. In the formation of elastomeric and thermoset polymers based nanocomposites, the swelling of the clay can be obtained with either monomers or pre-polymers. For example, in the synthesis of epoxy/clay nanocomposites conducted by Vaia et al [103], the monomer (diglycidyl ether of bisphenol A) and an organoclay in a solvent were used to swell the clay. The curing agent (poly(ether amine)) was then added. Lee and Jang [104] prepared an epoxy/clay intercalated nanocomposite by an in-situ polymerisation technique. They used bisphenol A and an epoxy pre-polymer in an emulsion media in the swelling of the clay.

The resultant swollen clay plays an important role in the structure of the nanocomposites. For example, clays with a low CEC can be exfoliated during swelling in epoxy resin before curing. This may be due to the homo-polymerisation of the epoxy resin during the swelling phase, causing diffusion of new epoxy molecules into the clay galleries. The large amount of space available between the clay layers would increase the diffusion of epoxy molecules. The swelling time of the clay with high CEC was found to be critical for the synthesis of an exfoliated nanocomposite [104]. In the synthesis of phenolic resin/clay nanocomposites reported by Chung et al [120], the nanostructure of the final nanocomposites was found to be the same as the nanostructure before the curing process.

When several monomers or pre-polymers are used in producing nanocomposites, the mixing method in the swelling treatment becomes very important. In the synthesis of unsaturated polyester/clay nanocomposites carried out by Park et al [119], the linear unsaturated polyester was used to mix styrene monomer and clay. Simultaneous and sequential mixing methods were tried for preparing the nanocomposites. In the

simultaneous mixing method, the unsaturated polyester, styrene monomer and clay were mixed together. In the sequential mixing method, the linear unsaturated polyester and clay were mixed in the first step, and then styrene monomer was added to the mixture of unsaturated polyester/clay and stirred. Intercalated structures were obtained in the case of the simultaneous mixing method. However both intercalated and exfoliated structures were achieved when the sequential mixing method was used.

Curing process

For the curing process, the effects of curing agents, concentration and the curing conditions on the structure of the resultant nanocomposites have been studied extensively [102-121]. In this review, the epoxy/clay system [106-110] is used as a typical example to explain the curing process in in-situ polymerisation.

A study of the curing of diglycidyl ether of bisphenol A in the presence of organoclays by Giannelis et al [106] showed that the *curing agent* used in the polymerisation process determined the structure of the nanocomposites. When bi-functional primary and secondary amines were used as curing agents, only intercalated epoxy/clay structures were obtained. When other curing agents (e.g. nadic methyl anhydride, benzyldimethylamine) were added, exfoliated epoxy-clay structures formed. Chin et al [107] reported that when using meta-phenylene diamine as the curing agent for epoxy, the nanocomposite structure was affected by the *concentration of the curing agent*. Only intercalated nanostructures were obtained when the molar ratio of diamine/monomer was equivalent or higher; exfoliated nanocomposites were formed using less than stoichiometric quantity of diamine or by auto-polymerisation of monomer without a curing agent. Cross-linking out of the clay tactoids occurred with higher concentrations of the curing agent.

Sometimes a suitable *catalyst* is necessary to achieve a complete exfoliation of an epoxy/organoclay system. When an anhydride is used as a curing agent without any promoter (*catalyst*), intercalated epoxy/clay structure always exists in the cured system [108-109]. *N,N*-dimethylbenzylamine was used as a *catalyst* to achieve complete exfoliation. The possible condition for complete exfoliation was that the heat of the intragallery curing process released before the gel point is larger than the Van der Waals attractive energy between the interlayers.

Kornmann et al [110] found that the key to exfoliate clays in epoxy systems is to control the balance between the intragallery and the extragallery curing rates. The curing temperature controlled both cure kinetics and diffusion rate of the clay and hence the exfoliation of the organoclay in epoxy systems.

In most other elastomeric or thermoset polymer/clay systems, the curing process is similar to the epoxy/clay system. The curing process normally helps in obtaining exfoliated structures. The selection of curing agent and the curing temperature for an elastomeric or thermoset polymer resin is critical in determining the intercalated and/or exfoliated nanostructure of the resultant nanocomposites. However, some thermoset polymer/clay systems show different behaviour [120]. In the synthesis of phenolic resin/organo-fluorohectorite nanocomposites, the curing process did not affect the intercalated structure. Also, in the case of phenolic resin/organo-montmorillonite system, de-intercalation occurred.

2.5.2 Solution synthesis

Solution synthesis has been widely applied to water soluble polymers to produce intercalated nanocomposites based on poly(vinyl alcohol) [8,124], poly(vinyl pyrrolidinane) [125], polyethylene oxide[21-22, 45, 123-124, 126-129] and poly(acrylic acid) [130]. This technique has been studied for polymer/clay composites since the 1960's [122-123]. However, the dispersion of clays on the nanoscale was not identified until the 1990's when it was applied to non-aqueous solvent soluble polymers, such as poly(L-lactide) [131], poly(ε-caprolactone) [132], PS [56, 133-134], PMMA [135], HDPE [51], polyimide [136-140], and polysulfone [141] to produce nanocomposites. The main method used for solution synthesis is shown in Figure 2-10. The synthesis comprises two steps, mixing and removal of solvent.

The synthesis begins with mixing polymer and clay (hydrophilic clay or organoclay) in a solvent/co-solvent. The mixing process can be carried out in three ways. The first one is mixing the solutions of clay and polymer. The second method is by adding powdered clay directly into a polymer solution. The third one is blending solid clay and polymer powders in the presence of a solvent/co-solvent. When the solvent is removed, the clay layers sandwich with the polymer to form an intercalated structure.

The mixing process is similar to the swelling process used in the in-situ polymerisation method. However, the mixing in solution synthesis is more difficult due to the involvement of polymers instead of monomers. The s*olvent/co-solvent* plays an important role in this process. The solvent/co-solvent has to be able to disperse clay and to dissolve the polymer. Water, toluene, chloroform, dichloromethane and *N,N*-dimethylacetamide are commonly used as solvents in solution synthesis. The intercalation reactions are normally carried out by stirring or using ultrasonic excitation.

Several methods are used to remove the solvent – evaporation, freeze-drying and precipitating using another solvent.

In evaporation, different techniques were used – natural evaporation in ambient conditions, static casting on a non-affinity substrate and roll-casting. All the techniques are followed by applying a vacuum to remove the final traces of solvent. Intercalated structures were obtained using this evaporation method to remove the solvent. [56, 127]

Freeze-drying is a method used to dry a material in a frozen state under high vacuum, which controls and allows humidity and moisture to be extracted from the material. Chang et al [133-134] used *freeze-drying* in their study of syndiotactic polystyrene/modified-clay nanocomposites. The reacted mixture of s-polystyrene and organoclay with adsorbed cetyl pyridium chloride (CPC) in hot dichlorobenzene was dried using this method. The freezing dried product was then dried further in a vacuum oven. X-ray diffraction and TEM results indicated that intercalated and exfoliated nanocomposites were obtained depending on whether the cationic surfactant CPC was applied.

The reacted products in solution synthesis can be also obtained from the solution by the precipitation of the solution into another solvent. For example, in producing high density polyethylene (HDPE) based nanocomposites [51], the reacted mixture of HDPE and an organoclay solution in the cosolvent of xylene and benzonitrile was precipitated into tetrahydrofuran to obtain HDPE/clay nanocomposites. In this case, intercalated nanocomposites were produced with an interlayer spacing of 1.77 nm.

The driving force for polymer intercalation in solution synthesis is that the entropy, which is gained by the desorption of solvent molecules, compensates the decrease of

conformational entropy in the intercalated polymer chains [193]. The major advantage of this method is that it is possible to synthesise intercalated nanocomposites based on polymers with low or even no polarity and to produce nanocomposite films with preferred orientation. However it is difficult to produce nanocomposites with exfoliated structures. Commercial application of this method is also a concern due to the use of large quantities of solvent.

2.5.3 Melt synthesis

Melt synthesis has become increasingly popular since it was first reported by Vaia et al. [23] in 1993. Recently this method has been recognised as a promising approach to produce nanocomposites since such a process can be carried out in conventional polymer processing equipment. Moreover, melt synthesis is environmentally benign. The intercalation between polymers and clays usually takes place in the melt phase with the aid of shear. If the surfaces of the clay layers are compatible with the chosen polymer, the polymer can flow into the interlayer space and form either intercalated or exfoliated nanocomposites.

The main method used to produce nanocomposites by melt synthesis is shown in Figure 2-11. The first route is mainly used in early stages of the research. The technique comprises two steps – blending the clay and the polymer followed by annealing the mixture above the glass transition temperature (Tg) for an amorphous polymer or the melt temperature (Tm) for a crystalline polymer, respectively. The quality of the nanocomposite via this route depends on a number of factors related to the polymers, the clays and the system as a whole. The factors for the clay are the cation exchange capacity (CEC) of the clay used, the chain length of the ammonium cations between the clay layers, the particle size of the clay and the clay content, while the polymer factors are polymer type and the molecular weight of the polymer. The combined system parameters are the thermodynamic character of the polymer/clay system, compatibility between the polymer and the clay, blending conditions and annealing conditions. [23, 24, 57-58, 142-146] These factors have similar effects on all the routes to produce polymer/clay nanocomposites in melt synthesis as discussed for in-situ polymerisation in Section 2.5.1.1. [23, 24, 46, 143-184,186]

The second and third routes are actively studied for most polymer/clay systems. These routes include melt compounding of the mixture of polymer, clay and other components above the Tg of amorphous polymers [148] or the Tm of crystalline polymers [149-150] to obtain polymer/clay nanocomposites. The second route comprises two steps. The first step is pre-blending the polymer and clay to optimise the polymer/clay interaction, sometimes with other additives; the second step is melt compounding. The third route is completed in one step – melt compounding.

The pre-blending step can be carried out in a mixer or just by shaking the mixture in a bag. The melt compounding step can be carried out by traditional polymer processing equipment such as two-roll mills [151-158], internal mixers [159-165], single-screw or twin-screw extruders [142, 149-150, 166-181, 186], injection moulding machines [182-183] or rotational moulding machines [184].

The majority of the melt compounding to produce polymer/clay nanocomposites is carried out through extrusion. The melt compounding processes of polymer/clay nanocomposites normally involves the distribution of clays in the polymer matrix in space and the separation of the clay particles into dispersed clay layers [185].

In the extruder, the aggregates of clay are broken up when the shear stress applied to them exceeds the strength of the particles. Nanocomposites are formed when the small particles are separated further so that polymer molecules can be inserted between the clay galleries [142]. Shear stresses and the diffusion of the polymer are important parameters here.

The important factors which affect the production of nanocomposites are the shear stress applied to the polymer and the clay, the viscosities of the mixture and the residence time in the extruder. These factors are determined by screw configuration, screw speed, processing temperature, feeding method and feeding rate.

The rheology of the polymer/clay system is an important parameter that affects the degree of exfoliation and properties of the final products. For example, in melt compounded PA 6/clay nanocomposites, a high viscosity polymer/clay system exhibited solid-like non-Newtonian behaviour; this was due to the high degrees of exfoliation of the clay, which increases the number of particle-polymer interactions [142]. A low viscosity polymer/clay system exhibited more Newtonian behaviour. The melt viscosity of the nanocomposites exhibited similar shear-thinning behaviour

as pure PA 6. However, the viscosity of the nanocomposites is significantly lower than that of the neat PA 6 [149]. Fornes et al suggested that a high melt viscosity exerted a greater stress on the clay tactoids so that the taller stacks are chopped into shorter ones by the stress shear. Low viscosity melts for the nanocomposites may be the result of higher clay layer alignment, smaller particle sizes and matrix molecular weight degradation [142].

The viscosity of the polymer normally decreases as temperature increases. There is a possibility that the processing temperature would play a very important role in the final nanocomposites produced in melt synthesis. However, Cho et al [149] reported that in the case of the PA 6/clay system, the final nanocomposite properties were almost independent of the barrel temperature over the range of processing temperatures (230 ° – 280 °C) typically used for PA 6.

The shear stresses and the residence time can be changed in an extruder via changing extruder type, screw configuration and speed. The extruders used in producing polymer/clay nanocomposites include single screw, co-rotating twin-screw and counter-rotating twin-screw extruders. Some studies described that shear stresses and residence time were important parameters to obtain exfoliated nanocomposites by melt compounding [149-150]. Paul et al used three types of extruders with a variety of screw configurations to introduce different shear stresses and residence times for melt compounding PA 6 and clays. Twin-screw extruders were found to give better exfoliation and dispersion of clays than single screw extruders. This is probably because the amount of shear in a single screw extruder is insufficient to get the same dispersion and expansion of the clay which is obtained in a twin-screw extruder. All twin-screw extruders were found to give improved exfoliation when the residence time increased [150]. Cho et al also mentioned that the exfoliation of a clay in polymer matrix was slightly improved by increasing the screw speed or a second pass of the polymer/clay mixture through the extruder [149]. However, other studies mentioned an opposite tendency [168, 174]. Davis et al [168] found that in polyethylene terephthalate/clay system, long residence time and high screw speeds resulted in low quality nanocomposites. Therefore, it appears that for each polymer/clay system, screw speed and residence time should be investigated to obtain high quality nanocomposites.

Surprisingly in the PA 6 based nanocomposites, the highest shear stress configuration did not give the best exfoliation and dispersion for both intermeshing and non-intermeshing counter-rotating twin-screw extruders. The best exfoliation and dispersion was obtained with medium shear stress in a non-intermeshing counter-rotating twin-screw extruder [150]. Therefore, shear stress does affect the exfoliation under certain conditions.

Paul et al also pointed out that with fully compatible PA 6/clay system, an exfoliated nanocomposite was formed via counter-rotating intermeshing extruder [150]. However, with marginally compatible PA 6/clay system, only partially intercalated nanocomposites were formed under the same processing condition. Therefore, the key parameter for exfoliation is the compatibility between polymer and clay. The effect of shear on the resultant nanocomposite structure depended on the compatibility between polymer and clay [180]. When shear was applied to a mixture with a fully compatible polymer/clay system, the exfoliation of clay took place in most processing conditions. Therefore in this case, the effect of shear was not significant. When a mixture with marginally compatible polymer/clay system was used, shear could be adjusted to obtain well-exfoliated nanocomposites. Where there was no apparent compatibility between the polymer and the clay, the shear applied during mixing is only responsible for the reduction of the size of clay tactoids. In this case, improving the compatibility between the polymer and the clay will play a crucial role to obtain an exfoliated nanocomposite.

The feeding rate and methods are very important in the exfoliation and dispersion of clay layers to obtain a high quality nanocomposite due to their effects on flow behaviour and shear stresses. For instance, Svoboda et al used a low feeding rate to achieve good mixing in a co-rotating fully intermeshing twin-screw extruder [170]. There is very little detailed study published on the effect of feeding rate and method on the final quality of the nanocomposites via extrusion. However, different feeding methods have been attempted using Brabender roller mixer. Park et al used an *indirect stepwise mixing method* and *simultaneous mixing method* in a polystyrene/clay system. In the *indirect stepwise mixing method*, the amorphous styrenic polymer was melt intercalated into organoclay followed by blending with syndiotactic polystyrene. In the *simultaneous mixing method*, all the components were melt mixed together simutaneously. The stepwise mixing method yielded more

intercalated structure while the simple simultaneous mixing method is more favourable to producing exfoliated structures [165].

Understanding the processing parameters for different polymer/clay systems is crucial in producing high quality nanocomposites by melt processing. Some commercial products have been produced using this method. In comparison with the materials produced from in-situ polymerisation, it was found that smaller, more disordered lamellae were observed in the in-situ polymerised nanocomposites whereas larger, more ordered lamellae were observed in melt-synthesised nanocomposites [181].

All the synthetic methods have their advantages and disadvantages. Further work is still required to use them efficiently and to develop commercial technology for manufacturing polymer/clay nanocomposites.

2.6 Properties of polymer/clay nanocomposites

Conventional polymer/clay composites have improved rigidity over pure polymers, but they often not only sacrifice strength, elongation and toughness, but also require a high clay loading. However a polymer/clay nanocomposite with a low clay content exhibit not only better mechanical properties, but also enhanced barrier properties, thermal stability and fire retardancy compared to its original polymer. In addition, the optical properties of the composite are not greatly affected by the presence of the exfoliated clay layers at low concentrations. [4]

2.6.1 Mechanical properties

2.6.1.1 Tensile properties

Significant improvement of tensile strength and modulus of polymer/clay nanocomposites has been reported [1, 68, 77, 114, 142, 147-150, 172, 186-187]. These properties are dependent on the structure of nanocomposites, the type of clay applied, clay content, manufacturing method and the properties of the polymer used. The conditions under which measurements are carried out also affect the tensile strength and modulus. The researchers in Toyota Central R&D Labs were first to report the improvement of tensile properties based on PA 6/clay systems produced

using in-situ polymerisation [1]. Their results showed that nanocomposites with only 4.7wt% clay content had a 42% increase in tensile strength and a 68% increase in tensile modulus at 23 °C compared to the pure polymer. At 120 °C, the tensile strength increased by 21% while the tensile modulus increased dramatically up to 221%.

Another advantage of nanocomposites over traditional composites is that elongation at yield does not reduce significantly. Most of the polymer/clay nanocomposites showed a small decrease in elongation at yield. However considerable decrease may occur if the clays in a nanocomposite are not well exfoliated. In some cases, elongation at yield could increase. For example, in PA 1012/clay nanocomposites, the elongation at yield showed a small decrease from 35% for pure PA 1012 to 28% for a nanocomposite with 5wt% clay content [77]. In PP based nanocomposites, the elongation at yield dropped from >150% for pure PP to 5.6% for nanocomposites with 7.2/21.6 wt% organoclay/maleic anhydride grafted PP content [186]. However, for a polyurethane (PU) based nanocomposite with 7.79 wt% clay content, its elongation at yield was nearly 2.5 times that of pure PU [114].

The clay content plays an important role in the improvement of the tensile properties. In the case of PA 6 nanocomposites obtained by melt intercalation, the tensile modulus of the nanocomposites increased with the increase of clay content. The tensile modulus approximately doubled as the clay content rose to 10 wt%. Above this clay loading, the tensile modulus levelled off. These changes corresponded to the change from totally exfoliated structure (<10 wt%) to partially exfoliated-partially intercalated structure (for ≥10 wt%) [147]. The tensile strength also increased with the increase of clay content within the studied range, 0-10 wt%. There was a substantial increase in the tensile strength when clay content was low (<2.5 wt%). When the clay content is over 2.5 wt%, the tensile strength began to level off. The elongation at yield of the nanocomposites decreased continuously as the clay concentration increased. It was explained that the improvement of the stiffness and strength was probably due to the integration of clay layers with the polymer matrix. The explanation for the decrease in elongation at yield is still in progress [172]. However in the PU/organoclay/glycerol propoxylate nanocomposites, both the tensile strength and the elongation at yield were increased with the increase in clay content in the range of 0–8 wt%. The maximum values of the mechanical properties

were reached at the 8 wt% clay loading. Above this range, both the tensile strength and elongation at break of PU/organoclay/glycerol propoxylate were decreased. This was explained as the result of the interaction between the PU and clay layers. When clay content was less than 8 wt%, the clay layers had a good compatibility and a strong interaction with the PU. When the clay content was higher than 8 wt%, the layers began to aggregate [114].

The tensile properties of nanocomposites were also influenced by the clays used. In Toyota's work [1], the nanocomposite produced from PA 6 with montmorillonite had a higher modulus than the composites with saponite which has a shorter length of the clay layers. This dependence clearly indicated that the tensile modulus of PA 6 based nanocomposites can be directly related to the average length of the layers. The higher the average length of the clay layers, the higher the modulus of the PA 6 based nanocomposites. Hence the tensile properties can be related to the aspect ratio of the dispersed clay layers since these clays have similar thickness in an individual layer, ~1 nm.

The tensile properties are also affected by the surface properties of clays. The improvement in tensile strength and modulus of nanocomposites is more significant when organoclays are used than hydrophilic clays. The decrease in elongation at yield is much less in PA 6/organoclay system than PA 6/hydrophilic clay system. This phenomenon is possibly caused by a higher extent of exfoliation in the polymer/organoclay system. [149]

The effect of manufacturing method on the tensile properties has been examined by Toyota for PA 6/clay nanocomposites with ~5 wt% clay content produced using in-situ polymerisation [1] and by other major active groups in this field using melt synthesis [68, 148-150]. The original polymers used by these researchers had similar tensile strengths between 64 and 68 MPa. However, the nanocomposites produced by in-situ polymerisation have higher tensile strengths than the nanocomposites produced by melt synthesis. In many cases, little improvement in mechanical properties has observed by melt synthesis [187].

For a particular synthetic method, different reaction parameters may result in differences in tensile properties. Paul et al used different shear rates in producing PA 6/15A nanocomposites via melt synthesis. The tensile strength and modulus reached

maxima when medium shear was applied. However, the elongation at yield reached the highest point when high shear rates were applied. This may be caused by the extent of exfoliation in the final nanocomposites [150].

The tensile properties of clay/polymer nanocomposites depend on the molecular weight of the original polymer. A higher molecular weight polymer often results in better improvement in tensile properties. The effect of the molecular weight of PA 6 on the tensile properties of the PA 6 based nanocomposites with different clay contents has been examined by Fornes et al [142]. Three PA 6's were chosen to represent low, medium and high molecular weight grades, their molecular weights $\overline{M}_n$ being 16400, 22000 and 29300 respectively. The addition of an organoclay (0-7.2 wt%) led to significant improvement in tensile strength and modulus of the nanocomposites for all three PA 6's. At any given clay content, the tensile moduli increased with the increase of the molecular weight although the tensile moduli of all the pure PA 6's were similar. Similar trends were observed in tensile strength. The high and medium molecular weight PA 6 based materials showed a steady increase in strength as the clay content increased, while the effect on the low molecular weight PA 6 composites was less significant. The elongation at yield of the high and medium molecular weight PA 6 based nanocomposites maintained reasonable levels of ductility at clay contents as high as 3.5 wt%, but the elongation at yield for low molecular weight polymer system decreased rapidly at very low clay contents.

The results on the tensile properties of polymer/clay nanocomposites suggest that the mechanical performance of nanocomposites is associated with the degree of exfoliation of the clay in the polymer matrix. A strong interaction between the polymer and clay layers optimises the number of available reinforcing elements for carrying an applied load and deflecting cracks. Clay layers behave in a similar way to chopped fibres in fibre-reinforced polymer composites. The coupling between the large surface area of the clay particles and the polymer matrix facilitates stress transfer to the reinforcement phase. Several explanations have been proposed for the reinforcement properties of polymer/clay nanocomposites based on interfacial properties and restricted mobility of the polymer chains. Shi et al. proposed interfacial effects where the direct binding (adsorption) of a polymer to clay layers would be the dominant factor [188]. Shia et al developed an interface model to predict the Young's modulus of elastomer/clay nanocomposites [189]. Usuki et al.

suggested that the strong ionic interaction between PA 6 and clay layers could generate some crystallinity at the interface, which may explain part of the reinforcement effect [190]. Another explanation related to interactions between the clay and the polymer at the interface is the formation of a constrained region in the vicinity of the clay layers. Kojima et al. proposed that the improvement of tensile modulus in a PA 6/clay nanocomposite could be accounted for by a constrained region where the polymer chains have a restricted mobility [1].

2.6.1.2 Compression

Limited improvements have been reported on the compressive behaviour for polymer/clay nanocomposites.

The behaviour of epoxy/clay nanocomposites in compression was studied by Massam et al. [191]. The compressive yield strength and the modulus of elasticity were increased by 17% and 27%, respectively, with a 10 wt% clay loading. Total exfoliation of the clay in the nanocomposite was required to obtain these improvements. The compression behaviour of the nanocomposites was directly affected by the interfacial interactions, platelet aspect ratios, layer charge densities and the factors previously mentioned that influence the interaction between the clay layers and polymer matrix [192].

Kornmann et al [193] found that the exfoliation of the clay was not that important for the improvement of compressive strength. Compression experiments on both nanocomposites and conventional composites were carried out based on a similar epoxy system to that used by used Massam et al [191]. The same improvement of the compressive strength was obtained for exfoliated nanocomposites, but the compressive strength of exfoliated nanocomposites was only 5% better than those of the conventional composite.

Adam et al demonstrated that the intercalated epoxy/clay nanocomposites did not show any measurable difference in either overall strength or compressive modulus [194].

Recently, Masenelli-Varlot et al [195] analysed PA 6 based nanocomposites in three deformation directions using a compression test. The samples were produced by melt synthesis followed by injection moulding. The reinforcement depended on the orientation of the montmorillonite layers in the polymer matrix. Compression

modulus and stress were increased by 70% and 66%, respectively in the orientated direction of the clay layers for an exfoliated PA 6 based nanocomposites with 6.5 wt% clay content, i.e. the best reinforcement was obtained along a direction parallel to the injection axis when compressing the nanocomposites.

2.6.1.3 Flexural properties

Significant improvements in flexural strengths and moduli of polymer/clay nanocomposites have also been reported. The improvements are dependent on various factors including clay type, clay loading and the manufacturing method of the nanocomposites [1, 165, 196-199]. The improvement of the flexural properties was first reported in PA 6 based nanocomposite produced by in-situ polymerisation. A nanocomposite with a clay content of 4.7 wt% showed 60% improvement in flexural strength and 124% in flexural modulus at 23 °C [1].

The effects of clay type and content on the flexural properties of PA 6 based nanocomposites containing 0-8 wt% clay loadings were studied by Ma et al [197]. A hydrophilic clay and three organoclays were used. Organoclay1, 2 and 3 were n-dodecylamine modified montmorillonite, 12-aminolauric acid modified montmorillonite and 1,12-diaminododecane modified montmorillonite, respectively. Both flexural strength and modulus were improved significantly with the addition of the clays. The improvement of the flexural properties was higher for the polymer/organoclay systems compared to the polymer/hydrophilic clay system. When a small amount of clay (0.99 wt%) was added, the flexural strength increased 40% for the polymer/hydrophilic clay system and 77% for the polymer/organoclay2 system. The flexural modulus increased 18% for the polymer/hydrophilic clay system and 68% for the polymer/organoclay2 system. In the case of organoclays, different clay modifiers affected the improvement of the flexural properties in nanocomposites. In these PA 6 based nanocomposites, 12-aminolauric acid and n-dodecylamine modified clays were more effective in increasing the flexural properties than 1,12-diaminododecane modified clay. The effect of clay type on the flexural modulus was more significant than on the flexural strength. The higher the clay content the higher the flexural strength and modulus. The increasing rate of the flexural strength was much higher at low clay content (<1 wt%) than at high clay

content (>2 wt%) while the increasing rate of the flexural modulus was not affected as much as that of flexural strength.

Limited studies are reported on the effect of synthetic methods on the flexural properties. It is too early to say that one method is better than the other to achieve the improvement in flexural properties. For example, in the case of PA 6/organoclay nanocomposite with 4.7 wt% clay content produced by solution synthesis [197], the flexural strength increased 93% which was better than that achieved in the material from in-situ polymerisation while the flexural modulus increased 107% which was lower than that achieved in the material from in-situ polymerisation [1]. Compared to the tensile properties, the flexural properties of polymer/clay nanocomposites were not much affected by the mixing method in melt synthesis.

2.6.1.4 Impact Resistance

Impact properties have been measured in a wide range of polymer/clay nanocomposites [1, 149, 170, 176, 197, 200-203]. Some of the studies showed a slight decrease in the impact strength, while others demonstrated a significant increase in the impact strength. For instance, in the case of a PA 6 based nanocomposite with 4.7 wt% clay content [1], the Izod impact strength was reduced by 16%, from 20.6 J/m to 18.1 J/m. The Charpy impact strength was decreased by 2.4%, from 6.21 kJ/m^2 to 6.06 kJ/m^2, compared to that of pure PA 6. However, in another PA 6 based nanocomposite system with 4.7 wt% clay content, the Izod impact strength was increased by 50% compared with that of the pure PA 6. The Izod impact strength increased to 114% when the clay content was 1 wt% [197].

The Izod impact strength is considerably affected by the impact testing temperature. The Izod impact strength for PA 6 based nanocomposites with 5 wt% clay content was examined at different temperatures. A PA 6/organoclay system, a PA 6/hydrophilic clay system and pure PA 6 were tested. At room temperature (25 °C), the impact properties of both the nanocomposites and PA 6 were similar. At high temperatures, the Izod impact strength of pure PA 6 was higher than those of the nanocomposites. When the temperature was over 78 °C, the PA 6/organoclay nanocomposites had higher Izod impact strength than both the pure PA 6 and the PA 6/hydrophilic clay nanocomposites [149].

The effect of the clay content on the impact properties was also studied. Most of the polymer/clay nanocomposites showed that the impact strength improved significantly at low clay contents, then decreased as the clay content increased. Some other nanocomposites showed that the impact strength either increased with the clay content or was hardly affected. The Izod impact strength increased significantly at clay content below 1 wt% and decreased with further increase of the clay content for three PA 6/organoclay systems. However, for PA 6/hydrophilic clay system, the Izod impact strength increased with the clay content [197]. The Izod impact strength of polypropylene/clay nanocomposites produced using maleic anhydride grafted polypropylene (PP-MA) and organoclay Cloisite 20A were hardly affected by clay content when the molecular weight of the PP-MA was 9,000 and 52,000. However, when PP-MA with a molecular weight of 330,000 was used, these polypropylene based nanocomposites showed that the Izod impact strength improved significantly at the clay content below 7 wt%, then decreased as the clay content increased [170].

The effect of the clay type on the impact properties was demonstrated in PA 6/clay systems [197]. The Izod impact strength of the PA 6/organoclay systems can be better or worse than the PA 6/hydrophilic clay system depending on the type of the organoclays used and qualities of the nanocomposites formed. This reflected the general trend of the effect of clay type on the impact properties as demonstrated in other papers [149, 200].

The impact properties have been measured for PA 6/clay nanocomposites prepared by in-situ polymerisation, solution synthesis and melt synthesis. Figure 2-12 summarises the percentage increase/reduction in the Izod impact strength of some PA 6/clay nanocomposites with ~5 wt% clay content produced by different synthetic methods, using the Izod impact strength of their corresponding original PA 6 as a comparison [1, 149, 176, 197]. It can be observed that the nanocomposites produced by in-situ polymerisation have lower impact strength than the nanocomposites produced by other synthetic routes. In melt synthesis, the improvement depends on the clay and the processing conditions used. For example, the impact strength of the PA 6/hydrophilic clay nanocomposite was better than that of the PA 6/organic ammonium salt modified clay nanocomposites; but it was worse than that of the PA 6/epoxy modified organoclay nanocomposites.

Processing conditions have significant effect on the impact strength. For example, PA 6 based nanocomposites produced by melt synthesis using a twin screw extruder had improved impact strengths while the materials using a single screw extruder had reduced impact strengths [149]. A second pass of the polymer/clay mixture through the extruder enhanced the improvement of impact strength when a twin screw extruder was used, but was more detrimental to the impact strength when a single screw extruder was used. Changing the screw speed of the twin-screw extruder had no clear effect on the impact strength of nanocomposites.

The molecular weight of the polymer also affected the impact properties of the resultant nanocomposites. The Izod impact strength for PA 6 based nanocomposites with different molecular weight in PA but the same clay loading have been studied [142]. A better impact strength was obtained using a higher molecular weight polymer. However, the Izod impact strength was relatively independent of clay content for the high and medium molecular weight polymer based nanocomposites up to 7 wt% clay content and gradually decreased with clay content for the low molecular weight polymer based nanocomposites.

The investigations have shown that significant improvement of mechanical properties can be obtained using polymer/clay nanocomposites compared to the base polymers. This has widened the use of polymers in industrial applications. In the automotive industry, General Motors and partners have used a thermoplastic olefin based nanocomposite to produce step-assist platforms for the 2002 GMC and Chevrolet vans [260]. There is also potential for utilisation of nanocomposites as door handles, engine covers and other parts of vehicles [257]. High performance polymer/clay nanocomposite adhesives and paints are also used in electronic, computer and other industrial applications [257-259]. Nanocomposites are currently being considered for the application for impellers and blades for vacuum cleaners, power tool covers and mower hoods [231].

2.6.2 Barrier properties

The improvement of barrier properties for polymers can widen their applications. The permeability of polymers to solvents, including water and gas is important. Polymer/clay nanocomposites have been found to have improved barrier properties.

2.6.2.1 Water Permeability

Water permeability of polymer/clay nanocomposites has been found to be substantially decreased compared to their base polymers. PA 6 [2], PA 1012 [77], poly(ε-capolactone) [204], PVA [205], poly(*o*-ethoxyaniline) [206], polyimide [137, 207-210], polyurethane [211], polyesterarnide [212] and vinyl ester resin [213-214] have been investigated. Their nanocomposites have lower water permeability than the original polymers.

The permeability is the product of the diffusion coefficient and the solubility coefficient:

Permeability = $D \times S$

where D is the diffusion coefficient and S is the solubility coefficient [215]. The experiment for obtaining water permeability is normally carried out by soaking a dried polymer or nanocomposite in deionised water for a fixed time, followed by drying the sample quickly between sheets of paper to remove the excess water to obtain the initial and the final weights of the sample. [2]

There are three ways to present the water permeability based on this experiment. A sorption curve – the amount of water absorbed in the sample M_t as a function of a square root of the soaking time divided by the thickness of the sample $\sqrt{t}/\Delta x$ can be plotted. [2]

The amount of water absorbed per 100 g polymer under certain conditions can be calculated from the increase in the weight of the sample. The final method is the percentage increase in the weight of the samples before and after being soaked in water using the following formula.

Water permeability (%) $W = (W_1-W_0)/W_0 \times 100$

where W_1 is the weight after soaking in water. W_0 is the initial weight of the sample before soaking.

Toyota researchers used the water sorption curve and the amount of water absorbed per 100 g polymer to assess the resistance to water permeation for PA 6/clay nanocomposites with 4.7 wt% clay content. The water absorption of nanocomposites was reduced compared to the pure polymer. However, the water absorption was increased with the increase in the soaking time. At a particular $SoakingTime/SampleThickness$, the water absorption was reduced by approximately half in the composite compared to the base polymer. In the case of PA 1012 based nanocomposites, water permeability (%) was used to characterise the water absorption, the water permeability was reduced by 45% for composites with 5 wt% clay content [77].

The resistance to water permeation is affected by clay content, clay type and manufacturing method.

The resistance to water permeation increased with the increase in clay content for most of the polymer/clay nanocomposites investigated so far. For example, the water absorption of PA 1012/clay nanocomposites decreased as the clay content increased [77].

The resistance to water permeation of polymer/clay nanocomposites is affected by the surface properties of clays. Generally a polymer/organoclay system improves the resistance to water permeation more than a polymer/hydrophilic clay system. For example, in Gu's work [208] on polyimide/clay polymer composites, the polyimide/organoclay nanocomposite has better resistance to water permeation than the polyimide/hydrophilic clay nanocomposite.

The effect of organoclays with different aspect ratios on water permeability of both partially and totally exfoliated poly(imide) (PI)-based nanocomposites has been investigated [207]. The results showed that as the aspect ratio of clays increased, the relative water permeability decreased drastically. Better barrier properties could be obtained in nanocomposites by using either hydrophilic clays or organoclays with a high aspect ratio.

The water resistance of the polymer/clay nanocomposites is affected more by the clay content when clays with high aspect ratios are used. For example, in PA 6/clay nanocomposites, the water absorption of the PA 6/montmorillonite nanocomposites

reduced much faster than that of the PA 6/saponite nanocomposites when the clay content increased [2].

The effect of manufacturing methods of the nanocomposites on the resistance to water permeation was also studied. For instance, with the same organoclay loading, PI based nanocomposites prepared by the solution synthesis have lower water absorption than those by the in-situ polymerisation [208].

2.6.2.2 Water Vapour, Solvent Vapour Permeability

In addition to liquid water, polymer/clay nanocomposites have reduced the permeability to water and solvent vapours [76, 140, 215-216].

The vapour transmission rate is defined as the mass of vapour transmitted through a unit area in a unit time under specified conditions of temperature and humidity. The test is normally carried out in controlled environments. Dry films are sealed to the open mouths of test bottles containing a desiccant and placed in a chamber controlled at specified relative humidity. Periodic weighing of the assembly allows the vapour transmission rate to be determined. The permeability P is calculated from the vapour transmission rate. The permeability of the polymer composites can also be expressed as relative permeability value, i.e. P_c/P_p, where P_c and P_p stand for the composite and the unfilled polymer permeability, respectively.

The clay content played an important part in reducing the permeability of water vapour and solvent vapour for polymer/clay nanocomposites. Different ways for representing permeability will be used in the following discussions.

The permeability to water and dichloromethane vapours of a poly(ε-caprolactone) based nanocomposite showed a strong dependence on clay content [215]. The permeability was calculated from the vapour transmission rate. Both water vapour and dichloromethane vapour permeability reduced significantly with the increase of clay content, particularly above 5 wt%. Chang et al [140] also studied the effect of clay content on the permeability of water vapour in polyimide (PI) based nanocomposite films using the relative permeability parameter P_c/P_p. There was an 82% reduction in the permeability for the PI/organoclay film with 4 wt% clay content, as compared to that of the PI film. Interestingly, the permeability of the composite was reduced by nearly an order of magnitude with only 8 wt % organoclay content in spite of the aggregation of clay particles in the polymer matrix.

The significant reduction of the permeability to water and solvent vapour is not only due to the formation of nanostructure in the polymer/clay system, but may also be related to the clay particle size.

2.6.2.3 Gas Permeability

Polymer/clay nanocomposites have lower gas permabilities than their base polymers. PA 6 [217], PP [40], polyaniline [218], acrylonitrile-butadiene copolymer [161], polyimide [219-220], poly(dimethylsiloxane) [221], ethylene-propylene-diene rubber [222] and cross-linked polyester [223] based nanocomposites exhibit a decrease in gas permeability.

Gas permeability is normally expressed as the actual amount of gas permeated through the unit area or as the relative permeability values such as P_c/P_p, where P_c and P_p stand for the composite and the unfilled polymer permeability, respectively.

The permeability of carbon dioxide (CO_2) for partially exfoliated polyimide based nanocomposites films has been studied [219-220]. The relative permeability values, P_c/P_p, have been reduced by more than five fold for low clay content in nanocomposites compared to the pure PI.

The clay content also played an important role in reducing gas permeability of polymer/clay nanocomposites.

The polyaniline based nanocomposite film at low clay loading (e.g., 0.25 wt %) showed dramatic reduction of air, oxygen (O_2) and nitrogen (N_2) permeability compared to the base polyaniline. With the increase in clay content, the air, O_2 and N_2 permeability decreased. However, a further increase in clay content resulted in only a slightly further enhanced gas barrier property of the nanocomposite materials when the clay content was over 0.25 wt%. [218]

A PA 6 based nanocomposite produced by in-situ polymerisation exhibited a four-fold improvement in oxygen barrier resistance and a three-fold improvement in carbon dioxide barrier resistance relative to PA 6 [217]. The gas permeability has significantly improved compared to current commercial packaging grades of PA 6. These enhancements open new opportunities for PAs in packaging applications such as high barrier multi-layer polyethylene terephthalate bottles for oxygen sensitive products.

Bayer has already commercialised a new grade of plastic films for food packaging, Durethan LPDU 601, based on PA 6 exfoliated nanocomposites which have improved gas barrier properties. In this case, the oxygen transmission rate has been reduced by half compared with the base PA 6. These new materials also have improved tensile modulus [224].

InMat LLC developed an aqueous, non-hazardous, rubber/clay nanocomposite coating under the trade name AIR D-FENSE(TM), which is commercially used in the sporting goods industry. The nanocomposite structure of the coating formulation provides a unique combination of barrier properties and flexibility. Using butyl rubber as the matrix, and a very high aspect ratio vermiculite filler, flexible coatings with gas permeability 30 to 50 times lower than butyl rubber have been produced. The coating products have been shown to be undamaged by significant strain. It has additional applications in any pneumatic rubber product, since one can get the barrier properties of 1 mm thick butyl rubber sheet in a thin (20-30 micron) coating. The largest target market is in automobile and truck tires, which currently use over $1 billion of butyl rubber to maintain a constant air pressure. [225]

2.6.2.4 Solvent resistance

The better barrier properties of polymer/clay nanocomposites contribute to solvent resistance. It was reported that epoxy/clay nanocomposites offered a better resistance to organic solvents including alcohols, toluene and chloroform [226].

A similar reduction in cyclohexane uptake was observed for cross-linked poly(dimethylsiloxane)/clay nanocomposite with 5 wt% clay content. However, the enhancement went far beyond simply limiting the uptake of solvent. The formation of the nanocomposites dramatically reduced the structural damage that normally occurs by the internal strain generated by the evaporation of solvent in a solvent saturated elastomer [221].

Other polymer systems reported include PA 6 [227], polycaprolactone [228], high-density polyethylene (HDPE) [229], polysiloxane [230] and nitrile rubber [15]. For example, nanocomposites based on HDPE were studied for potential fuel storage and automotive applications by Kenig et al [229]. The solvent resistance of containers produced from HDPE, co-extruded HDPE/PA 6 (92/8) composite, co-extruded HDPE/ethylene-vinyl alcohol (94/6) composite and HDPE/organoclay

nanocomposite was evaluated using xylene and 'Fuel C'. The nanocomposite containers with less than 5 wt% clay content showed a significantly lower level of permeation of both solvents compared to the pure HDPE container. The co-extruded polymer containers also demonstrated an improved barrier resistance to xylene compared to the pure HDPE container.

Other studies related to high barrier bottles, containers, sheets and films based on polyolefin resins are in progress [231].

The reasons for this improved permeability and solvent resistance have been explained in several ways. Most of the researchers suggested that when the clay layers were dispersed in a polymer, the impermeable clay layers form a tortuous pathway for mass transport of diffusates as shown in Figure 2-13 [14]. The enhanced barrier properties, including low water, water vapour, solvent vapour and gas permeability and high solvent resistance of polymer/clay nanocomposites are due to these hindered diffusion pathways through the nanocomposite.

2.6.3 Thermal stability

The thermal properties of a material are the properties measured as the sample is heated through a predetermined temperature profile. The most common techniques used in thermal stability analysis are thermogravimetric analysis (TGA) and differential scanning calorimetry (DSC). The thermal stability is significantly improved by the formation of polymer/clay nanocomposites. It has been suggested that the nanostructure formation is critical to improving thermal stability [3].

Blumstein [9] first reported an improvement of thermal stability in poly(methyl methacrylate) (PMMA)/clay intercalated nanocomposites. The nanocomposite was prepared by free radical polymerisation of methyl methacrylate intercalated with 10 wt% montmorillonite. This intercalated nanocomposite did not degrade under conditions which PMMA would degrade completely. TGA results showed that the composite had 40 °C to 50 °C higher decomposition temperature than that of the base polymer. Blumstein also proposed that the enhancement of thermal stability of the PMMA/clay nanocomposites was due to the difference in material structure and restricted thermal motion of the polymer chains between clay layers.

Huang and Brittain reported a 5 ° - 15 °C increases in glass transition temperature, T_g, and up to 60 °C increases in decomposition temperatures in both intercalated and exfoliated PMMA/organoclay nanocomposites compared to a conventional composite [87]. Similar results were also observed by Hwu and co-workers [135].

In the case of PA 6 based nanocomposites, it was reported that heat distortion temperature (HDT) of PA 6/clay nanocomposites produced by in-situ polymerisation was increased from 65 °C to approximately 160 °C depending on the formulations of the nanocomposites. [1, 17, 20]

The effect of clay type on the thermal stability of polymer/clay nanocomposites was studied. Many results showed that the thermal stability is not affected by clay type, but the organic cations inserted between the clay layers. Gilman et al [3] observed that there were no differences in thermal stability of aliphatic polyimide based nanocomposites using clays with different aspect ratios and CECs. However, when Zhu et al [232] studied the thermal stability of PMMA based nanocomposites using three different organoclays, they found the onset of degradation and the degradation process did depend on the type of the organoclays used. When the pure PMMA was compared with the three PMMA/organoclay nanocomposites, they found that one of the nanocomposites decomposed in two stages while the pure PMMA and the other two nanocomposites decomposed in three stages. There was 6% char formed in the first nanocomposite but no char from the pure PMMA. The results showed that the first nanocomposite had significantly enhanced thermal stability. It was proposed that the lack of initial stage degradation in that nanocomposite was due to the presence of weak links in the polymer chain [233]. The other two stages of the degradation were similar to the two stages that occurred in the degradation of the other two PMMA/organoclay nanocomposites. These two stages of the degradation were due to the confinement of intercalated PMMA chains within the clay interlayers which prevent the segmental motions of the polymer [234].

Clay content plays an important role in the thermal stability of polymer/clay nanocomposites. In general, the thermal stability is improved as clay content increases [80-81, 85, 235]. For example, in the case of PS based nanocomposites using VB16 and two other organoclays, N,N-Dimethyl-n-hexadecyl-(4-hydroxymethylbenzyl) ammonium chloride (OH-16) and phosphonium-Modified Clay (P-16), the onset temperatures of the degradation were found to be about 50°C

higher for the nanocomposites than for the base PS. The thermal stability was further improved with the increase in clay content for all three nanocomposites. However, according to the TGA curve for PS/P-16 nanocomposite, there was a second step (~30% of the degradation) in the degradation, which was absent in the other two materials. The authors explained that this was attributed to interactions between the clay and the polymer that served to stabilise the nanocomposite [81].

The thermal stability was studied for the polymer/clay nanocomposites produced by various synthetic methods. At present, it is not clear which method is better in improving thermal stability because different research groups used different raw materials. In the case of PS based nanocomposites produced using in-situ polymerisation and solution synthesis [85, 235], it was found that both nanocomposites had improved thermal stability. In this particular case, the materials produced from in-situ polymerisation had better thermal stability than those from solution synthesis.

The experimental conditions for thermal analysis could also influence the mechanism of degradation. For example, when heating ethylene vinyl acetate copolymer (EVA)/organoclay nanocomposite under helium and air flow, the nanocomposite only had a slight reduction in thermal stability (4 ^{o}C) under helium while a considerable increase (more than 40 ^{o}C) at the maximum DTG peaks occurred when heating in air. This might be associated with the char formation under oxidative degradation in air, the char acting as a physical barrier for heat transfer [236].

The TGA data also showed that an intercalated nanocomposite was more thermally stable than an exfoliated nanocomposite. Lee et al found that an intercalated poly(etherimide)/clay nanocomposite was more stable than an exfoliated poly(etherimide)/clay nanocomposite [237].

The improved thermal stability has also been reported in other polymer based nanocomposites. These polymers include PA 6 [196], PCL [238], PP [95], PI [140], Polydimethyl-siloxane(PDMS) [239], epoxy precursors [104], SAN [86], PEO[128], polyaniline [240], poly(*o*-ethoxyaniline) [206], polybenzoxazine [241], polybenzoxazole [242], cross-linked polyester [223] and poly(ethyl acrylate) [243]. In every case, an increase in the onset temperature of decomposition was observed.

The reasons for these effects on T_g and decomposition temperature are not clear. Several factors are mentioned for the significant improvement in thermal stability of polymer/clay nanocomposites. The first one is similar to that proposed by Blumstein, that is the difference in material structure and restricted thermal motion of polymer chains between the clay layers [87, 244-245]. The second factor is the strong interaction between the clay layers and polymer molecules which stabilise the nanocomposites [81]. The third one is the chemical nature of the base polymer and its degradation mechanism [239].

In summary, the improved thermal stability of nanocomposites can result from the superior thermal stability of the clay layers and the hindered diffusion of volatile decomposed gases in the composites. The improved thermal stability of nanocomposites can also result from the different base polymer structures and the restricted thermal motion of the polymer in the clay layers.

2.6.4 Flame retardancy

Early work on flame retardancy of polymer/clay composites appeared in a 1976 patent by Unitika on PA 6/clay composites [11]. Only recently the flame retardant properties of polymer/clay nanocomposites have been reviewed in detail [3]. Extensive investigations have been conducted using cone calorimetry. In a typical cone calorimetry experiment, a sample is exposed to a given heat flux. Parameters such as heat release rate (HRR), mass loss rate, smoke density and the time for ignition have been measured during the combustion of a sample. Additionally the composition of exhaust gas can be also measured. It is worth noting that reduction of the peak HRR, char formation and self-extinguishing phenomenon are the most straightforward evidence of the efficiency of a flame retardant material.

Polymer/clay nanocomposites exhibit very low flammability. The data of cone calorimetry for a variety of polymer/clay nanocomposites showed that the formation of a nanocomposite is effective in reducing the peak heat release rate. The polymer systems studied using cone calorimetry so far cover both thermoplastic polymers such as PA 6 [246-247], PS [80, 247], PP-g-MA [247], PMMA [232], poly(methylmethacrylate-co-dodecylmethacrylate) [248] EVA [236] and thermoset polymers such as vinyl esters and epoxies [249]. An exfoliated PA 6/clay

nanocomposite with 4.7 wt% montmorillonite had 63% reduction in the peak heat release rate, 50% decrease in the mean heat release rate, 50% increase in specific extinction area (SEA), without any increase in soot and carbon monoxide levels evolved during combustion compared to the pure PA 6 [247]. Similar behaviour was observed for all the polymer systems studied.

The effect of the nanostructure on the flame retardancy of polymer/clay nanocomposites is still under investigation. So far, there is no apparent difference between exfoliated, intercalated, or mixed intercalated-exfoliated nanocomposites as far as the flame retardant mechanism is concerned [154]. However, Wilkie reported that a PS based nanocomposite, PS/OH-16(N,N-Dimethyl-n-hexadecyl-(4-hydroxymethylbenzyl) ammonium chloride modified clay) nanocomposite, which contained mostly intercalated structure, gave a slightly larger reduction in the rate of heat release than did the other two PS/organoclay systems, which contained a significant exfoliated fraction [81]. Gilman et al [250], however, pointed out that possibly only exfoliated nanocomposites have reduced flammability. His conclusion was based on the flammability studies of different PS based nanocomposites.

It is notable that the clay content affected the flame retardancy. The flame retardancy normally increased with the clay content, e.g. the peak heat release rate reduced as the amount of clay increased. However, the situation can be very different at very low clay content. For example, in the improvement of flame retardancy in PS based nanocomposites with clay loading from 0.1 % to 10 %, both peak heat release rate and mass loss rate were affected by clay content. It appears that both parameters decreased as clay content increased. It was observed that the nanocomposites with as little as 0.1 wt% clay could reduce the peak heat release rate by about 40%. At low contents (< 1 wt% in this case), there was no clear relationship between the clay content and the heat release rate. At relatively high clay contents, the heat release rate decreased as the clay content increased. However, compared to the change of the peak heat release rate and the mass loss rate, other parameters were not affected as much by clay content in nanocomposites [80].

The effect of the clay type on the flame retardancy of polymer/clay nanocomposites was studied, but there is no general tendency observed at present. In a typical example, an intercalated PS/modified fluorohectorite nanocomposite had its peak heat release rate unchanged, whereas its counterpart – a PS/modified

montmorillonite nanocomposite had a 60% lower peak heat release rate compared to the pure PS or a PS mixed with Na^+ based montmorillonite (immiscible). Gilman et al mentioned that the result for the PS/modified fluorohectorite nanocomposite was possibly due to larger clay aspect ratio [250]. However, in the case of aliphatic polyetherimide based nanocomposites, the flame retardancy for nanocomposites produced from both fluorohectorite and montmorillonite were significantly improved compared to the base polymer [237].

The effect of the clay modifiers on the flame retardancy of nanocomposites has also been studied [80-81, 232]. The flame retardancy of PS with phosphonium-modified clay or ammonium-modified clay nanocomposites has been measured using cone calorimetry. Compared to pure PS, the peak heat release rate of the nanocomposites was reduced by 27-58%, depending on clay content. Studies on PS and PS based nanocomposites have also shown that an intercalated material is more effective than an exfoliated material in fire retardancy. Associated with the decrease in the heat release rate, there was a decrease in ignition time, the time to burn out, mass loss and specific extinction area (SEA) [81].

Zhu et al mentioned that the amount of organic ammonium ions between clay layers was not an important factor for the flame retardancy when the clay modification is based on the same hydrophilic clay. There was only a slight difference in the flame parameters obtained using cone calorimetry for three PS based nanocomposites with the clay being modified by the same ammonium salt with different concentrations - 140meq/100g, 125meq/100g and 95meq/100g [80].

In addition to the significant reduction in the peak heat release rate, nanocomposites could promote char formation [193, 228, 237, 249]. Kornmann [193] showed that the original geometry of the epoxy-clay nanocomposites samples was retained 2 hours after ignition at 1000°C. In another investigation on a polyetherimide based nanocomposite system, both intercalated and exfoliated nanocomposites had a high char yield and maintained their original dimensions [237].

General views on the mechanism for the improved flame retardancy of the nanocomposites were proposed. It is possible that the nanocomposite structure collapses during the combustion, but a high-performance carbonaceous clay char builds up on the surface during burning. The clay char may act as an excellent

insulator and mass transport barrier to the underlying material and slow the mass loss rate of decomposition products [3, 249-250]. However, further studies are needed for the verification of this proposed mechanism.

2.6.5 Optical properties

One of the attractive prospects of nanoscale dispersion of clay layers in a polymer is that the optical properties of the polymer can be maintained or only slightly reduced. Several investigations have shown that good clarity can be achieved in both thermoplastic and thermoset polymer based nanocomposites [40, 76, 140, 206, 223, 251-253]. In the case of thin films of PP/semi-fluorinated organoclay systems and thick films of PP-g-MA/organoclay systems [40], the UV/vis transmittance as a function of wavelength was measured. There was no marked decrease in the clarity due to the introduction of clay (for clay contents up to 9 wt%). The materials developed a haze observable by the naked eye for 3mm-thick films of PP-g-MA with clay content more than 9 wt%. The slightly loss of intensity in the UV region (for $\lambda <$ 250 nm) was primarily due to scattering by the clay particles.

The effect of clay content on optical properties was studied using PMMA, polyimide, poly(*o*-ethoxyaniline), cross-linked polyester and epoxy [76, 103, 140, 206, 223, 252]. With an increase in clay content, the optical properties tended to decrease. For example, the light transmittance of the cross-linked polyester/clay nanocomposites with different clay contents showed a negligible decrease in transmittance at 1 wt% clay content to very significant at 20 wt% clay content. At 10 wt% clay content, there was ~30% loss in transmittance due to scattering and absorption of the light by the clay [223]. Polyimide/hexadecylamine–montmorillonite nanocomposite films, prepared by solvent-casting are light brown in colour but highly translucent [140]. The level of translucency was found not to be affected by the clay content between 0 and 4 wt%. However the film with 8 wt% clay was slightly darker.

The optical properties are affected by the nanostructure formed. Exfoliated nanocomposites have better optical properties than intercalated nanocomposites. In the case of epoxy resin/organoclay nanocomposites [103], an exfoliated

nanocomposite film, 5mm thick containing up to 20 wt% organoclay, was optically transparent. However, the intercalated nanocomposites were opaque with relatively low clay content. In the case of PMMA based nanocomposites, UV/vis transmission spectra of pure PMMA and PMMA/clay nanocomposites with 1 and 3 wt% clay contents were measured using film samples with a thickness of ~180 μm. The spectra of PMMA/clay nanocomposites with 1 wt % clay show that the visible region (400-700 nm) was only slightly affected by the presence of the clay and retained high transparency due to primarily exfoliated structure. However, the spectra of PMMA/clay nanocomposites with 3 wt % clay exhibited low transparency due to primarily intercalated structure. For the ultraviolet wavelength, there was strong scattering and/or absorption, resulting in very low transmission of the UV light [76].

As long as the clay particle size is smaller than the wavelength of the light, the materials may be transparent; therefore, the dispersion and orientation of the clay layers in the polymer matrix may govern the optical clarity of the nanocomposites. If complete exfoliation and homogeneous dispersion of the clay layers can be achieved, it is possible that the material with high clay content may exhibit high optical clarity. However, if the agglomeration of clay particles occurs in nanocomposites, the transparency will decrease as clay content increases.

The improvement of major engineering properties by polymer/clay nanocomposites over the base polymer can be achieved at relatively low clay contents. This will lead to the materials with only minor changes in optical properties.

2.7 The prospect of commercialisation of polymer/clay nanotechnology

The characterisation and properties of nanocomposites produced by in situ polymerisation, solution and melt methods show that for all three synthetic methods both intercalated and exfoliated structure can be formed and that their mechanical, barrier, thermal, flame retardant and optical properties are much better than those of their base polymers. However, the *solution method* is limited in applications as the right polymer/solvent pair and clay are required and cannot be easily carried out in

industry due to the problem related to consuming a large amount of solvent. The *melt method* is a promising method since the process can be carried out using conventional polymer processing equipment. However this method is hindered by being less effective in layer expansion and exfoliation compared to the *in-situ polymerisation* technique. The property improvements of the nanocomposites produced from the melt method at present are not as good as the improvement achieved by in situ polymerisation. In some cases, little improvement in mechanical properties was obtained by melt intercalation [187].

Polymer/clay nanocomposites have numerous commercial potential applications in storage, packaging, automotive, aerospace and defence industries, due to their cost effective advantages as they are lightweight, offer high reinforcement, improved barrier properties, fire retardancy and optical properties over their base polymers. Several commercialised nanocomposites are already used in automotive applications [257]. For example, a PA 6/clay nanocomposite has been used to make a timing-belt cover by Toyota Motor Company. This was the first practical example of polymer/clay nanocomposites for automotive applications. Currently, the replacement of metals and high performance engineering thermoplastics by lower cost polyolefin based nanocomposite is an active area of industrial and academic research. Applications of polymer/clay nanocomposites in other areas have also been studied. HDPE based nanocomposites have been developed to produce containers with high barrier properties for hydrocarbon fluids like: xylene and fuel for storage and automotive applications [229]. Other polyolefin based nanocomposites have also been studied for bottles, containers, sheets, films with high barrier properties and image-receiving layers for inkjet imaging media [229, 258-259].

Figures for Chapter 2

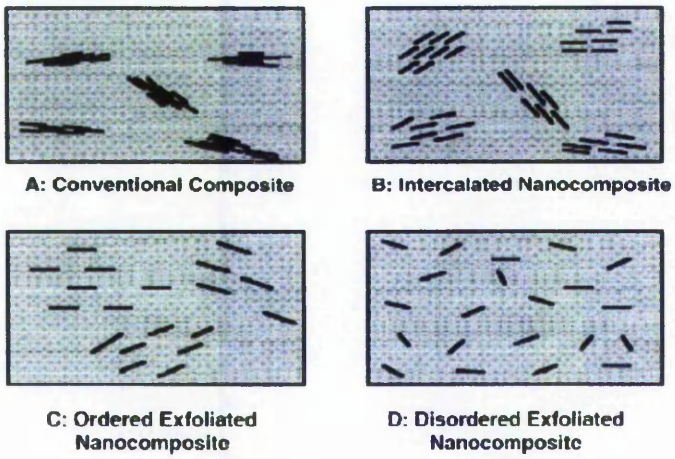

Figure 2-1 A schematic illustration of different types of structures in polymer/clay composites [4]

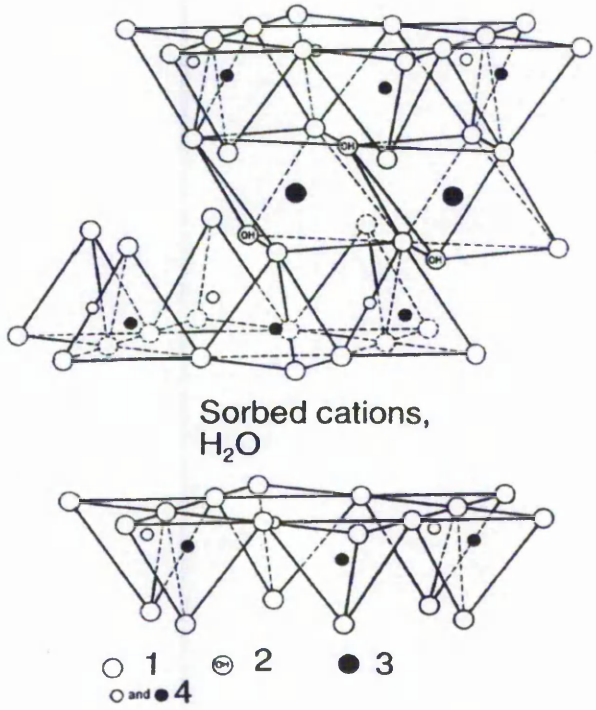

Figure 2-2 A typical structure of a layered clay (1- oxygen, 2- hydroxyl, 3- aluminium and magnesium, 4-silicon) [26]

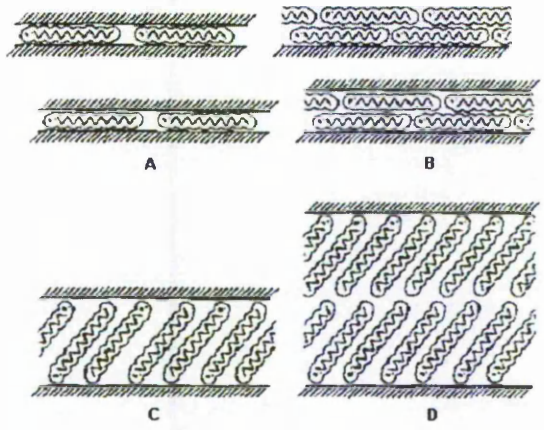

Figure 2-3 Conceptual arrangements of alkyl chain aggregations between two adjacent clay layers: A - lateral monolayer; B - lateral bilayer; C - paraffin-type monolayer; D - paraffin-type bilayer [27]

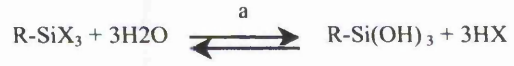

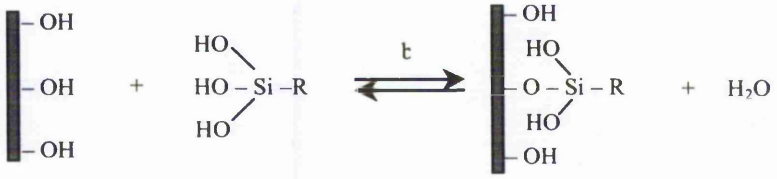

Figure 2-4 The hydrolysis of the silanes (a) and the possible reaction of a silanol group with a hydroxyl group present on an inorganic surface (b).

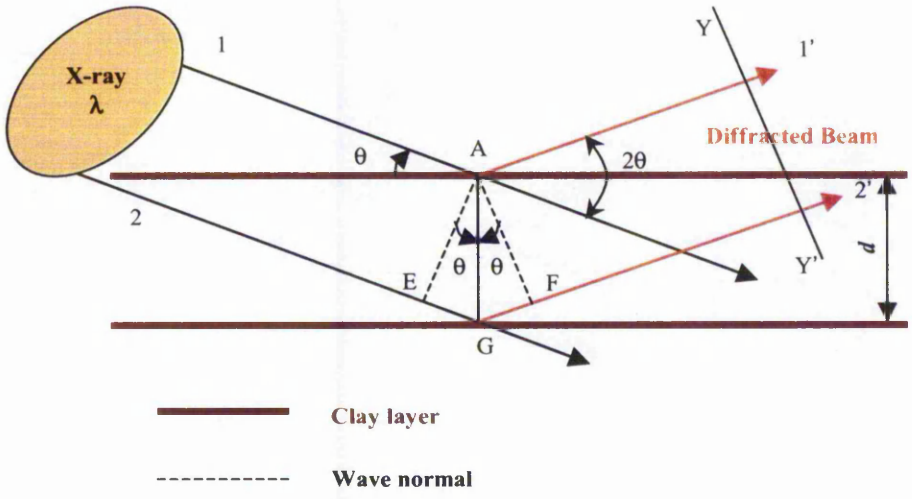

Figure 2-5 X-ray diffraction from two consecutive clay layers

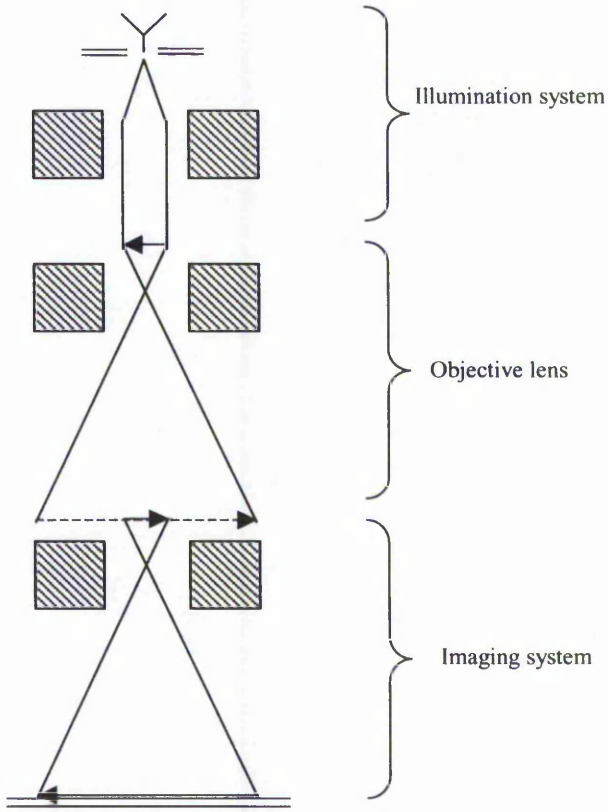

Figure 2-6 A schematic illustration of TEM image formation

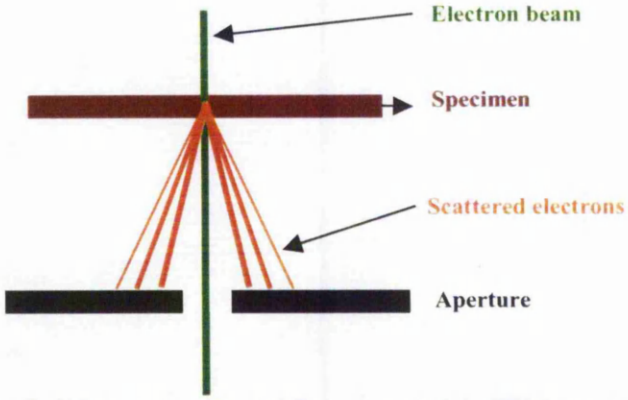

Figure 2-7 Schematic illustration of the bright field imaging method

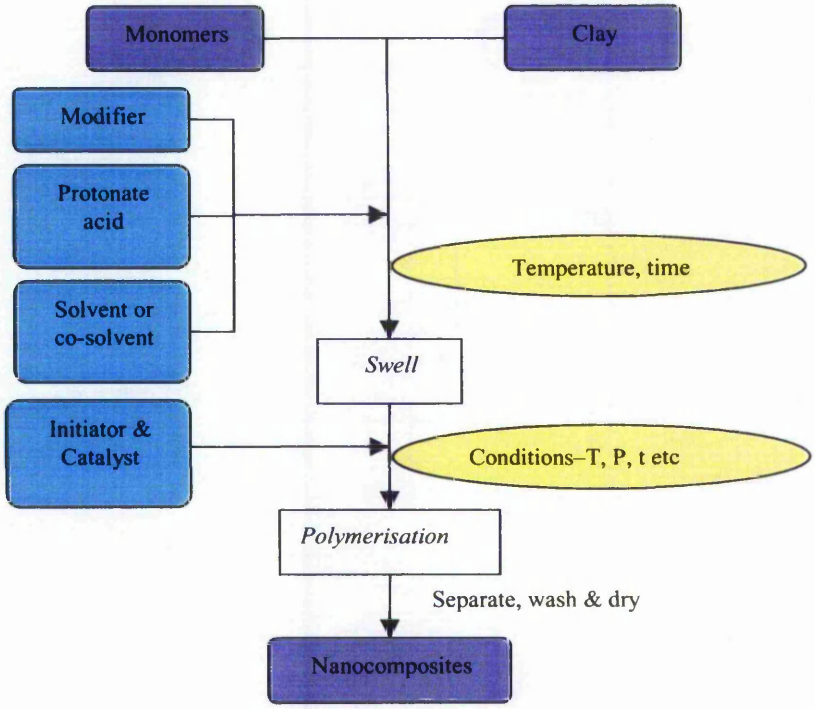

Figure 2-8 A schematic illustration of a typical process for using in-situ polymerisation to produce thermoplastic polymer based polymer/clay nanocomposites

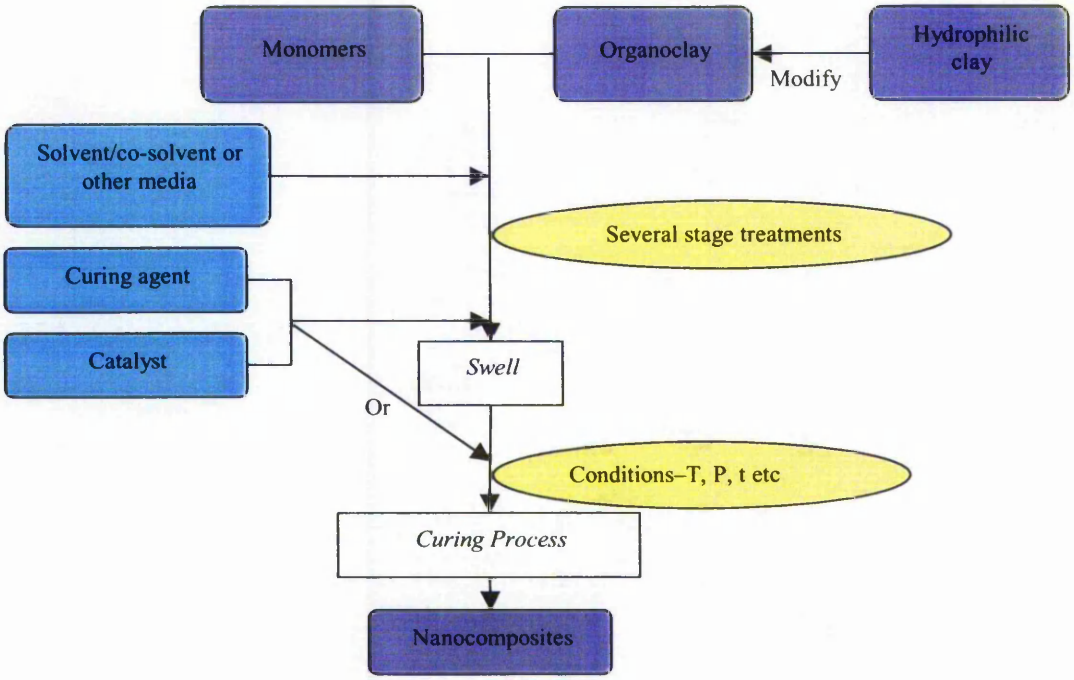

Figure 2-9 A schematic illustration of a typical process for using in-situ polymerisation to produce elastomeric or thermoset polymer based polymer/clay nanocomposites

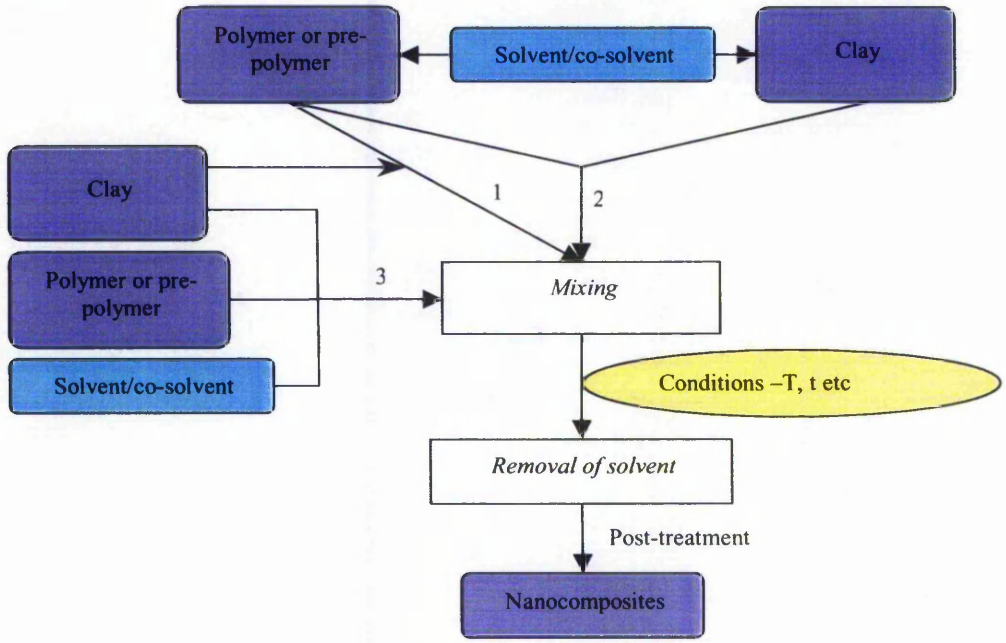

Figure 2-10 A schematic illustration of a typical process for using solution synthesis to produce polymer/clay nanocomposites

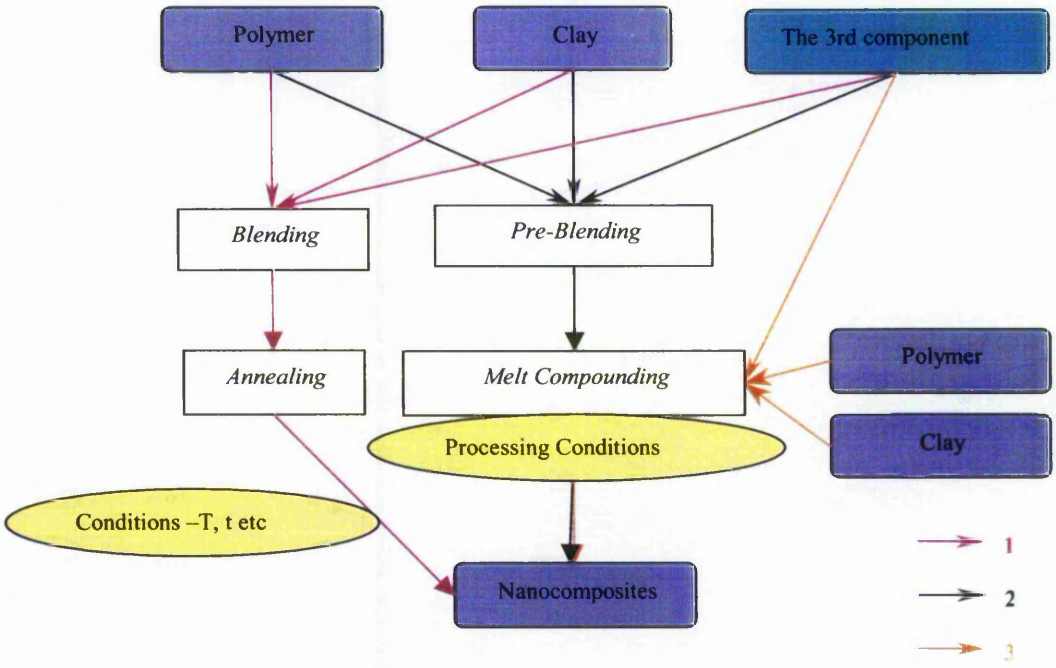

Figure 2-11 A schematic illustration of a typical process for using melt synthesis to produce polymer/clay nanocomposites

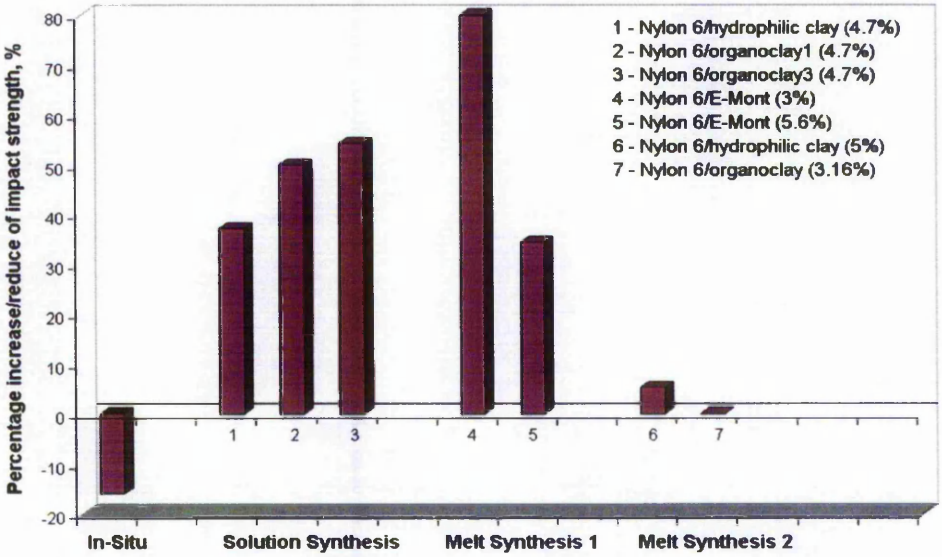

Figure 2-12 The percentage increase/reduction in the Izod impact strength of PA 6/clay nanocomposites with ~5 wt% clay content produced by using in-situ polymerisation [1], solution synthesis [197] and melt synthesis [176, 149] compared to that of the corresponding original PA 6

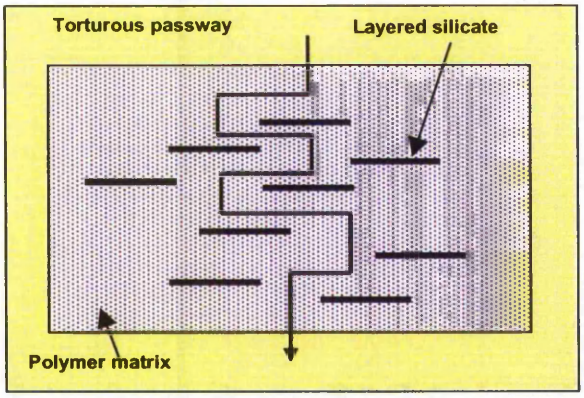

Figure 2-13 Proposed model for the torturous diffusion path in an exfoliated polymer-layered silicate nanocomposite when used as a gas barrier [14]

Tables for Chapter 2

Table 2-1 The classification and the nominal chemical formula of 2:1-layered silicates [27]

Mineral Group (Layer charge)	Subgroups	
	Dioctahedral	Trioctahedral
Pyrophyllite-Talc (x~0)	Pyrophyllite $Al_2Si_4O_{10}(OH)_2$	Talc $Mg_3Si_4O_{10}(OH)_2$
Smectite (0.2<x<0.6)	Montmorillonite $M_x^+(Al_{2-x}Mg_x)Si_4O_{10}(OH)_2$	Saponite $M_x^+Mg_3(Si_{4-x}Al_x)O_{10}(OH)_2$
	Beidellite $M_x^+Al_2(Si_{4-x}Al_x)\,O_{10}(OH)_2$	Hectorite $M_x^+(Mg_{3-x}Li_x)Si_4O_{10}(OH)_2$
Vermiculite (0.6<x<0.9)	Dioct. Vermiculites $(M_x{\bullet}nH_2O)^+Al_2(Si_{4-x}Al_x)\,O_{10}(OH)_2$	Trioct. Vermiculites $(M_x{\bullet}nH_2O)^+Mg_3(Si_{4-x}Al_x)O_{10}(OH)_2$
Mica (x~1)	Phlogopite, Biotite, Annite $K(Mg,Fe^{2+},Al^{3+})_3(Si_3Al^{3+})O_{10}(OH)_2$	Muscovite, Paragonite $(K,Na)(Al,Fe^{2+})(Mg,Fe^{2+})(Si_3Al)O_{10}(OH)_2$

x represents layer charge per formula unit; M^+ represents a univalent or equivalent compensating cation.

Table 2-2 Interlayer spacings of organo-montmorillonites (x-MMT) and PS-based nanocomposites together with the clay dispersibility within the polymerisation medium [72]

	Interlayer spacing, nm		
Clay	In clay	In PS/clay	Dispersibility[a]
Na+-montmorillonite	1.18	1.42	-
Bz-MMT	1.91	3.40	++
Eh-MMT	2.04	2.85	+
Ta-MMT	3.27	3.29	+

a: It was judged by the appearance of the montmorillonite dispersion in styrene monomer: (++) fully dispersible; (+)partly dispersible; (-) non-dispersible.

Table 2-3 Peak intensity (I_m) and interlayer spacing (d) of PA-6-based nanocomposites prepared in the presence of different acid derivatives by the one-pot technique [20]

Acid	Peak Intensity Im, cps	Interlayer spacing, nm
Phosphoric acid	0	0
Hydrochloric acid	200	2.17
Isophtalic acid	255	2.02
Benzenesulfonic acid	280	1.93
Acetic acid	555	2.03
Trichloroacetic acid	585	2.13
No acid	1840	1.86

Chapter 3 EXPERIMENTAL METHODS

3.1 Materials studied

3.1.1 Clays

Seven commercial clays and two polymers were used for polymer/clay nanocomposite synthesis. The clays used in this study include hydrophilic clays and organoclays supplied by Nanocor, Inc. and Southern Clays Products. The physical properties of these clays are listed in Table 3-1. The clays from Nanocor Inc were Nanomer ® G105 PGW (G105), Nanomer ® I.28MC (I.28), and Nanomer ® I.30TC (I.30). G105 is a highly pure sodium-based montmorillonite and has a cation exchange capacity (CEC) of 145meq/100g±10%. This clay is hydrophilic, it is white with individual layer thickness approximately 1 nm, an aspect ratio of 200 – 400 and a specific gravity of 2.6. The other two products supplied by Nanocor were organoclays, I.28 and I.30. These clays are white and their specific gravity is 1.9.

The clays from Southern Clays Products were Cloisite ® Na^+ (NA^+), Cloisite ® 93A (93A), Cloisite ® 20A (20A) and Cloisite ® 15A (15A). Cloisite ® NA^+ is a natural sodium-based montmorillonite with a CEC of 92.6meq/100g and a specific gravity of 2.86 [261]. It is a hydrophilic clay. The other Cloisite ® clays are organoclays. As listed in Table 3-2, Cloisite ® 93A has been modified by a methyl, dihydrogenatedtallow, ternary ammonium salt with a concentration of 90 meq/100g clay [262]. While Cloisite ® 20A has been modified by a dimethyl, dihydrogenatedtallow, quaternary ammonium salt with a concentration of 95 meq/100g clay [263]. Cloisite ® 15A has been modified by the same ammonium salt as 20A but the concentration of the ammonium ion was higher, i.e. 125 meq/100g clay [264].

3.1.2 Polymers

The two polymers used in this study were polyethylene oxide and polystyrene. The physical properties of both polymers are listed in Table 3-3. The polyethylene oxide

was supplied by BDH Chemical Ltd in powder form with an average molecular weight of ~600,000 and has melting temperature, Tm = 65 °C.

The polystyrene was supplied by Aldrich Chemicals in granule form with an average molecular weight of ~230,000, density ρ = 1040 kg/m^3, melt flow index MFI = 7.5g/10min and glass transition temperature T_g = 94 °C. The polystyrene was ground to powders with the size below 150 μm before use.

3.2 Synthetic methods

3.2.1 Solid Intercalation

Solid intercalation was developed to produce polymer/clay nanocomposites. Different combinations of dried polymer powders and clays, with a total weight of 2.0 grams in each case, were mechanically blended for 15 minutes; the mixture was then evenly stacked between two flat steel plates which had been covered with aluminium foil. The solid mixtures were firstly hand-pressed flat, which resulted in approximately circular discs, and then subjected to uniaxial compression under 30 tonnes force at room temperature (25 °C) for 5 minutes using a compression moulding machine to produce a tablet. The actual compaction pressure for each tablet was calculated based on the final cross-sectional area. The value was around 330 MPa for all the samples. Clay loadings of 5 wt%, 7 wt%, 10 wt%, 15 wt%, 20 wt% and 50 wt% were used to investigate the effect of the clay loading on the extent of the intercalation in polymer/clay system. As the clay loading increases, the volume of the mixture decreased, but the cross-sectional areas were fairly constant with the main differences being in the thicknesses of the samples.

A study of the processing conditions of solid intercalation was carried out using PEO and G105 clay. The effect of moisture on the samples was examined by conditioning the polymer/clay samples in a controlled atmosphere of 0%, 25% and 69% relative humidity, for an hour. A second set of samples were prepared and were conditioned for 24 hours, 48 hours and 7 days at 69% relative humidity. The samples were compressed for 5 minutes at 25 °C and 30 tonnes.

The effect of pressure on solid intercalation was studied by preparing samples and pressing them at 25 °C with forces of 6, 10, 20 and 30 tonnes, which corresponded to pressures of 66, 110, 220 and 330 MPa respectively.

The effect of the temperature was examined by storing samples at 6 °C, 20 °C or 25 °C for two hours prior to compressing the samples with a force of 30 tonnes, corresponding to approximately a pressure of 330 MPa as before.

3.2.2 Solution Synthesis

Solution synthesis was also used to produce polymer/clay nanocomposites. In this method, Different combinations of polymer and clay with a total weight of 5.0 grams were used in each case. PEO was dissolved in de-ionized water at 50 ° – 70 °C and mixed using a magnet stirrer on a hot plate. The clays were dispersed in de-ionized water in a similar manner. The clay suspension was then mixed with the PEO solution. The mixture was stirred for 6 hours at 50 ° – 70 °C and then poured onto a transparent sheet of acetate to dry naturally at room temperature to obtain the nanocomposite film. Clay loadings of 5 wt%, 20 wt% and 50 wt% were used in the solution synthesis.

3.3 Characterisation of nanostructure

The nano-structure of the nanocomposites was characterised using X-ray diffractometry (XRD) by measuring the interlayer distance between clay layers and the stacking height of the clay tactoids. The experiments were carried out using a Philips X-ray diffractometer using CuKa (λ=1.54Å) as radiation source. The equipment had a position sensitive detector covering a 3–125° scanning range.

Samples for the XRD experiment were prepared using different techniques depending on the integrity of the materials. Powdered materials were either ground using a marble pestle and mortar and then dispersed onto adhesive tape or compressed into discs with a diameter greater than 16 mm under a pressure of 330 MPa. The discs were then placed in the XRD sample holders. Film samples were cut into a rectangular shape 16mm×20mm, or larger, and then fixed into aluminium sample holders.

Since the clays used have a layered structure, the basal *00l* series, (001), (002), (003) ..., reflections will be changed during intercalation. These changes depend on the nature of the cations and molecules intercalated between the clay layers. The interlayer spacing, *d*, can be determined using the angle of the *00k* peaks in the spectrum

According to Bragg's equation

$$2d\sin\theta = n\lambda$$

in which λ is the wavelength (in this case, 0.154 nm for Cu Kα1), θ is Bragg angle and n is the number of the *00l* order. When n = 1, the corresponding d is the distance between the adjacent two clay layers. Therefore the interlayer spacing, $d_{(001)}$, can be calculated using the position of the (001) peak.

$$d_{(001)} = \lambda/(2\sin\theta)$$

The dimension of a clay tactoid can be determined using the intensity of corresponding peaks. Theoretically, if the width at half peak height, β, is known, the average dimension along a line normal to the reflecting plane, L, can be determined using the Scherrer equation,

$$L = K\lambda/(\beta\cos\theta)$$

in which K is Scherrer parameter. This is the shape factor and is estimated to be 1.84 for (00*l*) and 1 for (*hk*0). In the case of clay, K = 1.84 will be used to calculate the average stacking height of the clay tactoid, Lc, based on the width at half height of (001) peak and K = 1 will be applied to obtain the average diameter of the clay sheets in the layer direction, La, based on the width at the half height of (110) peak, as shown in Figure 3-1 (b). [265-266] In a real application, β is influenced by the equipment settings. Therefore the dimension of the crystal size measured using the distance at half peak height is not an accurate value. However, the ratio of Lc over La, calculated from the same spectrum, should be an adequate estimation of the aspect ratio of clay tactoids. This parameter is defined as the apparent aspect ratio (Lc/La)e, which can be calculated using the following equation

$$\left(L_c/L_a\right)_e = \frac{K_c\beta_a Cos\theta_a}{K_a\beta_c Cos\theta_c}$$

in which θ_a is the Bragg angle corresponding to the (110) peak, θ_c is the Bragg angle corresponding to the (001) peak, β_a is the width at half peak height of the (110) peak and β_c is the width at half peak height of the (001) peak.

3.4 Characterisation of microstructure

The microstructure of clays and polymer/clay composites was characterised using scanning electron microscopy (SEM). An ISI-DS 130 Scanning Electron Microscope was used with an operating acceleration voltage of 25 kv, and a magnification range of 1000 – 18400.

Samples for the SEM experiment were prepared differently depending on their structure. Powdered materials were dispersed on an aluminium sample holder which was coated with a conductive carbon adhesive disk. The sample was then gold coated for 4 minutes under vacuum. Film and disk samples were cut into 4mm×4mm squares. They were also fixed on sample holders using conductive carbon adhesive disks before being gold coated.

3.5 Fire assessment

The fire performances of PEO and its nanocomposites were assessed by a natural burning method using a Bunsen burner. Aluminium foil was used to support the sample during the test. A sample was placed on a sheet of aluminium foil and ignited using a Bunsen burner. When a sample was ignited and developed sustained burning, the Bunsen burner was removed. The burning phenomenon of each sample was recorded. The burned residues were examined using an Olympus stereomicroscope. Micrographs were taken using a camera.

3.6 Annealing test

An annealing test was designed to investigate the clay layer expansions in the polystyrene/clay composites produced using solid intercalation. The tablets produced by solid intercalation were heated at a temperature of 120 °C, which is just above the glass transition temperature of polystyrene, for two hours in a vacuum oven. The annealed tablets were then examined by XRD. The changes in the clay layer expansion were shown in the XRD patterns.

3.7 Nanoindentation test

The mechanical properties of the nanocomposites were characterised using nano-indentation testing by MicroTesting Ltd. This experiment was conducted using a NanoTest equipment produced by MicroTesting Ltd. The NanoTest is a platform-based system that is capable of carrying out indentation, scratching and impact tests.

The principle of the nanoindentation test is shown in Figure 3-2. During the test, a sample is mounted vertically, perpendicular to the displacement transducer. A very small-calibrated diamond indenter is used to produce an indentation on the surface of the sample. The movement and the force applied are controlled by a coil and magnet located on the top of the pendulum. The resultant displacement of the diamond indenter into the surface of the composite as a function of load can be measured and the results displayed and stored on a computer. To produce accurate hardness and modulus results, the equipment is required to be calibrated before the measurements are made. This can be carried out automatically by the equipment.

Depth-controlled indentation method was employed in this project. In this method, repeat indentations at a depth of 1908 nm were carried out on each sample. The loading process was stopped and reversed when the pre-set depth of 1908 nm was reached. An initial load of 0.03 mN was used to detect contact. The loading rate was 0.06 mN/s whilst a 60 seconds dwell time was used. A line of 10 indentations, each separated by 25 μm from the adjacent indents were made and measured for each sample. All the data was analysed by using a revised Oliver and Pharr method [270].

3.8 Characterisation of thermal properties

3.8.1 Thermogravimetric analysis

The thermal behaviour of clays, polymers and polymer/clay composites were characterised using a thermogravimetric analyser.

Approximately 10 mg of sample was used in each experiment. The experiments were carried out in either air or nitrogen atmosphere. The thermogravimetric analysis (TGA) was mainly carried out in nitrogen atmosphere. The data from TGA in air was used to investigate the decomposition of the material in real polymer processing conditions. The heating rate applied was 10 °C/min.

3.8.2 Thermal aging test

Organoclay degradation was investigated using a thermal aging test. During the thermal aging test, organoclays were heated at 200 °C for 5 minutes in air on a hot plate. When the samples had cooled to room temperature, they were then examined using X-ray diffractometry. The changes of the interlayer spacing in the organoclays were shown in XRD patterns.

Figures for Chapter 3

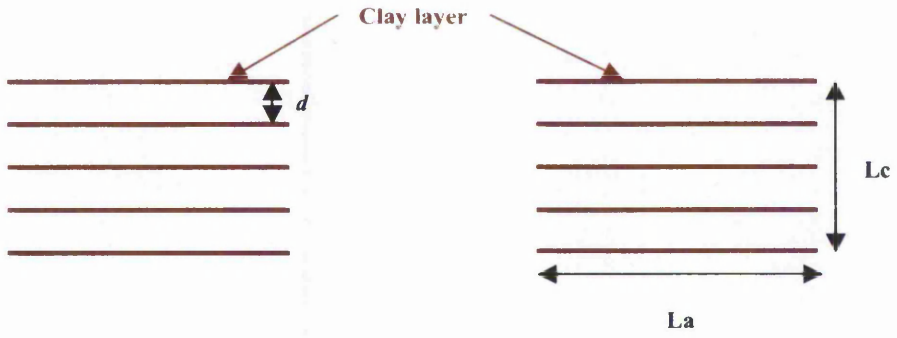

d – Interlayer spacing

La – average particle length for (110)
Lc – average particle length for (001)

(a) (b)

Figure 3-1 A schematic illustration of the parameters for clay characterisation

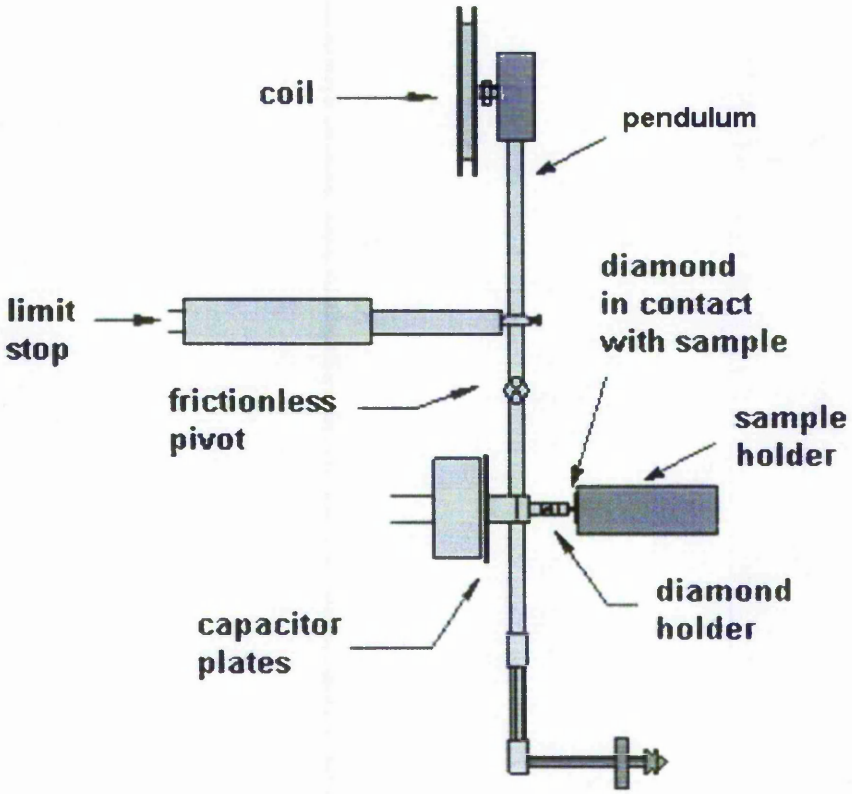

Figure 3-2 A schematic illustration of the nanoindentation equipment

Tables for Chapter 3

Table 3-1 Physical properties of clays used (Manufacturers' Data)

Clay Name	Manufacture Name	CEC, meq/100g	Specific Gravity	aspect ratio	appearance
Hydrophilic clay					
Nanomer ® G105 PGW	Nanocor Inc.	145	2.6	200-400	White powder
Cloisite ® Na^+	Southern Clays Products	92.6	2.86	-	Off White powder
Organoclay					
Nanomer ® I.28MC	Nanocor Inc.	-	1.9	-	White powder
Nanomer ® I.30TC	Nanocor Inc.	-	1.9	-	White powder
Cloisite ® 93A	Southern Clays Products	-	1.88	-	Off White powder
Cloisite ® 20A	Southern Clays Products	-	1.77	-	Off White powder
Cloisite ® 15A	Southern Clays Products	-	1.66	-	Off White powder

Table 3-2 Organic modifiers and concentration of Cloisite ® organoclays [261-263]

Clay Type	Organic Modifier *	Modifier Concentration
Cloisite ® 93A	methyl, dihydrogenatedtallow ammonium salt	90 meq/100g clay
Cloisite ® 20A	dimethyl, dihydrogenatedtallow, quaternary ammonium salt	95 meq/100g clay
Cloisite ® 15A	dimethyl, dihydrogenatedtallow, quaternary ammonium salt	125 meq/100g clay

*Hydrogenated Tallow (~65% C18; ~30% C16; ~5% C14); Anion: HSO4

Table 3-3 Physical properties of polymers used (Manufacturers' Data)

Polymer Name	Molecular weight	m.p. °C	Tg °C	Density kg/m^3	MFI, g/10min	Appearance
Polyethylene Oxide	~600,000	65	-	-	-	White powder
Polystyrene	~230,000	-	94	1040	7.5	Clear granules

Chapter 4 RESULTS AND DISCUSSION

In this chapter, the results and discussion are presented with a view to investigating the hypothesis that the polymer chains will intercalate between the clay galleries and with relatively strong and effective bonding being formed between the polymer chains and the clays. This is the key to the formation of high quality polymer/clay nanocomposites. X-ray diffractometry is used to study this, since the insertion of the polymer chains between the silicate sheets can be assessed by determining the changes in the d-spacing. The four main factors which were expected to affect the extent of intercalation of the polymer chains into the clay galleries are:

- Chemistry of the interlayer, in particular if it is hydrophobic or hydrophilic
- Original interlayer spacing and the potential of the clay layer expansion
- Polarity of species in the polymer chains
- Crystallinity of the polymer

These effects have been investigated using seven commercially available clays and a combination of the two selected clays and two polymer matrices utilised in this study.

Scanning electron microscopy is used to demonstrate the micro-morphology which will show how easily the clay can be dispersed in the polymer matrix at the micrometer scale. The thermal behaviour of the clays will make clear whether the clays can be used in conventional melt processing to produce polymer/clay nanocomposites.

With the problem of thermal degradation of the clay that arises in conventional melt processing, a novel synthetic method of polymer/clay nanocomposites, solid intercalation, is developed. The formation of nanocomposites based on either crystalline or amorphous polymer matrixes by solid intercalation will show the effectiveness of this method.

In order to elucidate the mechanism of solid intercalation, the differences between the micro-morphologies of the original clays and the corresponding nanocomposites produced by both solid intercalation and solution synthesis will clarify whether the

clay structures are changed at the micrometer scale. A natural burning test is easy to carry out and the results will reflect the structural differences at the molecular scale.

To optimise the processing conditions of the solid intercalation, a preliminary study of the effect of moisture, pressure and temperature on solid intercalation was carried out. Moisture is normally ignored in polymer processing since most of the thermoplastic polymers are not affected much by water. It can be very important, however, when a water soluble polymer is used. Temperature and pressure are the key parameters in solid intercalation processing. To explore the thresholds of temperature and pressure that can be used to process the mixture of polymer and clay to produce a nanocomposite material will further promote the potential of this method.

To explore the potential of solid intercalation in commercial applications, the mechanical properties and thermal stability of the composites were investigated. The improvement of the mechanical properties is one of the main aims of the nanocomposite approach. The nanoindentation technique is ideal in this case since only small quantities of materials were made in the laboratory. The thermal stability of the resultant composites will be crucial to be used as itself or as master batches for melt processing.

4.1 The Structure and Thermal Stability of Commercial Clays

The structure and thermal stability of clays plays an important role in the formation of polymer/clay nanocomposites. It is essential to gain an understanding of the nanostructure, micro-morphology and thermal behaviour of the main commercially available clays before the development of suitable synthetic methods for producing polymer/clay nanocomposites can be successfully undertaken. In this study, several commercial clays were investigated in order to identify the problems associated with the current development of polymer/clay nanotechnology.

4.1.1 The nano- and micro-structures of major commercial clays

4.1.1.1 The Nanostructure of the Clays

The major commercial clays currently used for polymer/clay nanocomposite application are montmorillonites, saponites and synthetic micas. In this project, commercial clays obtained from the Nanocor Inc and Southern Clays Products were investigated. The clays from Nanocor Inc include Nanomer ® G105 PGW (G105), Nanomer ® I.28MC (I.28), and Nanomer ® I.30TC (I.30). The clays from Southern Clays Products are Cloisite ® Na^+ (NA^+), Cloisite ® 93A (93A), Cloisite ® 20A (20A) and Cloisite ® 15A (15A). G105 and Cloisite Na+ are hydrophilic clays while the other clays are organoclays.

The nanostructure of the clays was characterised using X-ray diffractometry (XRD). In the XRD pattern of a clay, two parameters are important with regard to polymer/clay nanocomposite formation, the interlayer spacing and the stacking height. Both parameters can be calculated from the XRD pattern as discussed in Chapter 3. Interlayer spacing refers to the distance between two adjacent clay layers – d, as shown in Figure 3-1 a. According to the Bragg equation, $d = \lambda/(2\sin\theta)$, the interlayer spacing changes with the Bragg angle position. A smaller angle is equivalent to a larger interlayer spacing. The stacking height is the number of the clay layers in a clay tactoid which is measured by the ratio (Lc/La)e, which is the apparent aspect ratio of the clay tactoids, as described in Section 3.3. According to the Scherrer equation, $L = K\lambda/(\beta\cos\theta)$, a sharp high intensity peak corresponds to a

large stacking height of clay tactoids, while a broad low intense peak indicates a small stacking height of clay tactoids.

The X-ray diffractometry patterns of the hydrophilic and organophilic clays studied are shown in Figures 4-1 and 4-2 respectively.

The (001) peaks of both of the hydrophilic clays have relative high intensities at 2θ angles of 7.30 ° and 7.46 ° for G105 and NA^+ respectively. The corresponding interlayer spacing is 1.20 nm for G105 and 1.18 nm for NA^+. The calculated apparent aspect ratio of clay tactoids are listed in Table 4-1, the (Lc/La)e for NA^+ is 0.44 which is lower than that for G105, 0.76. This data indicates that G105 and NA^+ have similar interlayer spacing but different aspect ratios.

The relative intensity of (001) peaks for the organoclays are much higher than those of hydrophilic clays. The (001) peak positions are at 2θ = 3.68 °, 3.68 °, 3.78 ° and 3.76 ° for I.28, I.30, 93A, and 20A respectively. For 15A, the angle of (001) peak is out of the measurement range of the XRD equipment. However, the interlayer spacing can be calculated using Bragg's equation from other *00l* peaks which are clear in the XRD pattern. The (002) peak position at 2θ = 4.82 ° was used for the 15A clay. The corresponding interlayer spacings of I.28, I.30, 93A, 20A and 15A, calculated using either (001) or (002) peaks are 2.40nm, 2.40nm, 2.33nm, 2.35nm and 3.66nm respectively. The interlayer spacings of the organoclays are much higher than those of the hydrophilic clays. The organoclays from the different suppliers have very different interlayer spacings. For the Nanocor organoclays, I.28 and I.30, the interlayer spacing is the same while for the Cloisite series clays 93A, 20A and 15A, the interlayer spacing increases in the sequence listed. For the Nanocor organoclays, the reasons that the interlayer spacing is the same are unclear since the information on the surfactants used in making the clays is not available. In the case of the Cloisite organoclays, different surfactants have been used. A methyl, dihydrogenatedtallow, ternary ammonium salt was used to produce 93A and a dimethyl, dihydrogenatedtallow, quaternary ammonium salt was used to make 20A and 15A. The methyl, dihydrogenatedtallow, ternary ammonium salt is less hydrophobic than the dimethyl, dihydrogenatedtallow, quaternary ammonium salt. Together with the XRD information in Section 4.1.1.1, both the concentration and hydrophobicity of the ammonium salt used for 93A were not as high as those used

for the clay 20A. For organoclays 20A and 15A, though they were modified by the same quaternary ammonium salt, the concentration of the ammonium salt in 20A was lower. These results indicate that the extent of layer expansion is dependent on the type and concentration of surfactants applied. The shapes of the (001) peaks are also different in the organoclays. This depends on clay suppliers as shown in Figure 4-2.

According to the calculated (Lc/La)e of the clay particles as listed in Table 4-1, the Nanocor organoclay I.28 has a (Lc/La)e of 2.44 which is the lowest amongst all the organoclays studied while the Nanocor organoclay I.30 has a higher value of (Lc/La)e. This indicates that I.28 and I.30 have different aspect ratios even though they have the same interlayer spacing. For the Cloisite organoclays, except the (Lc/La)e data for 15A which is not available due to the lack of (001) peak in the XRD pattern, the (Lc/La)e of the 93A is greater than that of the 20A. Both of the values are above the (Lc/La)e of the I.28 clay.

In summary, the organoclays have higher (Lc/La)e values than the hydrophilic clays. If some organoclays are produced from the same hydrophilic clay and the size of the clay tactoids in the layer direction is maintained during the modification processes, the stacking heights of the organoclays would be increased due to the insertion of the organic cations which causes the clay layer expansion. Therefore, the stacking heights of the organoclays are affected by clay modification. However, the modification processes may reduce the size of the clay tactoids and decrease the stacking height of the clay tactoids. The interlayer spacing of the clay is also affected by the type and concentration of clay modifiers used.

4.1.1.2 The Micro-morphology of the Clays

The micro-morphology of the clays was investigated using scanning electron microscopy. Figures 4-3 to 4-9 show the SEM micrographs of the hydrophilic clays and organoclays, respectively. Different magnifications were used in order to identify the differences in structure, particle size and particle size distribution between these materials. Although these clays have layered structures at the nanometer scale, their appearance on the micrometer scale is very different.

The micrographs for the hydrophilic clay, G105, are shown in Figure 4-3. The clay tactoids appear to be crumpled and irregular in shape. Some individual clay tactoids

can be observed in the high magnification micrographs. These tactoids appear similar to "jellyfish". This indicates that the clay layers are really crumpled and irregular in shape since the clay tactoids are composed of many clay layers. The majority of the tactoids are aggregated into larger particles. The clay tactoids in the particles are entangled with each other. The shape and appearance of these particles appears very similar with a relatively small particle size distribution. The maximum particle size is around 55 μm while the minimum size is about 6 μm. However, the majority of particles are approximately 10-20 μm. The entanglement of the clay layers between different clay tactoids may affect their dispersion in solvents and polymers.

For the hydrophilic clay, NA^+, as shown in Figure 4-4, the appearance is very different compared to that of G105. The layered structures can be clearly seen for most particles and tactoids in the micrographs at higher magnifications. The clay particles appear to be rigid. Most of the particles look like slate fragments and comprise of various clay tactoids. The individual clay tactoids can be identified in the micrographs at higher magnifications. The typical tactoids are thicker than those of G105. The clay particles have a wider size distribution compared to those of G105. The size of the large particles exceeds 70 μm while the size of the small ones is less than 1 μm. However, the size for the majority of the particles is below 25 μm. There is less entanglement of the clay layers between different clay tactoids in the particles. This leads to the formation of particle shapes essentially like slate fragments. Such a structure suggests it may be easier to disperse at the micrometer scale compared to the structure of G105.

Combining the micro-morphology observations of the hydrophilic clays with their XRD data, the results indicate that most of the clay particles observed in micrometer scale were clay aggregates instead of clay tactoids. The low aspect ratio of NA^+ is associated with small tactoid size which can be observed in the micrographs.

The organoclay, 93A, micrographs are shown in Figure 4-5. Layered structures can be clearly seen for most particles and tactoids in the higher magnification micrographs. The clay tactoids appear to be more crumpled and irregular in shape than those of NA^+. The typical tactoids are thinner than those of NA^+. Most of the particles comprise of various loose clay tactoids. Their appearances are different

compared to those of NA^+ as there are no tiny particles distributed over the clay. The size range of the 93A clay particles is much narrower than the hydrophilic clay NA^+. Only a few large particles have a size of up to 40 μm while the size of the small ones is below 2 μm. The sizes for the majority of the particles are between 5 μm and 15 μm.

Cloisite 20A and 15A have similar morphology and particle size to 93A as shown in Figures 4-6 and 4-7.

The similarity in microstructure of all the Cloisite organoclays may imply that these organoclays might be manufactured by the modification of Cloisite NA^+. However the particle size distribution becomes narrower and the layered structured particles become thinner and more crumpled and irregular in shape for the organoclays.

The micro-morphology observations and the XRD data between the hydrophilic clay, NA^+ and the organoclays, 93A, 20A indicate that the high aspect ratio in the organoclays is associated with clay layer expansion and the change in particle size distribution.

For Nanocor organoclay, I.28, as shown in Figure 4-8, the layered structures for most particles and tactoids can be clearly seen in the high magnification micrographs. The clay tactoids appear to be more even than those of the hydrophilic clay G105. Most of the particles comprise of various lose clay tactoids. Only limited individual clay tactoids can be observed clearly in the micrographs. The size range of the I.28 clay particles is much narrower compared to the hydrophilic clay G105. The large particles are around 50 μm while the small ones are below 2 μm. The size for the majority of the clay particles is between 10 μm and 20 μm. According to the micro-morphology, it does not appear that I.28 was produced from G105.

For Nanocor organoclay, I.30, as shown in Figure 4-9, the structure is similar to that of the hydrophilic clay G105. The particle size distribution is wider than that of G105. The maximum particle size is approximately 45 μm while the minimum one is about 5 μm. The majority of the clay particles are between 6 – 20 μm. It appears that I.30 might be modified from G105 due to the similarity in the shape and the appearance of the clays. This means that if the separation of the G105 clay layers can be achieved, the clay layer expansion of I.30 should be easily obtained by a similar technique.

The micro-morphology observations and the XRD data of the hydrophilic clay, G105 and the organoclays, I.28 and I.30 indicate that the high aspect ratio in the Nanocor organoclays is also associated with clay layer expansion and the particle size distribution change.

From the analyses of the XRD patterns and SEM micrographs of all the clays, it can be concluded that although these clays have layered structures at the nanometer scale, their appearance at the micrometer scale is very different even though some of the organoclays were possibly obtained through the modification of the same base clay.

4.1.2 The thermal stability of major commercial clays

The thermal stability of the clays was investigated using thermogravimetric analysis (TGA) and thermal aging tests.

The TGA data of the hydrophilic clays and organoclays shown in Figures 4-10 and 4-11 were obtained in a nitrogen atmosphere. The corresponding residue yields for all the clays are listed in Table 4-2. For the hydrophilic clays, as shown in Figure 4-10, there is a small weight loss of 1.5% - 2% before 150 °C possibly due to the release of water absorbed in the clays. The decomposition temperature, where the major weight loss occurs, exceeds 500 °C. The clays were very stable when the temperature was over 800 °C. The residue yields for G105 and NA^+ were 93.6% and 92.3%, respectively. The major weight loss is possibly caused by the release of intercalated water, and the water formed from dehydration reactions.

For the organoclays, as shown in Figures 4-10 and 4-11, the first stage weight loss was at temperatures below 150 °C and is less than 1%. This weight loss is due to the release of free water in the clays. This first stage weight loss is slightly less than that for hydrophilic clays. However, there is a big difference between hydrophilic clays and organoclays in the temperature range of 200 ° – 500 °C. The onset temperatures of the major weight losses for the organoclays are much lower than those for hydrophilic clays, approximately 170 °C or lower. The decomposition behaviour also depends on the clay sources.

For the Cloisite organoclays, there is only one major weight loss which is in the temperature range of 170 ° – 500 °C. Both the onset temperature of the major weight

loss and the residue yield change due to the different clay modification method used. The onset temperature of the major weight loss of 93A is more than 10 °C higher than that of 20A. The residue yield of 93A is 2.7% more than that of 20A. The onset temperature of the major weight loss of 20A is about 10 °C higher than 15A. The residue yield of 20A is 7.4% higher than that of 15A. The major weight loss is probably caused by the release of intercalated water, and the evolution of long-chain alkyl volatiles formed from the degradation of the organic modifiers used for clay modification. The difference between the TGA results of these organoclays is due to the decomposition of the organic modifier between the clay layers and the concentration of the organic modifier used in clay modification. The higher the concentration of the organic modifier or the longer the organic group chain in the modifier, the greater the weight loss is.

For the Nanocor organoclays, I.28 and I.30, there are two major weight losses in the temperature range 170 ° – 500 °C. The first major weight loss occurred in the temperature range 170 ° – 325 °C and the second major weight loss occurred in the temperature range 325 ° – 500 °C. Both organoclays have the same amount of residue yield, 64.2%. However, I.28 has slightly lower decomposition temperature than I.30. Both major weight losses of the organoclays are probably caused by the release of intercalated water, and the evolution of the volatiles formed from clay modifiers. In the Nanocor organoclays the ammonium salts, which were used as clay modifiers, may have two major stages of degradation which appear exactly the same in both the organoclays and result in the same residue yield.

The TGA curves of 93A and I.28 show that there is another weight loss in the temperature range of 500 – 800 °C corresponding to the inorganic minerals. This weight loss may be caused by the loss of the water formed from dehydroxylation, as is observed in the hydrophilic clays. However, the onset temperatures of the weight losses for the organoclays are lower than those for hydrophilic clays. The organoclays were different in their weight loss behaviour to the hydrophilic clays when the temperature was over 800 °C, the organoclays continued to lose weight. Xie's explanation [267] of thermal decomposition of other organoclays may be applicable to this case. In his explanation, the weight loss in this region is associated with the secondary and further decompositions of onium ions in the condensed phase on the clay surface.

In real polymer processing, air is always involved; therefore TGA testing of the organoclays in an air atmosphere was also carried out. The results are shown in Figure 4-12. In order to see the onset temperature difference of the major weight loss for the organoclays studied, the clays were tested between 50 °C and 500 °C.

The first stage weight losses of the organoclays at temperatures below 150 °C are similar to the results obtained in a nitrogen atmosphere. However, the onset temperatures of the major weight losses for the organoclays are similar or slightly lower in air compared to those tested in a nitrogen atmosphere. The decomposition behaviour also depends on the clay type.

For the Cloisite organoclays, the onset temperature of the major weight loss and the residue yield changed compared to the results tested in a nitrogen atmosphere. All the onset temperatures of the major weight loss for the Cloisite organoclays are nearly 10 °C lower than those in nitrogen. The residue yields are higher than those obtained in the tests in nitrogen atmosphere. The difference in the onset temperature of the major weight losses among the three organoclays is similar to those under nitrogen. However, the difference between the residue yields did change. The residue yield of 93A is 5.8% more than that of 20A. The difference in the residue yield between 93A and 20A in air is more than doubled compared to those in a nitrogen atmosphere. The residue yield of 20A is 72.6%, which is only 3.4% higher than that of 15A. The difference of the residue yield between 20A and 15A in air is much less than that in nitrogen. The results indicate that the ternary ammonium salt formed more residues in air than the quaternary ammonium salt did. The quaternary ammonium ions between the clay layers decreased less during the testing in air than in nitrogen. This indicates that the combustion in air of the organic ammonium salt between the organoclay layers was incomplete which resulted in the formation of a carbon soot or char which increased the residue yield.

The Nanocor organoclay, I.30, had only one major weight loss in the temperature range 170 ° – 500 °C instead of the two major weight losses in nitrogen. The major weight loss occurred in the temperature range 170 ° – 400 °C. The onset temperature of degradation is similar to that in nitrogen at 170 °C. The residue yield, 79.2%, is 15% more than that in nitrogen. This is most possibly due to the incomplete combustion of the organic fragments from the degradation of the organic ammonium salt.

The results of the TGA show that the onset temperature of the major weight loss and the residue yield are both related to the clay modifier. The type and the concentration of organic modifier affected the stability of the organoclays directly. The higher the concentration of the organic modifier or the longer the chain of the organic group in the modifier, the greater the weight loss is and the lower the residue yield is.

As the TGA data in air show, the decomposition temperatures of most of the current available organoclays are below 200 °C, which is lower than the common melt processing temperatures of polymers. In a nitrogen atmosphere, the situation is better, but quite a few organoclays started to degrade in the temperature range 170 – 230 °C. When these organoclays are used directly in the melt method to produce polymer/clay nanocomposites using traditional polymer processing equipment, they will degrade and affect the intercalation reaction.

The change of interlayer spacing corresponding to organoclay degradation was also investigated using X-ray diffractometry. The XRD patterns of the samples before and after the thermal aging test were examined and are shown in the Figures 4-13 and 4-14, for the Nanocor organoclays and Figures 4-15 – 4-17 for the Cloisite organoclays.

The (001) peaks of both the Nanocor and Cloisite organoclays after the thermal aging test shifted to the right which indicates that the interlayer spacing of the clays have decreased. These (001) peaks have relatively high intensity in the 2θ angle range of 6.36 ° – 6.80 °. The corresponding interlayer spacing varies between 1.30 – 1.39 nm depending on the clay source and clay modification as listed in Table 4-3. The samples after the thermal aging test have interlayer spacings similar to those of the hydrophilic clays. This indicates that the expanded layered structures in organoclays collapsed during the heating process.

The collapse of the expanded structure of the organoclays during TGA and thermal aging test shows that the organic cations between the clay layers degrade and the decomposed components are released from the clay layers. However, the basic layered structure of the clay is still maintained.

When the temperature reaches 200 °C, volatiles are evolved as the organic cations decompose, as illustrated in Figure 4-18. When the temperature is maintained, more and more organic cations are degraded. Since the basic layered structure of the clay

is maintained under the testing condition, the decomposed organic cations keep diffusing through the clay layers until the decomposition is completed.

When these organoclays are used in the melt processing of polymer/clay nanocomposites, the similar situation would occur. As illustrated in Figure 4-19, the volatiles produced from the organoclay itself will try to escape out of the clay galleries while the polymer melt is driven by the capillary effect and the intermolecular bonding force between the polymer and the remaining surfactants to flow into the clay galleries. There would be a balance between these two driving forces. If the organic cations between the clay layers decompose easily at high temperatures, more volatiles will be generated. The balance will be dominated by the volatiles escaping from the clay layers which would prevent the polymer melt flowing into the clay layers, thus the efficiency of the intercalation would be affected.

Therefore, the stability of the organic cations existing between the clay layers plays a key role in the development of polymer/clay nanocomposites. High efficiency of intercalation in melt processing would be expected if the thermal stability of organoclays could be improved.

In general, the Nanocor clays are relatively pure and have narrower size distribution compared to Cloisite products, thus the subsequent investigations are essentially based on the clays obtained from Nanocor. Nanocor organoclays, I.28 and I.30 have very similar characteristics except that I.28 has a lower stacking height compared to I.30. This means that the clay layers of I.28 can be expanded more quickly when the clay tactoids are fully dispersed in the polymer matrix. The behaviour of I.30 will be better understood if the expansion and dispersion of the hydrophilic clay, G105 in polymer/clay nanocomposites is examined first due to the similarity in microstructure between these two clays. Therefore the hydrophilic clay, G105 and the organoclay, I.28 were used in this study.

In order to avoid the decomposition of organoclays in melt processing, two possible solutions can be investigated. One is to produce more stable organoclays and the other would be to stabilise the clays by introducing pre-intercalation between the clay layers with a polymer below the clay degradation temperature. At present, several attempts have been investigated towards the development of thermally stable

organoclays. This includes Singh's work using tetra-phenyl phosphonium compounds [254], Gilman's recent work on synthesising four thermally stable trialkylimidazolium salts to modify montmorillonite or fluorinated synthetic mica for the preparation of nanocomposites [174] and other research groups are attempting to use other stable surfactants/compatibility agents [255-256]. However these researches have not yet led to a commercially available product. The surfactants used were too expensive.

The approach used in this project was to develop a novel technology to introduce pre-intercalation between polymers and clays at a temperature below the degradation temperature of the organoclays. When the polymer would enter the space between the clay layers, as shown schematically in Figure 4-20, it is anticipated that the application of the pre-intercalated products in melt processing would be more efficient in intercalating clays to produce polymer/clay nanocomposites.

The technique developed was named as "solid intercalation". In this technique, a high pressure was applied to a solid polymer/clay mixture at ambient temperature to introduce intercalation. Since no high temperature was involved, there was no degradation of the organoclay. The following section will discuss details of the changes in nano- and micro-structure of polymer/clay composites in solid intercalation, the possible mechanism of the intercalation and the potential applications of solid intercalation based on the Nanocor clays.

4.2 The Intercalation during compression of solid polymer/clay mixtures

A technique to intercalate clay layers with a polymer in the solid phase, solid intercalation, has been developed in this project to produce polymer/clay nanocomposites. The solid intercalation processing involves blending and compression of the mixture of solid polymer and clay at ambient temperature.

There are a number of benefits from using this technique. This technique does not use high temperatures during processing so that degradation of the organoclay during melt processing can be avoided. Secondly, the processing is carried out using a solid mixture; therefore, there is no solvent involved. Thirdly, the processing can be carried out using traditional compression machines, thus the polymer processing industry can use existing polymer processing equipment to manufacture polymer/clay nanocomposites.

In this project, a crystalline polymer, poly(ethylene oxide) (PEO) and an amorphous polymer, polystyrene (PS) were used with a hydrophilic clay and an organoclay to produce nanocomposites using solid intercalation. The polymer/clay composites were produced under dried conditions for characterisation. This section will give details of the results obtained using X-ray diffractometry.

Poly(ethylene oxide) was selected as the crystalline polymer due to its potential use in polymeric electrolytes for lithium batteries and in producing master-batches to be used in similar structured polymers. Polystyrene was studied because it is a commonly used amorphous polymer and its glass transition temperature is far above the process temperature for solid intercalation. The effectiveness of solid intercalation in such a material has the potential to produce master-batch materials commercially.

4.2.1 PEO/clay Mixture System

The resultant XRD patterns of the composites produced from PEO with different loadings of the hydrophilic clay G105, PEO-G105, prepared by solid intercalation are shown in Figure 4-21. The (001) peaks of the clay have been shifted to lower angles for most the composites. This indicates that the interlayer spacing of the clay

in these samples has been expanded. The extent of layer expansion is a function of clay content. The interlayer spacing increased significantly when the clay content was below 10 wt%. With a clay loading of 5 wt%, the interlayer spacing expanded from 1.20 nm to 1.74 nm as listed in Figure 4-21. The extent of this expansion is similar to those of the composites produced by solution and melt syntheses [24, 124]. However, when the clay content is above 10 wt%, both expanded and original clay layers exist in the polymer/clay composites. As shown in Figure 4-21, the position of the (001) peak at $2\theta = 5.12°$ is replaced by a broad peak in a range of $2\theta = 5.12°$ to 6.84 °. The 2θ angle 6.84 ° corresponds to the original clay layer distance. The remaining 2θ angles in this range represent different degrees of clay layer expansion. As the clay content further increases, the ratio of $2\theta = 6.84°$ to $2\theta = 5.12°$ increases. When the clay content increased to 50 wt%, the sharp (001) peak was obtained at $2\theta = 6.84°$ and there was virtually no peak at $2\theta = 5.12°$. This indicates that the initial clay layer distances are retained. Only very limited expanded clay layers exist in the polymer/clay system. Therefore, as the clay content further increases, there are less and less expanded clay layers in the polymer/clay system.

Layer expansion also occurs when an organoclay is used. Figure 4-22 shows the XRD patterns of the composites produced from PEO with different loadings of organoclay I.28 (PEO-I.28) using solid intercalation. The results show that the (001) peaks of the composites have been shifted from the original 2θ at 3.68 ° to values below 3 °, which is the limit of the XRD equipment. However, the (002) peaks of the clay in Figure 4-22 are clearly visible so that the interlayer spacing can be calculated from the angle of the (002) peaks according to the Bragg equation. The calculated interlayer spacing data are listed in Figure 4-22. The data indicates that layer expansion occurred in the PEO-I.28 composites. The layer expansion of the clay appears to be independent of the clay content in the composites, which is different from the results obtained from the PEO-G105 composites. The interlayer spacing has been increased from 2.32 nm to over 3.11 nm. The variation in the interlayer spacing data between the composites may be associated with the fluctuation of the pressure applied during processing. Unlike the (001) peaks for PEO-G105 composites, which become broader as the clay content increases, the width at half of the maximum intensity of the (002) peaks is similar for all these samples.

Two possible changes may occur during the solid intercalation processing. A simple clay layer expansion which is constrained by residual stresses in the polymer/clay system may occur. Alternatively a valid intercalated structure, which is similar to that of nanocomposites produced by other methods, has been formed.

In the first situation, the layer expansion would be caused by the compression stresses perpendicular to the layers and would not involve the insertion of polymer between the clay layers. If this takes place, the layer expansion could occur if the clays were compressed under the same compression conditions as applied to the polymer/clay system.

However when both the hydrophilic clay and organoclay were compressed under the same compression conditions, no layer expansion occurred in either of them, as shown in Figures 4-23 for the hydrophilic clay G105 and Figure 4-24 for the organoclay I.28. The position and shape of the (001) peak remained the same. Only the relative intensity changed slightly.

These results indicate that the layer expansion is not caused by compression residual stresses which are applied in a direction perpendicular to the clay layers. Thus, intercalation between the PEO and the clays does occur during solid intercalation, and the polymer penetrates into the clay layers.

The mechanism of solid intercalation for PEO nanocomposites is possibly similar to that of melt synthesis. PEO is a crystalline polymer and is composed of two phases, a rubbery amorphous phase and a crystalline phase. In melt synthesis the polymer melts and flows into the clay layers. However in solid intercalation, it is most likely that the amorphous phase of the polymer inserts itself into the clay galleries, causing layer expansion. The crystalline phase in the polymer will have very limited flow at room temperature. With high pressure, the crystalline phase in the polymer will resist deformation more than an amorphous phase. The flow of the amorphous phase in the crystalline polymer above its glass transition temperature, T_g, may be enhanced significantly by high pressure. When the hydrophilic clay G105, is used, the extent of intercalation will depend on the amount of the amorphous phase in the polymer. The clay layer interfaces need to be wetted by the amorphous phase of the polymer. As the clay content increases, the amount of the amorphous phase available for intercalation in the mixture becomes less and less. At high clay contents, the amount

of the amorphous phase in the mixture will be insufficient to wet and flow into the clay galleries. This may be the reason for the decrease in the degree of layer expansion for the hydrophilic clay G105, as shown in Figure 4-21.

In the case of the organoclay, I.28, the interlayer spacing of the clay is already wetted and filled with hydrocarbon based ammonium cations. A small quantity of the amorphous phase of the polymer in the polymer/clay system is sufficient to flow into the clay galleries. As a consequence, the extent of layer expansion of the clay is not affected.

Additionally PEO has both hydrophilic and hydrophobic segments in the molecules, which increases the compatibility between the clay and the polymer which allows PEO to flow more easily into the clay layers.

4.2.2 PS/clay Mixture System

The solid intercalation technique was also applied to polystyrene which is a brittle amorphous polymer. The hydrophilic clay, G105 and the organoclay, I.28 were used. The XRD patterns of the composites of polystyrene with different loadings of the clays are shown in Figures 4-25 and 4-26 respectively.

For the polystyrene with hydrophilic clay G105 composites, PS-G105, the (001) peaks in XRD patterns only shift slightly to the left and the shape of the peaks remains similar. This indicates that only a minor expansion of the clay layers has occurred. The Bragg equation was used to calculate the interlayer spacings, which are listed in Figure 4-25. The results show that the interlayer spacing was increased from the original 1.20 nm to 1.29 nm for all the composites with different G105 loadings, which indicates that the extent of clay expansion is independent of clay content.

The results for the polystyrene with organoclay I.28 composites, PS-I.28, were different compared to those for the polystyrene with hydrophilic clay G105 composites. The (001) peaks have been shifted below 3^{o}. Only (002) peaks can be seen in the XRD patterns. The interlayer distances calculated from the (002) peaks are listed in Figure 4-26. The data indicates that significant layer expansion occurred in the PS-I.28 composites. The interlayer spacing has been increased from 2.40 nm to 3.11 – 3.74 nm. The XRD patterns also indicate that the extent of the layer

expansion is independent of the clay content in the composites. The peak shapes are similar for all the PS-I.28 composites. As the clay content increases, the width of half the maximum intensity of the (002) peaks remains similar. The fluctuation of the interlayer spacings between the composites may be associated with the fluctuation of the pressure applied during processing.

An annealing experiment was designed to investigate whether the clay layer expansions were caused by compression residual stresses. The samples were placed in a vacuum oven at a temperature of 120 °C which is just above the glass transition temperature. Figure 4-27 show the X-ray diffraction patterns of PS-I.28 composites with different clay loadings produced by solid intercalation process followed by annealing at 120°C for two hours. The results indicate that when samples are heated to 120 °C, little change in nanostructure for the PS-I.28 composites occurred. This indicates that the expanded structure did not collapse, thus the clay layer expansions were not caused by compression residual stresses.

The above discussion clearly reveals that the intercalation between polystyrene and organoclay did occur during the solid compression. However, there was little change between the polystyrene and the hydrophilic clay. In contrast to PEO, polystyrene is an amorphous polymer whose glass transition temperature, T_g, is much higher than the temperature applied in the solid compression. The polymer at this processing temperature in the solid compression is much more brittle than the amorphous phase in the PEO and hence exhibits very limited flowing behaviour. The layer expansion in these composites mainly depends on the compatibility or interactions between the polystyrene and the clay. In the case of hydrophilic clay, G105, the compatibility between the polystyrene and the clay is poor. The limited flow of polystyrene is not sufficient to cause intercalation between the polymer and the clay. In the case of organoclay, I.28, significant intercalation occurs which is possibly due to the following reasons. The organoclay is more compatible to polystyrene since polystyrene is more hydrophobic. However, with very limited flowing behaviour of the brittle polymer, the intercalation cannot be significant. It is possible that the interactions between the polystyrene and the pre-inserted hydrocarbon ammonium cations in I.28 are caused by the brittle polystyrene "dissolving" into the ammonium ions between the clay galleries under the high pressure.

In summary, the differences in nanostructure in the materials produced by the solid intercalation processing, which have been studied by X-ray diffractometry, indicate that significant layer expansion has occurred in PEO and polystyrene with the organoclay in the range of the clay content studied and PEO with the hydrophilic clay at relative low concentration. The layer expansion is unlikely to be associated with the residual stresses introduced in compression and hence is more likely to be caused by the intercalation between the clays and the polymers. In the subsequent section, the mechanism of the intercalation will be explored via a SEM study and a comparison investigation of the difference between solid intercalation and solution method.

4.3 A comparison between solid intercalation and other synthetic methods

4.3.1 The microstructure of nanocomposites

In order to elucidate the mechanism of solid intercalation, the microstructure of the polymer/clay nanocomposites was investigated using SEM. The nanocomposites produced by solution synthesis were also studied so that the difference between solid intercalation produced nanocomposites and those produced by other synthetic methods could be understood.

PEO-G105 nanocomposites with 5 wt% clay content (PEO-5wt% G105 nanocomposite) produced by solid intercalation and solution synthesis and PS-I.28 nanocomposite with 5 wt% clay content (PEO-5wt% I.28 nanocomposite) produced by the same methods were investigated.

The micrographs from scanning electron microscopy of hydrophilic clay, G105 and PEO-5 wt% G105 nanocomposite produced using solid intercalation at high magnification are shown in Figure 4-28. Figure 4-28 (a) shows the "jellyfish" structure of the clay as discussed in Section 4.1.1.2. The clay tactoids are entangled together. Figure 4-28 (b) shows the structure of the clays in the composite. The entangled structure of the clay has been separated in the polymer matrix. The clay layers or tactoids are stretched in the same direction in some regions. The surface of the clay layers and their edges does not appear as sharp as the image for the original clay. This may indicate that the surface of the clay layers is covered by a thin layer of the polymer.

At lower magnifications, as shown in Figure 4-29, the fractured surface of the composite shows many clay layers pulled out of the surface. Few clay layers in the composite have the "jellyfish" structure. The original clay structure in Figure 4-29 (a) cannot be seen in the composite structure in Figure 4-29 (b). The entangled clay layers have been expanded and flattened as the PEO intercalated into the clay layers.

In the macro-scale, a photograph of a PEO-5 wt% G105 nanocomposite film produced by the solid intercalation is shown in Figure 4-30. The photograph shows that only part of the sample edge appears white while other areas of the sample are translucent. This is a clear indication that melting of the PEO occurred during the

compression of the sample. In fact, the solid intercalation of PEO/clay composites can be described as a melt processing at low temperatures.

However it is surprising that the entangled jelly-fish structure in the original clay has been separated in the solid intercalation processing at low shear rate. This may be associated with the relatively high shear stresses introduced in the laminate flow in the solid intercalation processing. Although the shear rate applied in this case was low compared to traditional melt processing, the extremely high shear viscosity might cause significantly high shear stresses under limited laminate flow leading to the effective separation of the entangled clay structure. In contrast, a high shear rate applied to a low viscosity polymer system in melt processing may not always result in high shear stresses.

The microstructure of PEO/clay nanocomposites with 5wt% clay loading produced using solution synthesis was also studied. Figures 4-31 (a) and (b) show the SEM micrographs of the composite at different magnifications. The morphology of the clay in this composite was very different to the composites produced by solid intercalation. The original morphology of the "jellyfish" structure of the clay is retained in the composite. The formation of such a structure may be associated with either volume shrinkage during the removal of the solvent/co-solvent in the composites or insufficient separation of the entangled structure of the clays during solution synthesis.

To compare the solid intercalation and solution synthesis, the XRD patterns of PEO-G105 composite with 5 wt% clay content produced by the two synthetic methods were plotted in the same chart in Figure 4-32. The patterns showed that almost identical XRD patterns have been obtained from the composites produced by the two different methods. The (001) peaks for the composite from both the synthetic methods are in the same position. A similar extent of clay layer expansion has occurred, therefore in terms of nano-structure, there is little difference between the two composites. The difference of the two composites is in their micro-structure. The solid intercalation method is more effective in the separation of the entangled clay tactoids.

The mechanism of solid intercalation in the amorphous polymer, polystyrene and its composite produced with the organoclay I.28 with a 5 wt% loading, produced by solid intercalation, was studied using SEM.

The micrographs of both the clay and the composite at high magnification are shown in Figure 4-33. Figure 4-33 (a) shows the loose flower structure of I.28, as discussed in Section 4.1.1.2. Some clay tactoids are aggregated as particles. The micrograph in Figure 4-33 (b) shows the image of half pulled-out clays on a fractured surface of the PS-5 wt% I.28 composite sample. The polymer and the clay have been integrated into a continuous structure. The clay layers or tactoids in the polymer can be observed as stiff separated layers at the micro-scale. Some clay tactoids are covered by the polymer. Melting behaviour could not be observed at the macro-scale. Such an observation may support the speculation described in the previous section, that the surfactant in the organoclay possibly playing an important role in the intercalation.

4.3.2 Mechanistic studies of solid and other synthetic methods through burning

In order to investigate the distribution of the intercalated clay structure in the whole composites, the natural burning test as described in the experimental methods section was applied to investigate PEO-G105 composites produced by both solution and solid synthetic methods. The structure of the char formed by combustion of a polymer is dependent on the molecular structure of the polymer. An investigation of the difference in charring behaviour of the nanocomposites produced by both synthetic methods would provide an understanding of the mechanism of intercalation at the molecular level.

The burning behaviour of the pure PEO film was also carried out for comparison purposes. Figure 4-34 shows the morphology of the burning residue formed from the pure PEO film. During burning, the PEO film was first melted and then started to flow on the aluminium foil which was placed underneath the sample. The PEO then burnt with a blue flame. The flame continued till the sample burnt itself out. Little residue was produced following the burning.

The composites produced by solution synthesis, did not visibly melt. The samples changed from a transparent light beige colour to various colours depending on clay content during the burning. The morphology of the final burned residues is shown in Figures 4-35 (a) – (c). With 5 wt% clay content in the composite, an integrated char

has been formed. The original shape of the film has been retained. The residue had a dark brown/black colour. As the clay content increases, the residues became stronger and harder. The colour of the residues changed from a dark brown/black to a shining metallic colour. With 50 wt% clay loading, the composite was very difficult to ignite. Only the edge of the composite film could be burnt.

The burning behaviour of the PEO/clay composites produced by solid intercalation was very different from what was observed for solution synthesised materials. Figures 4-36 (a) – (c) show the burned residues of the composites with three different clay contents. During the burning, all of the solid intercalated composites exhibited melt flow behaviour. At low clay content, 5 wt%, the burning behaviour was similar to the original polymer. As shown in Figure 4-36 (a), the residue formed from PEO-5 wt% G105 composite appears similar to that from the base polymer in Figure 4-35 except that more yellow and black residue was formed. As the clay loading increased to 20 wt%, as shown in Figure 4-36 (b), there were some unburned areas and black loose powders in the residue. Figure 4-36 (c) shows the burning residue of the composite with 50% clay loading, the residue was essentially a black powdery char.

The morphology of the burned residues are associated with the distribution of the intercalated structure in the composites. The integrated structure of the residues formed from the solution synthesised products may indicate that perhaps all polymer molecules have participated in the intercalation during the formation of the polymer/clay nanocomposites and thus has led to the formation of integrated char during the burning. The situation may be similar to the diagram illustrated in Figure 4-37.

In solid intercalation, the results indicate that the nanocomposites formed are not homogenous. Only parts of polymer molecules have participated in the intercalation process so that the un-reacted polymer molecules melt and flow during burning. As shown in Figure 4-38, the polymer/clay system is possibly composed of two phases. One phase is the intercalated/exfoliated structure which is formed when some of the polymer flows into the clay layers; the other phase is the rest of the polymer outside the clay galleries which does not participate in the intercalation process. It appears that the flow of the polymer is very limited even though melting behaviour has been

observed. The reason of this behaviour may be associated with the high viscosity of the polymer under the processing conditions.

In summary, there are differences between solid intercalation and solution synthesis in both crystalline and amorphous polymer/clay systems.

In the solid intercalation processing of the crystalline polymer PEO/hydrophilic clay G105 system, the polymer melts during the processing and the molecular movement is limited to the region close to the clay layers. Un-reacted polymer molecules remain in the composites. During the burning, the un-reacted polymer melts and flows in the way similar to the original polymer.

In the solution synthesis of the crystalline polymer PEO/hydrophilic clay G105 system, almost every polymer molecule participated in the intercalation reaction. This uniformly intercalated structure results in the formation of an integrated char which increases the thermal performance of the material. However the micrographs indicate the limitation of using this method to produce exfoliated polymer/clay nanocomposites using the current clays since the entangled clay structure can be re-formed during the removal of the solvent.

In the solid intercalation of the brittle amorphous polymer polystyrene/clay system, the mechanism of the intercalation has not yet been fully understood. The micro-structure from SEM showed the evidence of the formation of an integrated structure. However polystyrene only has very limited flow at the processing temperature. Intercalation does occur and may be associated with the "solvent effect". In other words, the pre-inserted organic groups between the clay layers "dissolve" the polystyrene under the high pressure leading to the intercalation.

4.4 A preliminary study of the processing conditions on solid intercalation

The results described in the previous sections were based on the composites produced under a fixed set of processing conditions. In this section, the effect of processing conditions on solid intercalation will be discussed. These factors include moisture, pressure and temperature. The investigations were carried out based on PEO with 5 wt% hydrophilic clay G105.

4.4.1 Moisture

Before studying the effect of moisture on solid intercalation, the influence of moisture on the original hydrophilic clay, G105, was investigated. The study was carried out by dispersing the clay in water and then drying the clay to produce clay samples with different moisture contents. Figure 4-39 shows the XRD patterns of these clay samples. The clay layer expansion depends on the water content in the clay. When the clay was dispersed in water, a gel was formed. In this case, there is no (001) peak of the clay in the corresponding XRD pattern since the clay layers were randomly dispersed in water. As the water gradually evaporated, the (001) peak of the clay appears in the XRD patterns. The interlayer spacing decreases with the reduction of water content and the order of the stacking sequence of the clay tactoids is recovered.

The effect of moisture on solid intercalation was investigated under different relative humidities. Dried samples and samples conditioned in 25% and 69% relative humidity atmospheres were used. The material used was PEO with 5 wt% G105 clay. The mixture was exposed to a humid atmosphere for an hour before applying high pressure for solid intercalation. The processing conditions used were the same as the conditions for the samples described in the previous sections. As shown in Figure 4-40, with the increase of moisture content, the (001) peak splits into two overlapping peaks at $2\theta = 4.98°$ and 6.72°. The ratio of the peak at $2\theta = 4.98°$ over 6.72° is decreased. It appears that solid intercalation is more effective when the polymer and the clay are dry than when moisture is present for a short period of time. When the mixture was exposed to a humid atmosphere for a longer period of

time, the resultant XRD patterns are shown in Figure 4-41. The ratio between the peak at 2θ = 4.98° and the peak 2θ = 6.72° is reversed. In this case, moisture was a benefit to the clay layer expansion.

A possible explanation for this could be that when the polymer and the clay are dry, the intercalation is mainly by the melt flow of the polymer, under pressure, into the clay galleries. When there is sufficient water present to dissolve the polymer to make a solution, the intercalation is then by solution synthesis where the polymer solution flows into the clay layers. Therefore in the case of the samples which only experience a humid atmosphere for a short period of time, the moisture might affect the melting of the polymer under high pressure while the moisture content in the mixture was insufficient to convert the mixture into a "solution", leading to the decrease of the extent of intercalation as the increase of moisture content. When the mixture was exposed to moisture for a long time, the polymer was sufficiently wet so that the mechanism of the intercalation was switched to the situation similar to that which occurred in solution synthesis.

4.4.2 Pressure

The effect of pressure on the solid synthesis was investigated under compression pressure of 66 MPa, 110 MPa, 220 MPa and 330 MPa for PEO with 5 wt% G105 mixtures using the same conditions as applied to the dried sample, i.e. dry polymer and clay at 25 °C. The X-ray diffraction patterns of the samples are shown in Figure 4-42. There are two peaks between 2θ = 4 ° and 7 ° at lower pressures, 66 MPa and 110 MPa. When the pressure increases, the relative intensity of the (001) peak at 2θ = 4.98 ° increases; while the peak intensity at 2θ = 6.72 ° decreases. The peak intensity at 2θ = 6.72 ° nearly disappears when the compression force reaches 220 MPa. This indicates that the extent of intercalation is dependent on the pressure applied during processing. Significant layer expansion of all clay tactoids did not occur at low pressures. When the pressure was increased to more than 220 MPa, almost all the clay layers are intercalated.

It appears from these results that the low pressure is not sufficient to create enough melting of the polymer for a high degree of intercalation to take place. High pressure is required for intercalation of the polymer and clay.

4.4.3 Temperature

The effect of temperature on solid intercalation was investigated at three different temperatures, 6 °C, 20 °C and 25 °C based on a mixture of dried PEO and 5 wt% dried clay G105 using a pressure of 330 MPa. Figure 4-43 shows the XRD patterns of the composites processed at these temperatures. The relative peak intensity of the (001) peak increases at $2\theta = 4.98$ ° while the peak intensity decreases at $2\theta = 6.72$ °, as the temperature rose. The ratio of the peak intensity between $2\theta = 4.98$ ° and $2\theta = 6.72$ ° increased from 9:11 to 2:1 as listed in Table 4-4. This indicates that the level of intercalation is a function of the processing temperature. When the temperature is below 20 °C, the intercalation is only slightly affected by the processing temperature. When the temperature is above 20 °C, the intercalation increases significantly as the temperature rises. More clay layers have been intercalated by the polymer at the higher temperature. At 25 °C, nearly all the clay layers were expanded to a significant extent.

This is expected. As the increase of temperature would increase the mobility of the polymer molecules, which leads to a higher level of intercalation between the polymer and the clay.

In summary, the processing conditions play an important role in solid intercalation of PEO and clay. Small amounts of moisture in the polymer/clay system may decrease the extent of melt and flow of the polymer in the mixtures leading to low efficiency in intercalation. However, when sufficient moisture is present in the polymer/clay system, the clay layer expansion increases and the intercalation improves. The mechanism of intercalation in this case may be dominated by the mechanism of solution synthesis. High pressure and temperature improve the melt and flow of the polymer in the solid intercalation process and benefit the intercalation.

4.5 Mechanical properties and thermal stability of the nanocomposites produced using solid intercalation

In order to explore the potential of solid intercalation in commercial applications, the mechanical properties and thermal stability of the composites were investigated using the nanoindentation testing and thermogravimetric analysis.

The nanoindentation technique is particularly suitable for small-scale laboratory studies as only small quantities of materials are required. A depth sensing micro-indentor has been used to study the elastic and plastic properties of the samples during load and unload cycles. The hardness (H) of the sample is determined from the load curve and the reduced modulus (Er) which is a function of Poisson's ratio and Young's modulus, can be calculated from the unload curve, using the Oliver and Pharr analysis.

$$\text{Hardness } H = \frac{P_{max}}{A}$$

where P_{max} is the maximum load and A is the projected contact area of the indentor at maximum load.

The reduced modulus can be calculated using the following equation:

$$\frac{1}{Er} = \left[\frac{(1-\upsilon_s)^2}{E_s}\right] + \left[\frac{(1-\upsilon_i)^2}{E_i}\right]$$

Where E_s is Young's modulus for the sample, E_i is Young's modulus for the indenter (1141GPa), ν_s is Poisson's ratio for the sample and ν_i is Poisson's ratio for the indentor (0.07). [268, 269]

The materials studied were PEO based nanocomposites containing both hydrophilic clay (G105) and organoclay (I.28) produced by solid intercalation and solution synthesis and pure PEOs produced by using the same conditions as those materials described in Section 4.2 to 4.3.

4.5.1 PEO/Hydrophilic Clay Composites

The hardness H and reduced modulus Er in the PEO/hydrophilic clay composites produced by solid intercalation were measured by applying the depth-controlled indentation method as described in Section 3.7. Polyethylene oxide based composites with 7 wt% and 15 wt% clay loadings were used in this investigation. The depth-controlled indentation procedure provided useful information about the differences in hardness and elasticity between the samples.

The results of hardness and reduced modulus for the PEO/hydrophilic clay composites produced by the solid intercalation process are shown in Figures 4-44 and 4-45. The hardness of the PEO-G105 composites increases with the addition of the hydrophilic clay. For the PEO based composites with 7 wt% clay loading (PEO-7wt% G105), the hardness increased by more than 37% compared to that of the pure PEO. However, the hardness of the PEO based composites with 15 wt% clay loading (PEO-15wt% G105) appears anomalously low, as it only increased by 3% compared to that of the pure PEO.

The reduced modulus of the PEO based composites increased significantly with the addition of hydrophilic clay, Figure 4-45. The Er of PEO-7 wt% G105 increased by 58% and the Er of PEO-15 wt% G105 increased by more than 31% compared to that of the pure PEO.

It appears from these results that the efficiency of intercalation is reduced at high clay loadings. This may be associated with the extent of intercalation. As shown in the XRD patterns in Figure 4-21, PEO-7 wt% G105, has an intercalated nanostructure with interlayer spacing of 1.72 nm while PEO-15 wt% G105 is essentially a micro-structured composite with little change in the interlayer spacing having occurred. Both the nanoindentation test and XRD data indicate that the nanocomposite is superior to the micro-composite. In the nanocomposite, the excellent mechanical properties of the individual clay layers have been enhanced by the layer expansion and exfoliation. These clay layers behave in a similar way as short fibres do in fibre-reinforced composites, to reinforce the polymer at the nanometer scale. However in the case of the micro-composite with 15% clay loading, the reinforcement component is not these clay layers but clay tactoids which

do not possess good mechanical properties, especially in the through thickness direction of the layered structure.

4.5.2 PEO/Organoclay Composites

The mechanical properties of the composites produced using organoclay were also studied. The hardness and reduced modulus of PEO-I.28 composites produced using solid intercalation and solution synthesis were measured by the depth-controlled nanoindentation test. The results enable a comparison between the two composites processing techniques to be made as shown in Figure 4-46 and 4-47.

The hardness of the PEO-I.28 composites increases with organoclay content. With 7 wt% clay loading, the hardness increased by 22% while with 15 wt% clay loading, the hardness increased by nearly 38% compared to the pure PEO.

A similar tendency occurred in the reduced modulus of the PEO-I.28 nanocomposites with the reduced modulus increasing more significantly, Figure 4-47. The composite with 7 wt% I.28 had an increase in the Er of 42% and for the composite with 15 wt% I.28, the Er increase was 58% compared to the pure PEO.

As the XRD patterns in Figure 4-22 indicated that both the PEO-I.28 composites have intercalated nanostructure. These reduced modulus results indicate that the improvement in the mechanical properties is due to the increase of nano-structured reinforcing elements.

In addition, the hardness and reduced modulus of the PEO-I.28 composites are much higher than those of the PEO-G105 composites. The variation of the nanoindentation behaviour between PEO/hydrophilic clay composites and PEO/organoclay composites is associated with the extent of intercalation or the formation of some exfoliated structures in the PEO/organoclay composites. The XRD patterns of PEO/hydrophilic clay composites and PEO/organoclay composites in Figures 4-21 and 4-22 show that intercalated layered nanostructures were formed in both composites. However, greater interlayer spacing in the clay has been achieved in the PEO/organoclay composites. However, the XRD results cannot provide definite information about the exfoliated and disordered nanostructures of the materials and it is possible that some exfoliated structure was formed in PEO-I.28 composites produced by solid intercalation.

As a comparison, the nanoindentation tests for PEO/organoclay nanocomposites produced from solution synthesis were carried out. The results are also shown in Figures 4-46 and 4-47.

The hardness of the PEO-I.28 nanocomposites produced from solution synthesis shows the same trend as those materials produced by solid intercalation. However, the rate of increase in the hardness with respect to clay content for the materials from solution synthesis is higher than the rate of increase for the solid intercalated materials. The values of the hardness for the materials produced using solution synthesis is not as high as those for the composites produced by solid intercalation when the clay loading is below 15 wt%.

A similar tendency can be also observed for the reduced modulus of the PEO/organoclay nanocomposites as shown in Figure 4-47. The increase rate in Er with respect to clay concentration for the materials from solution synthesis is similar to that for the materials produced by the solid intercalation method. However, the values of the Er for the materials produced by solution synthesis are much lower than those by solid intercalation for clay loading below 15 wt%.

The XRD patterns for both the PEO-I.28 composites from solution synthesis have intercalated nanostructures, Figure 4-48. The improvement in the mechanical properties is due to the formation of the nanostructures.

The differences of the mechanical properties between the materials produced by the two methods have been not yet understood completely with the limited experimental data and investigations. These differences may be associated with different phases existing in the composites produced from the two methods. In the composites produced by solid intercalation process, there are possibly the isolated polymer phase and intercalated/exfoliated structure phase. The isolated polymer phase would mainly be composed of crystalline structures. In the composites produced by solution synthesis, there are mainly intercalated structure phase. Both the exfoliated structure and crystalline structure maybe provide extra improvement in hardness and Er of the materials produced by solid intercalation process. It may also be affected by the differences in crystallinity, crystal size and density of the PEO in the nanocomposite system resulting from the two synthetic methods.

The improved mechanical properties of the solid intercalated composites offer the potential for the direct application of solid intercalated products for small components such as polymer electrolytes in the future.

4.5.3 Thermal analysis of the PS/organoclay composites

The results obtained on polystyrene/organoclay composites, described in Section 4.2.2, has shown that up to 80 wt% polystyrene can be used to form intercalated polystyrene/clay nanocomposites using solid intercalation. In order to explore the potential of using this approach to produce a master batch for melt processing, thermal analysis of a PS/clay nanocomposite was carried out using TGA. The TGA results for PS-5 wt% I.28 composite produced by solid intercalation, in a nitrogen atmosphere are shown in Figure 4-49. The TGA of the base polymer, polystyrene, and the organoclay, I.28, tested in a nitrogen atmosphere were also shown in Figure 4-49. The thermal behaviour of PS shows two-step weight loss process. The first step weight loss is less than 3 wt% which is probably due to the release of the water from the sample. The second step is the major weight loss. The onset temperature for this weight loss is 350 °C. The peak temperature of major weight loss for the composite is 424 °C. There was no residue left after the test. The thermal behaviour of the organoclay I.28, as mentioned in Section 4.1.2, is a three-step weight loss process. The first stage weight loss was at temperatures below 150 °C and is less than 1%. The onset temperature of the major weight loss was 170 °C with two stages which corresponded to two rapid weight loss temperatures are between 170 °C and 400 °C. The residue of I.28 was 63.8 wt%. The thermal behaviour of PS/5 wt% I.28 composite has a two-step weight loss process. The first step weight loss is less than 3 wt% which is similar to that of I.28. The onset temperature of the second step weight loss, which is the major weight loss, was 368 °C. This is 18 °C higher than the onset temperature the second step weight loss of polystyrene. The temperature of the sharpest weight loss for the composite is at 440 °C. This is 16 °C higher than the major weight loss temperature of polystyrene. It is also much higher than the major weight loss temperature of I.28.

The results indicate that the thermal properties of the PS/I.28 nanocomposite produced by solid intercalation process are significantly improved due to the formation of the nanostructure.

One of the problems of using organoclays in producing polymer/clay nanocomposites is that they decompose at temperatures below the processing temperature of the polymer. The results of this research indicate that polymer/clay nanocomposites, produced by the solid intercalation process, are able to protect clay from degradation to some extent. This behaviour is extremely important in the further development of polymer/clay nanotechnology and offers the opportunity to use the existing available organoclays to produce high quality nanocomposites by using a combined approach involving both solid intercalation and melt processing.

Figures for Chapter 4

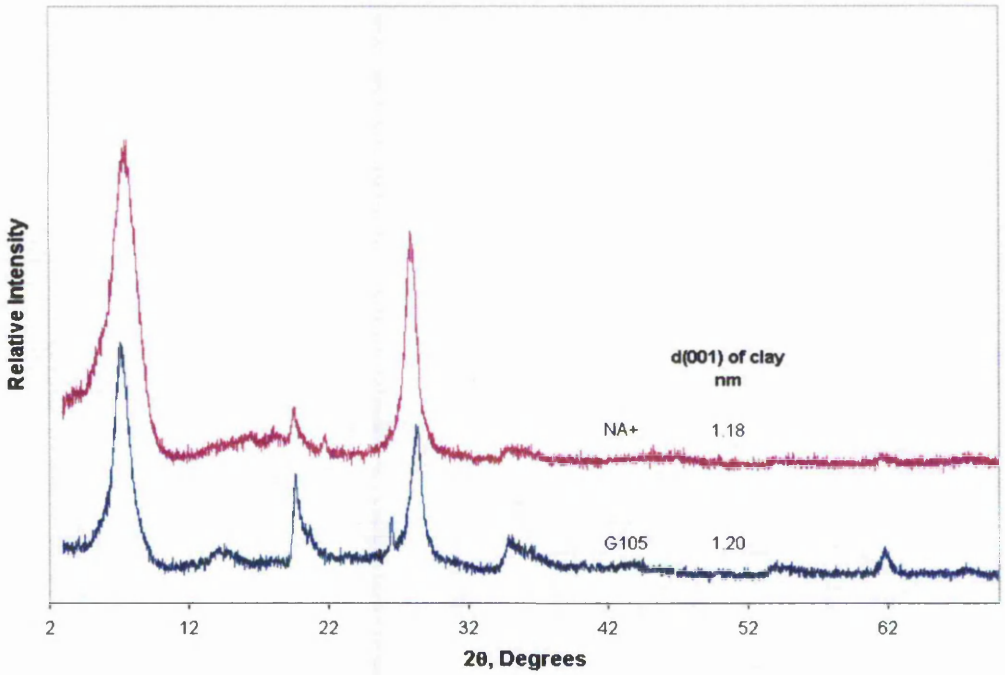

Figure 4-1 XRD patterns of the commercial hydrophilic clays, G105 and NA^+

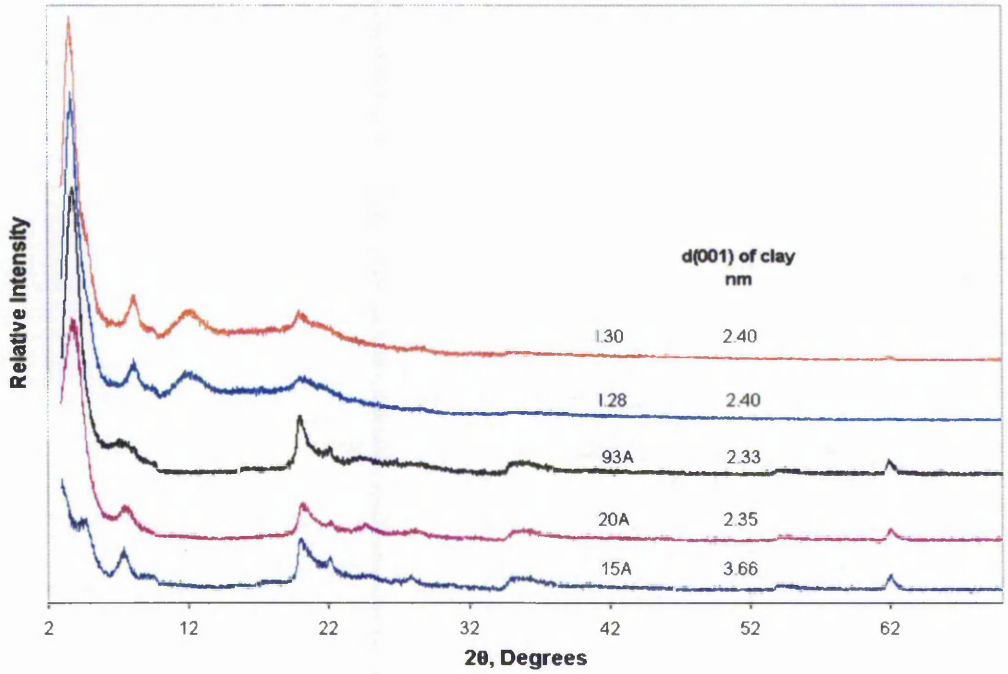

Figure 4-2 XRD patterns of the commercial organoclays, 15A, 20A, 93A and I.28, I.30.

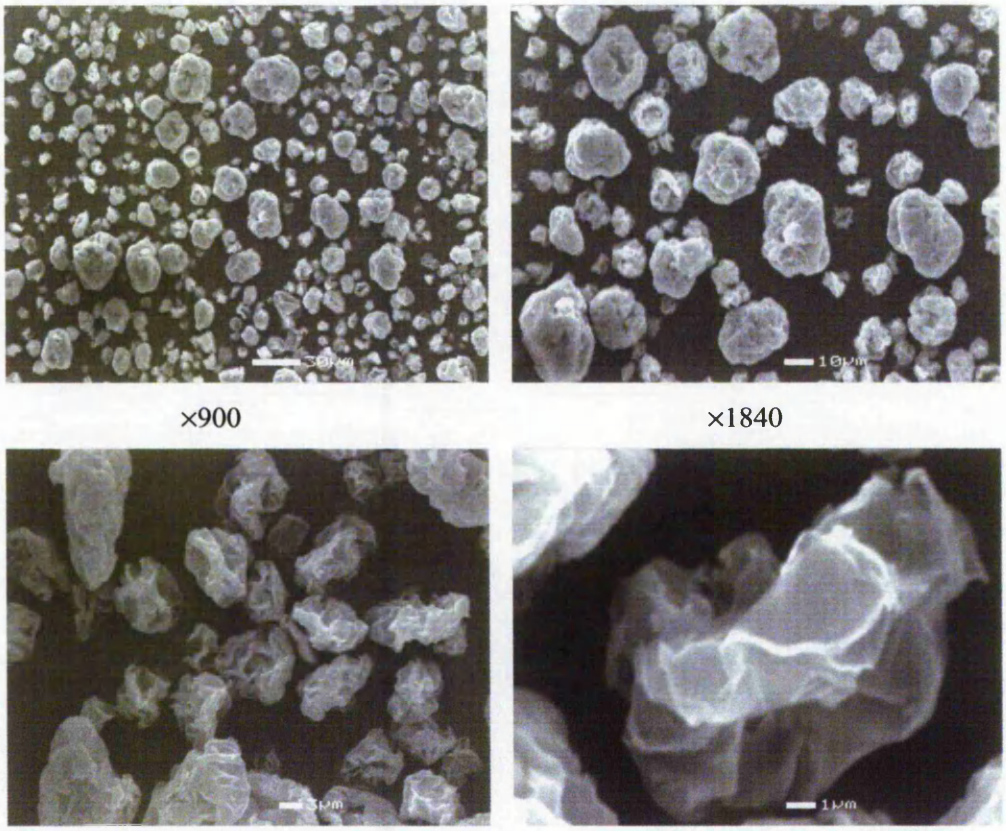

×900 ×1840

×4460 ×18400

Figure 4-3 SEM micrographs of the hydrophilic clay, G105

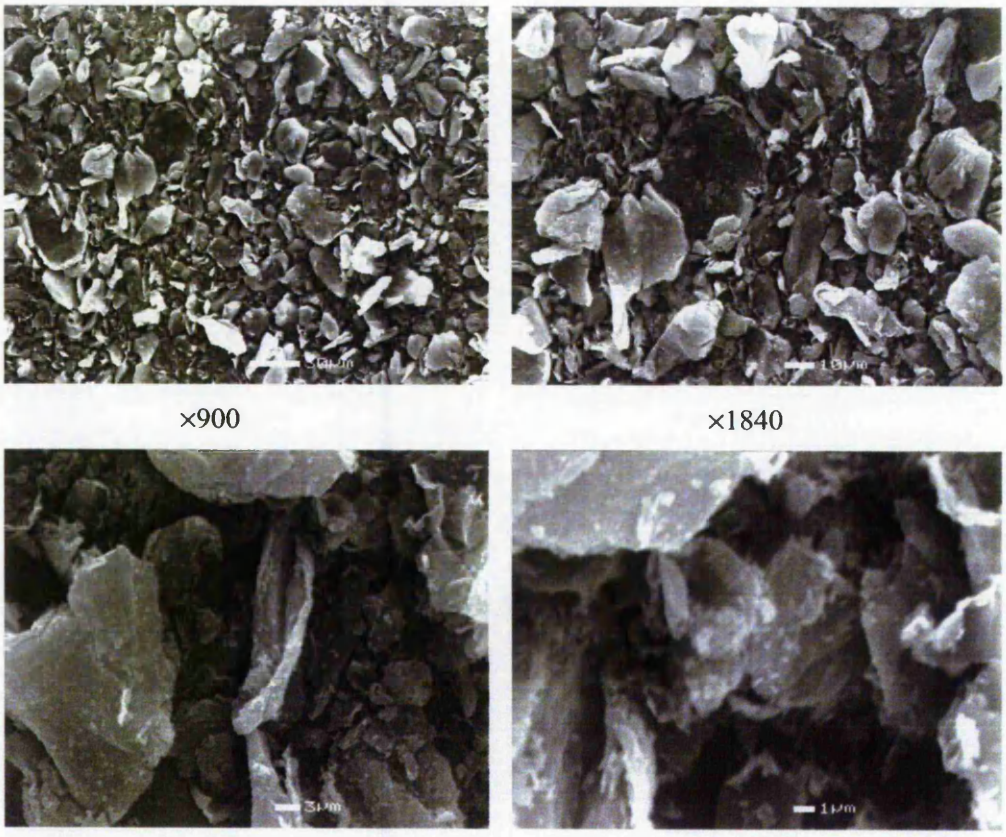

×900 ×1840

×4460 ×14800

Figure 4-4 SEM micrographs of the hydrophilic clay, NA^+

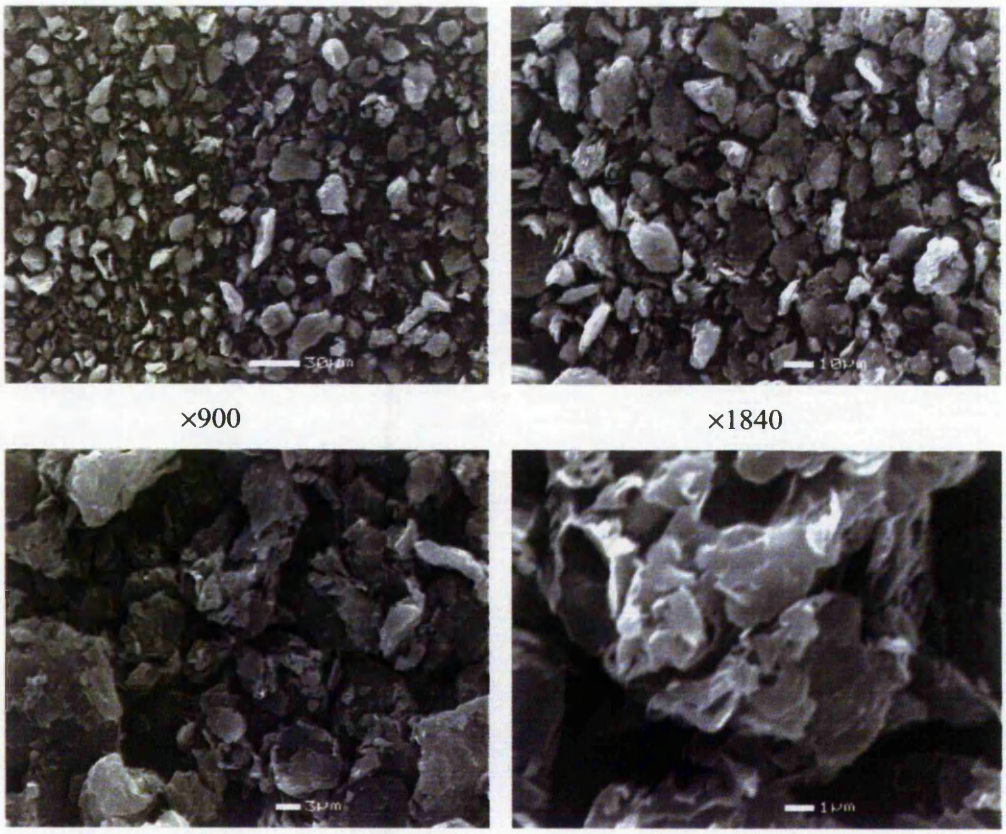

×900 ×1840

×4460 ×18400

Figure 4-5 SEM micrographs of the organoclay, 93A

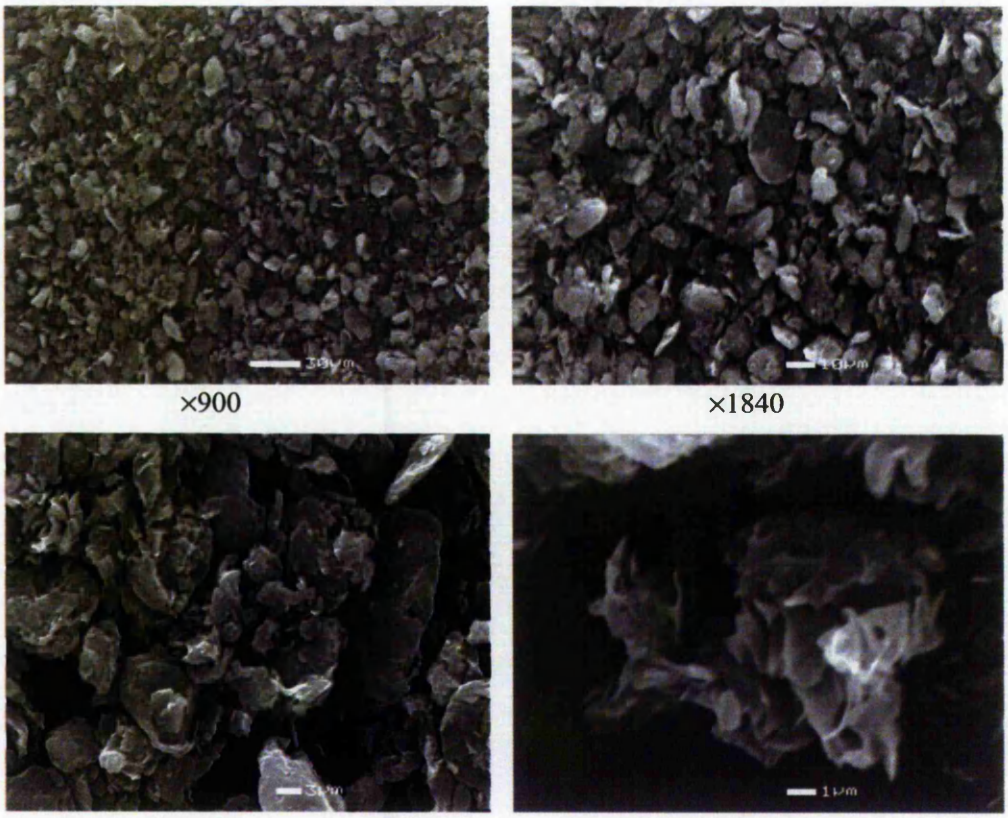

×900 ×1840

×4460 ×18400

Figure 4-6 SEM micrographs of the organoclay, 20A

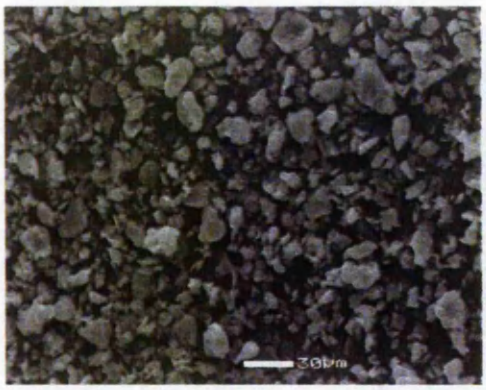

×900

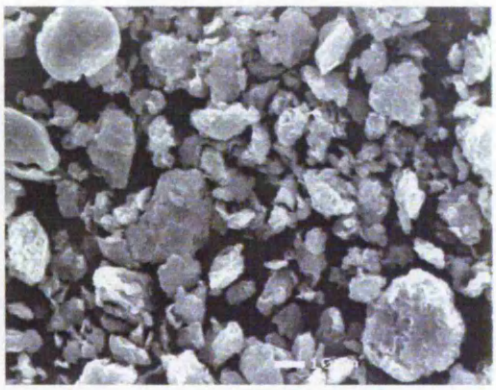

×1840

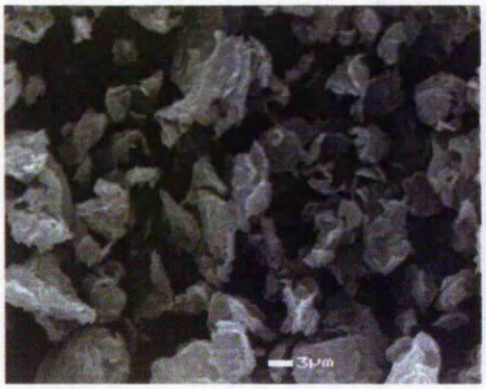

×4460

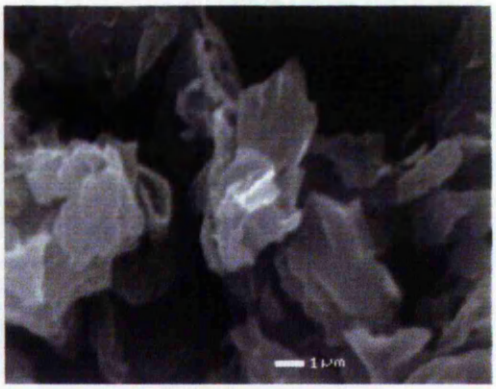

×18400

Figure 4-7 SEM micrographs of the organoclay, 15A

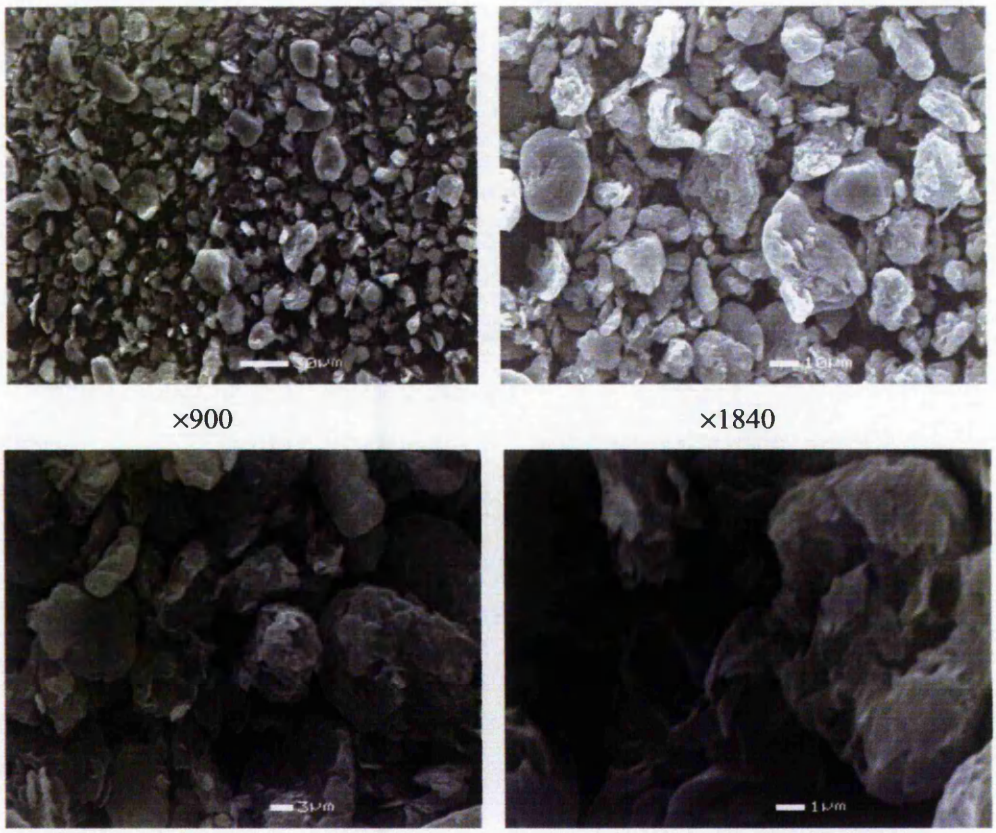

×900 ×1840

×4460 ×18400

Figure 4-8 SEM micrographs of the organoclay, I.28

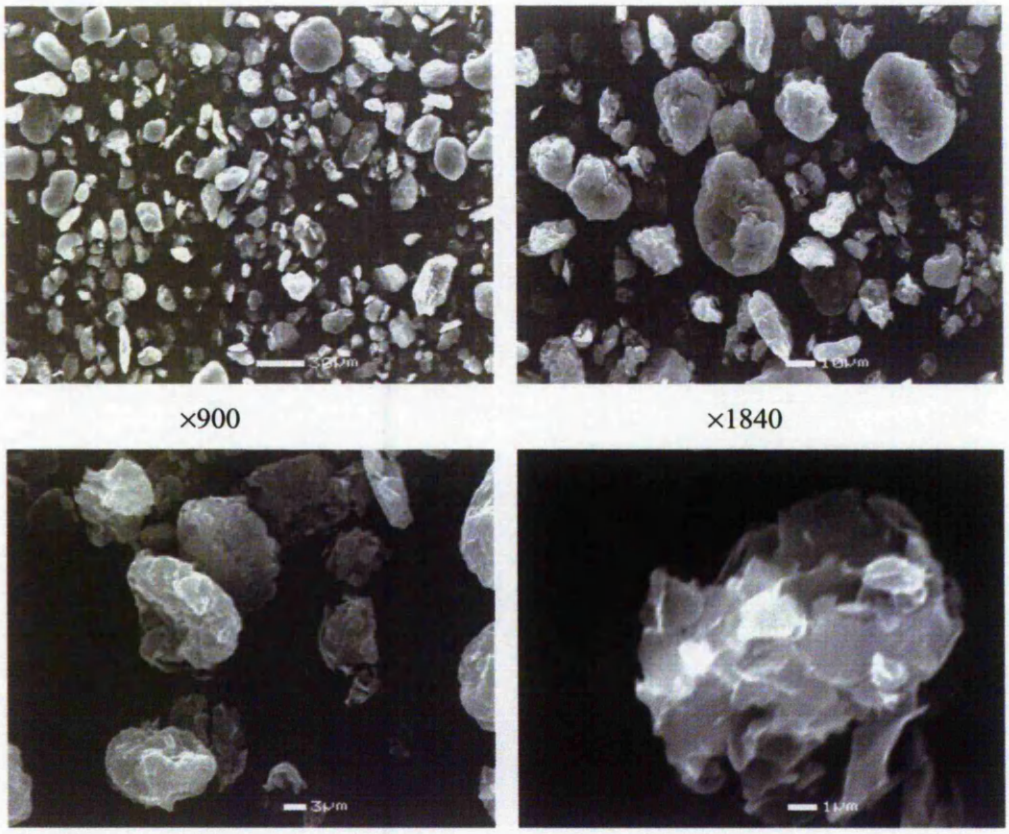

×900 ×1840

×4460 ×18400

Figure 4-9 SEM micrographs of the organoclay, I.30

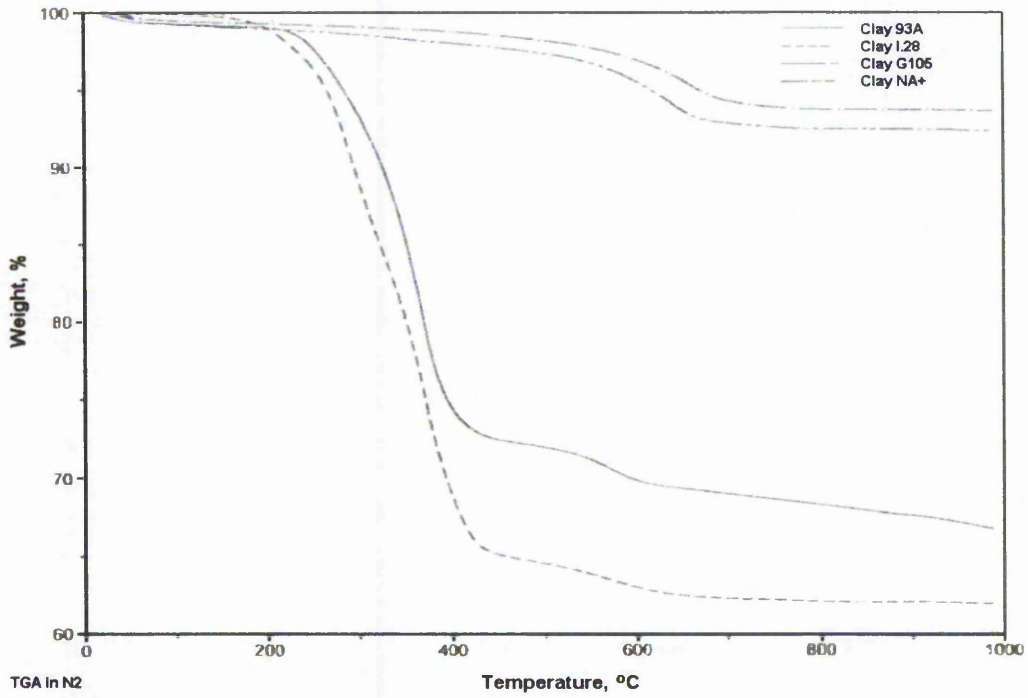

Figure 4-10 TGA results in nitrogen for hydrophilic clays and organoclays

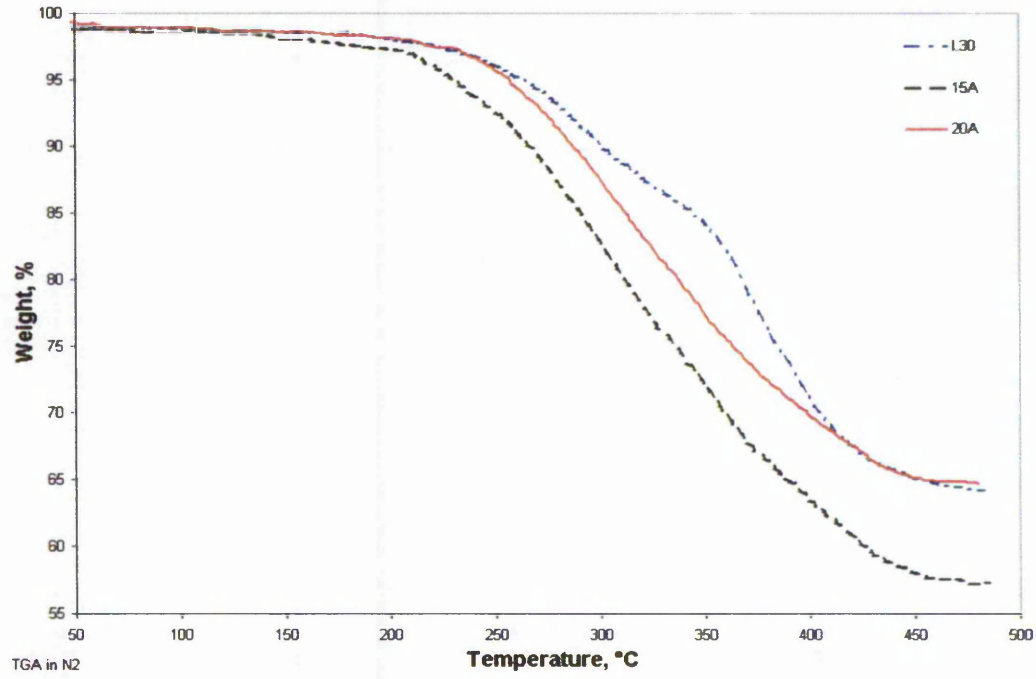

Figure 4-11 TGA results in nitrogen for organoclays

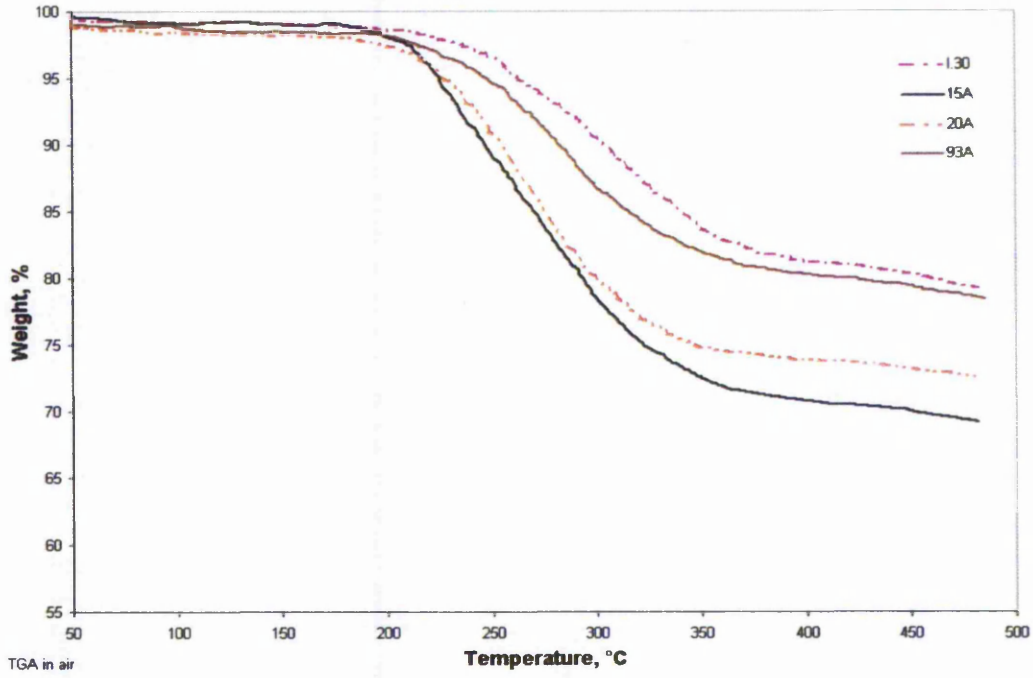

Figure 4-12 TGA results in air for organoclays

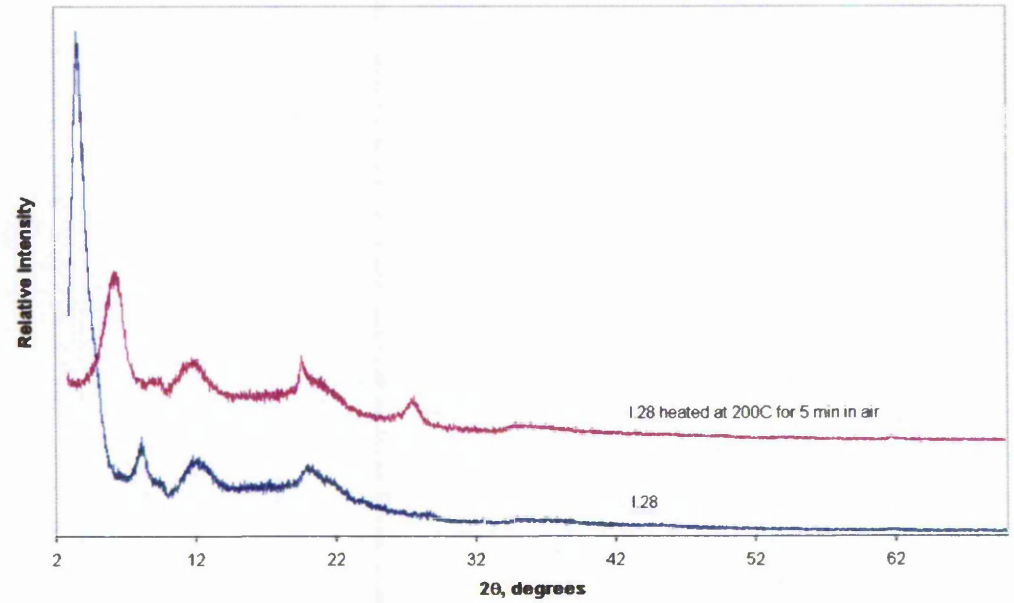

Figure 4-13 XRD patterns of I.28 and the heated I.28

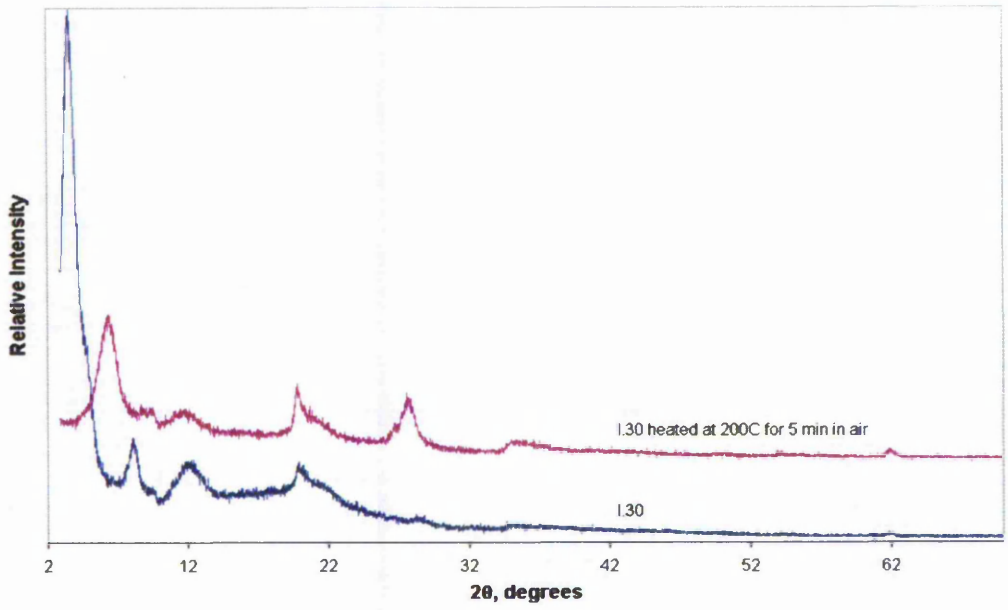

Figure 4-14 XRD patterns of I.30 and the heated I.30

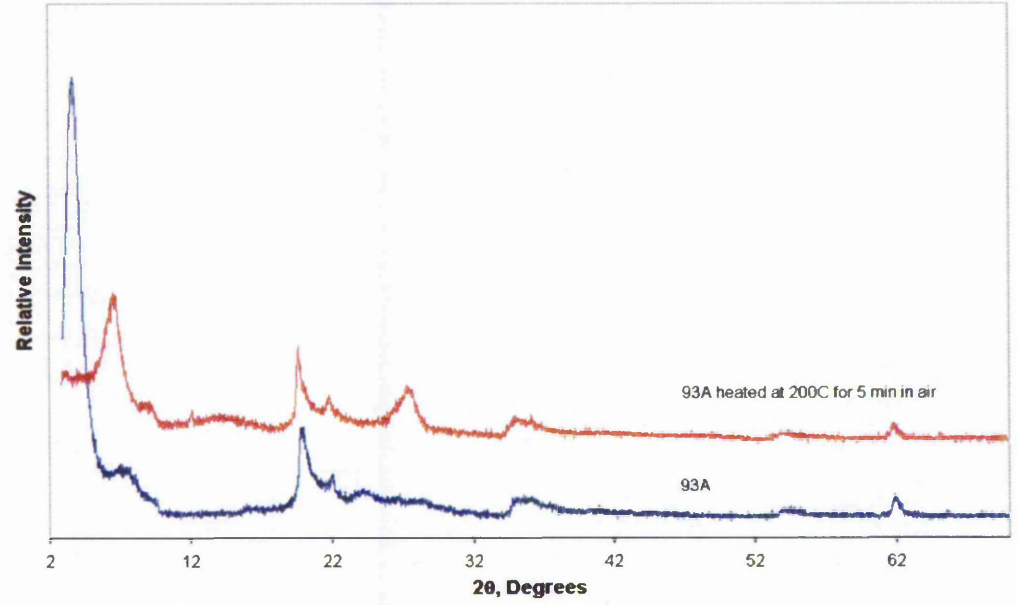

Figure 4-15 XRD patterns of 93A and the heated 93A

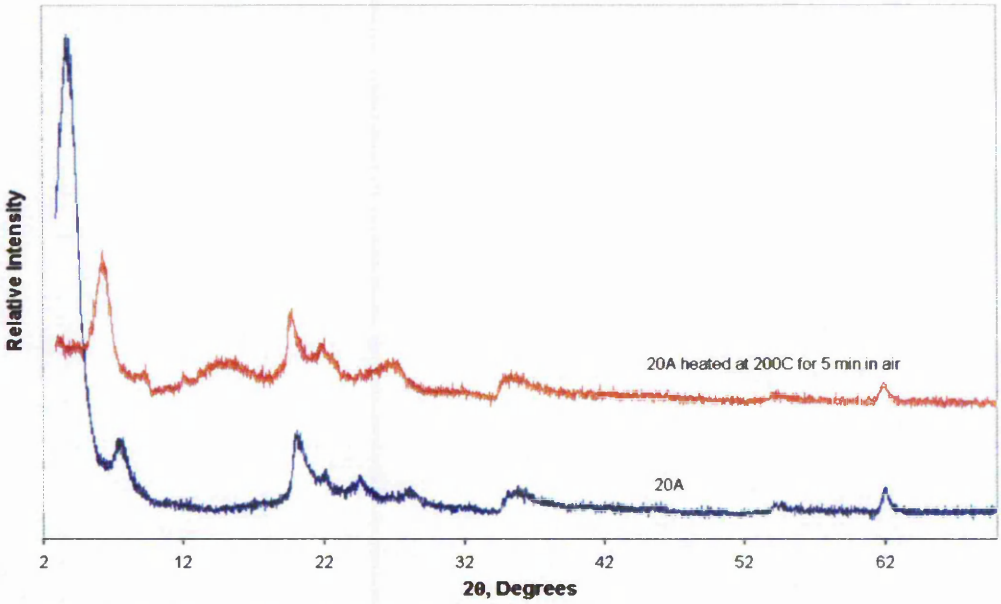

Figure 4-16 XRD patterns of 20A and the heated 20A

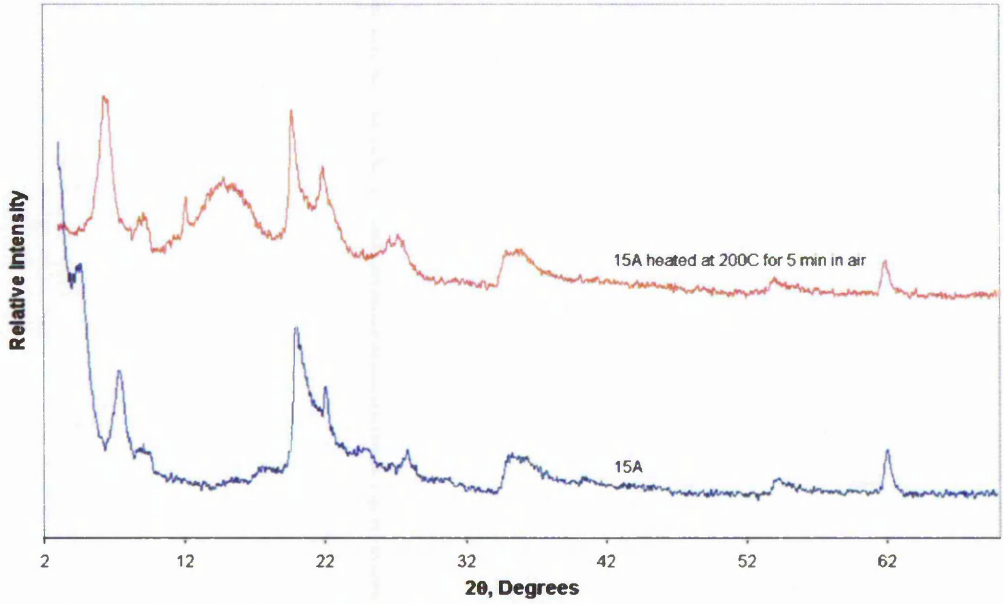

Figure 4-17 XRD patterns of 15A and the heated 15A

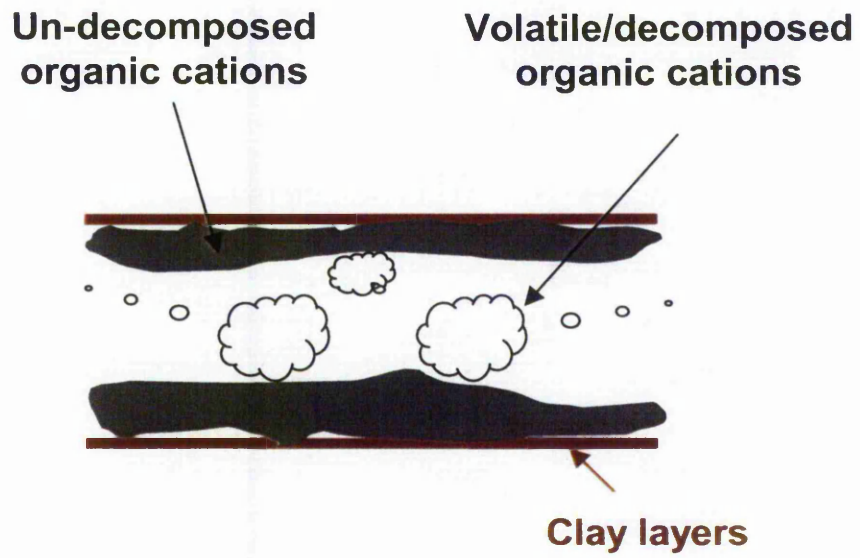

Figure 4-18 Diagram of the thermal degradation for organoclays

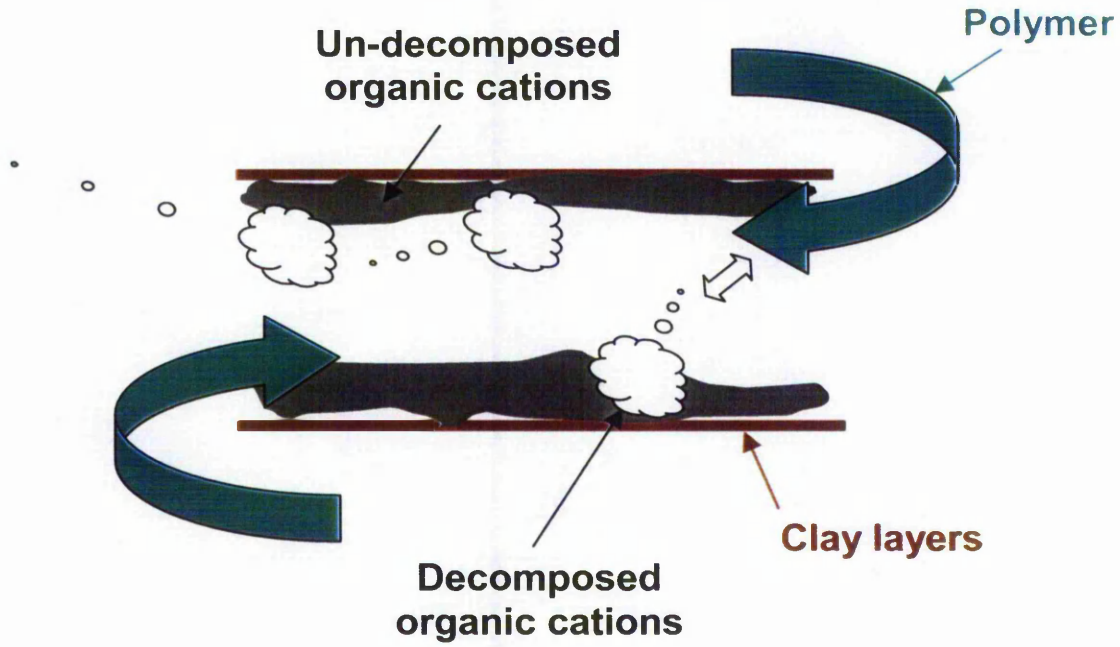

Figure 4-19 Diagram of the thermal degradation for organoclays in the presence of polymer

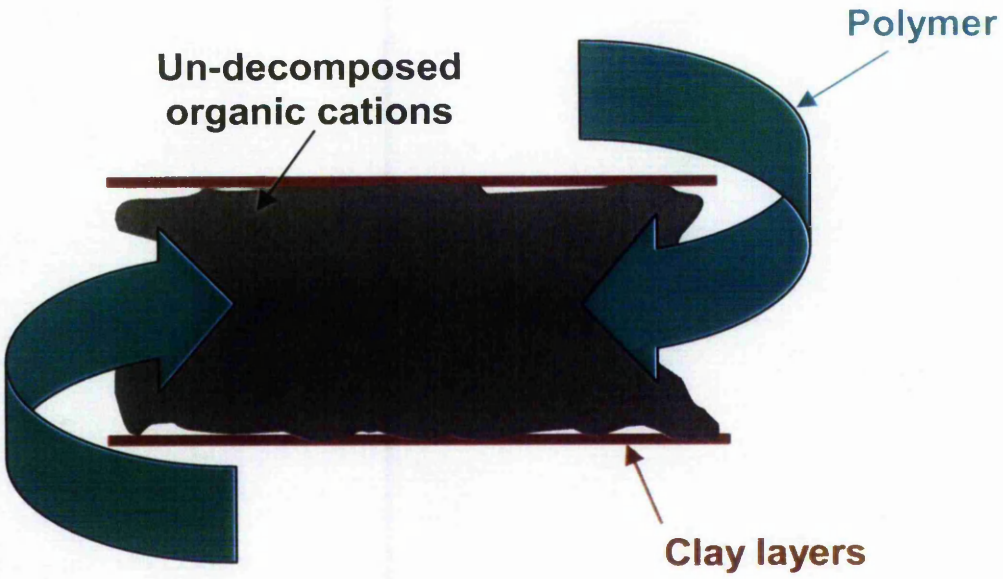

Figure 4-20 Diagram of the advantage of solid intercalation

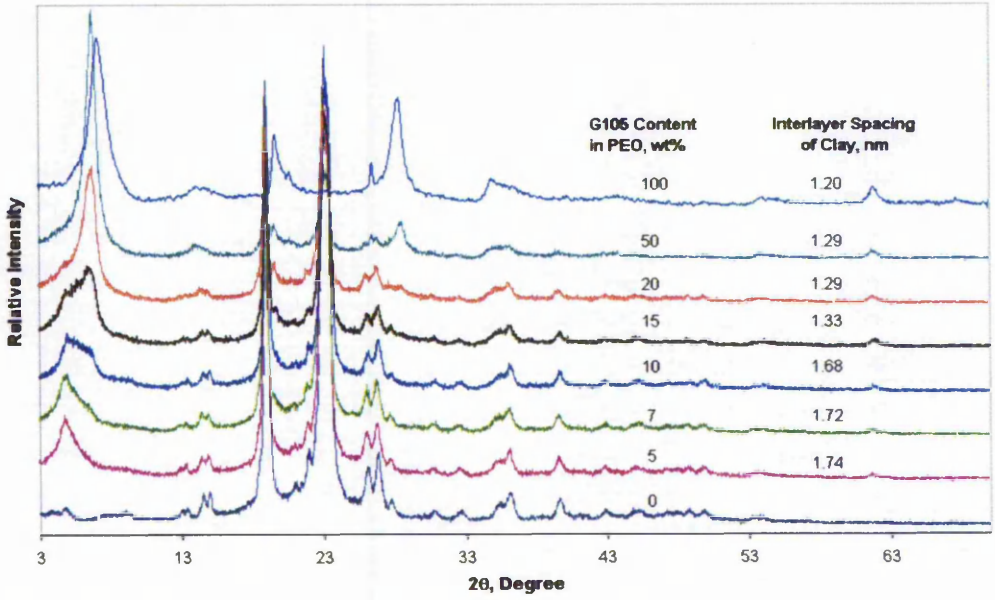

Figure 4-21 XRD patterns of the composites produced from the PEO and the hydrophilic clay, G105, by solid intercalation.

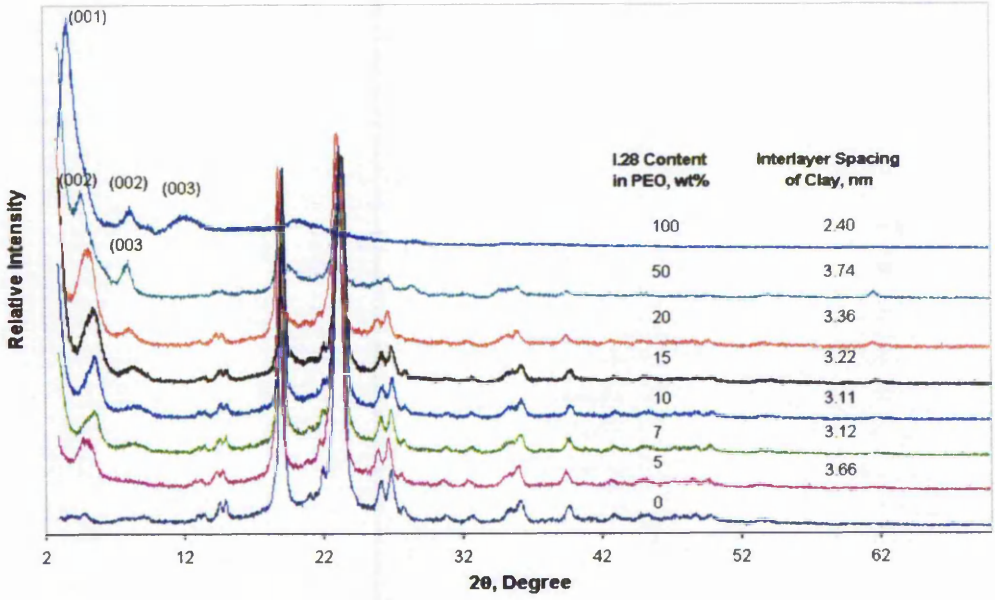

Figure 4-22 XRD patterns of the composites produced from the PEO and the organoclay, I.28, by solid intercalation.

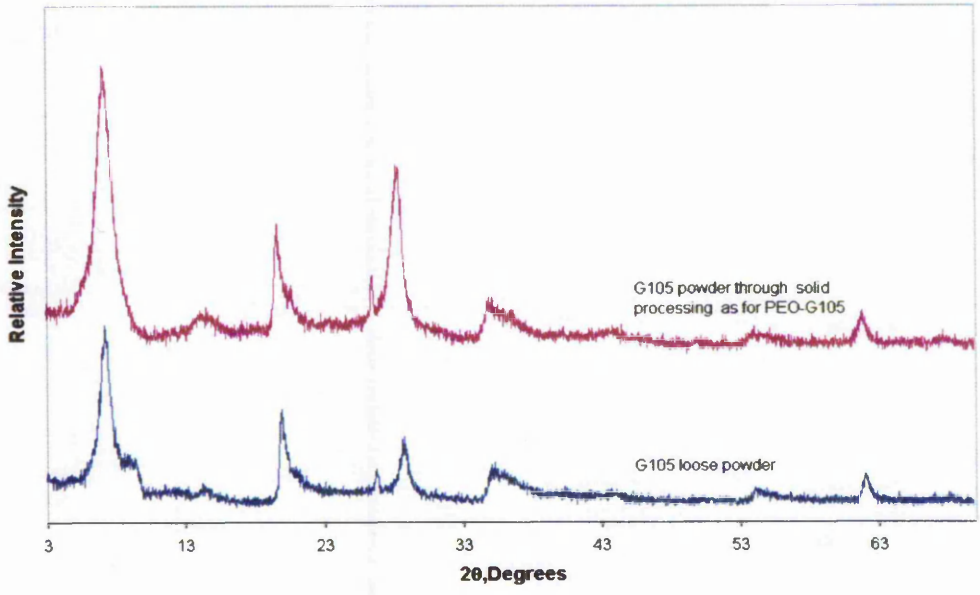

Figure 4-23 XRD patterns of the hydrophilic clay G105 loose power and G105 power compressed using the same condition as applied to the PEO-G105 composites

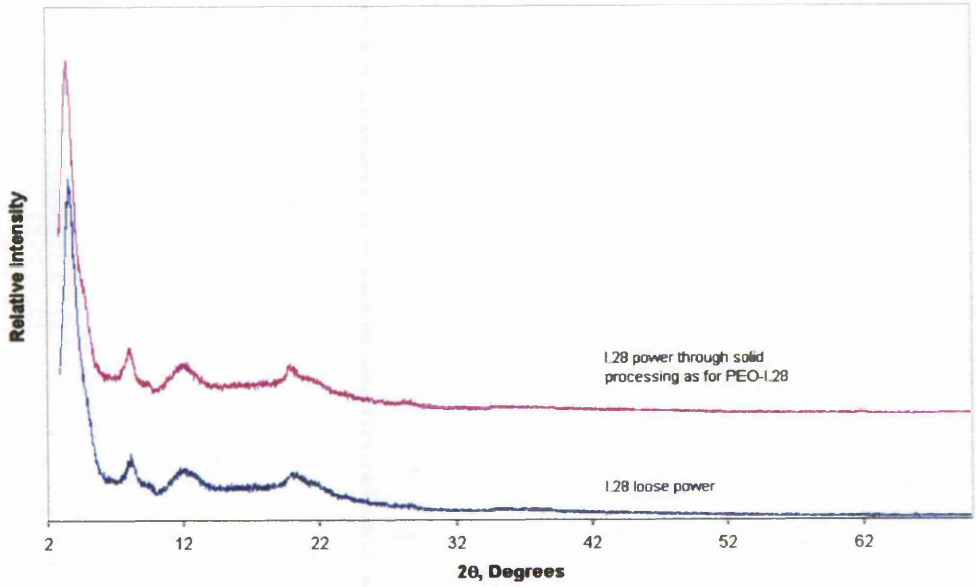

Figure 4-24 XRD patterns of the organoclay I.28 loose power and I.28 power compressed using the same condition as applied to PEO-I.28 composites

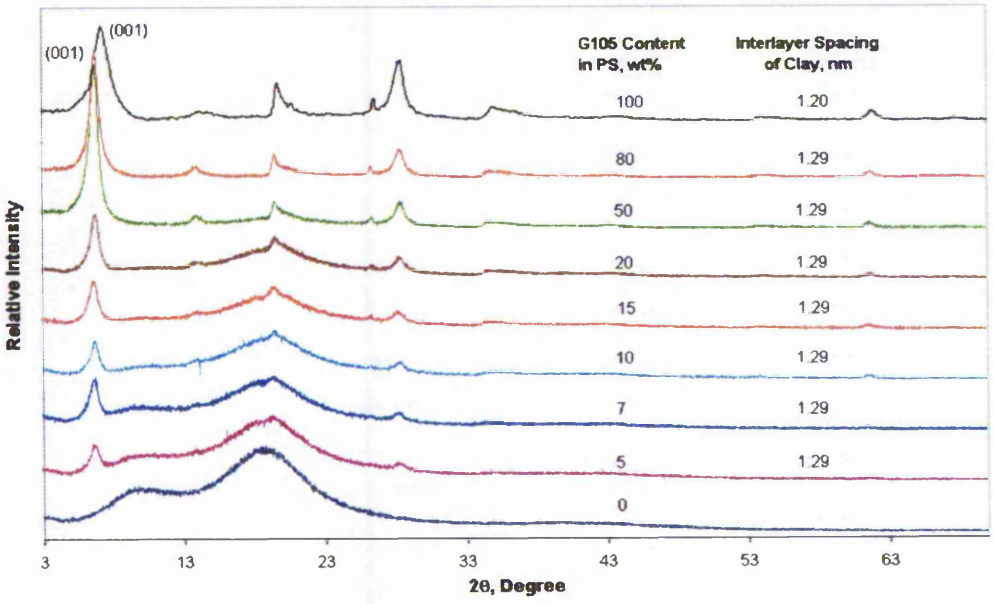

Figure 4-25 XRD patterns of the composites produced from the polystyrene and the hydrophilic clay, G105, by solid intercalation.

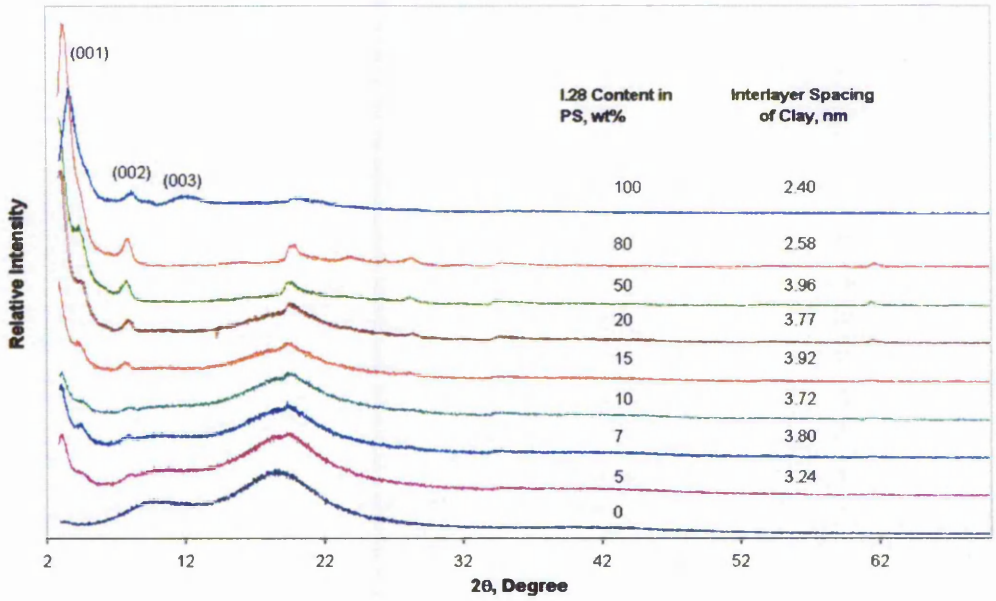

Figure 4-26 XRD patterns of the composites produced from the polystyrene and the organoclay, I.28, by solid intercalation.

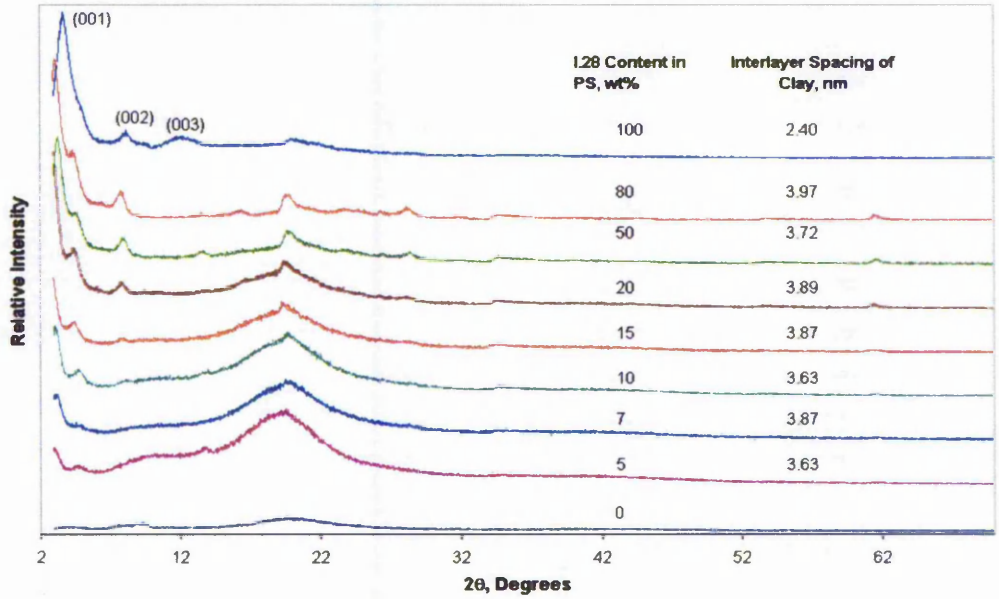

Figure 4-27 XRD patterns of the composites produced from the polystyrene and the organoclay, I.28, by solid intercalation, annealing at 120 °C for two hours in vacuum.

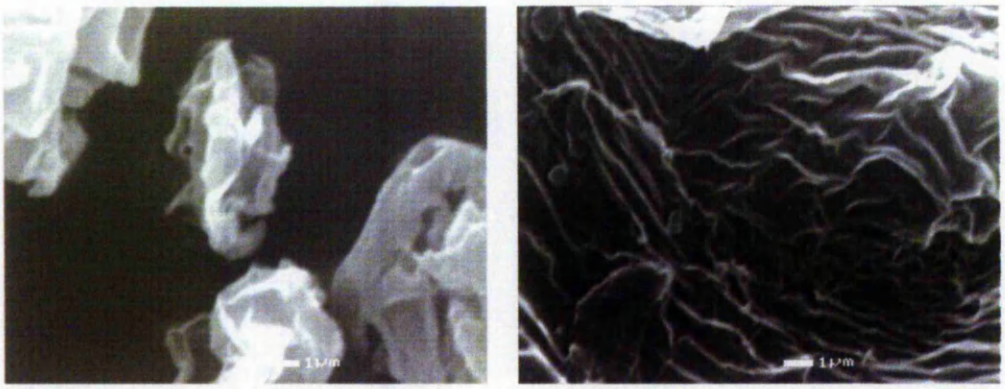

(a). Hydrophilic clay, G105 (×18400) (b). PEO-G105 nanocomposite (×18400)

Figure 4-28 SEM micrographs of hydrophilic clay G105 and PEO-G105 nanocomposite produced by solid intercalation at high magnification

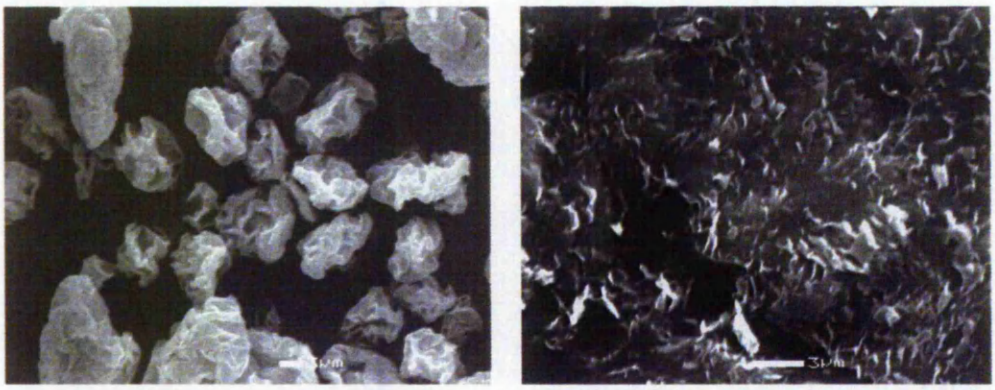

(a). Hydrophilic clay, G105 (×4460) (b). PEO-G105 nanocomposite (×9000)

Figure 4-29 SEM micrographs of hydrophilic clay G105 and a fractured surface of PEO-G105 nanocomposite produced by solid intercalation at a relatively low magnification

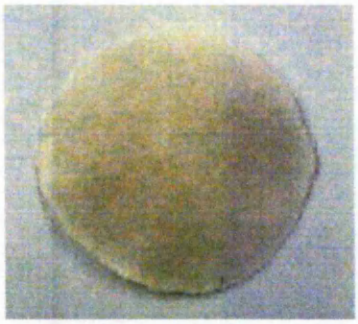

Figure 4-30 The morphology of solid polymer/hydrophilic clay G105 mixtures following the compression (same size as the sample)

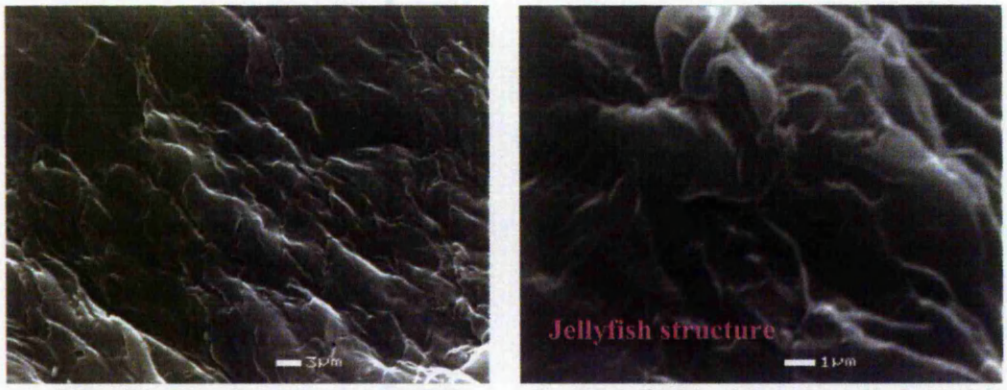

(a). PEO-G105 nanocomposite (×4460) (b). PEO-G105 nanocomposite (×18400)

Figure 4-31 SEM micrographs of PEO/clay nanocomposites with 5wt% clay content produced using solution synthesis

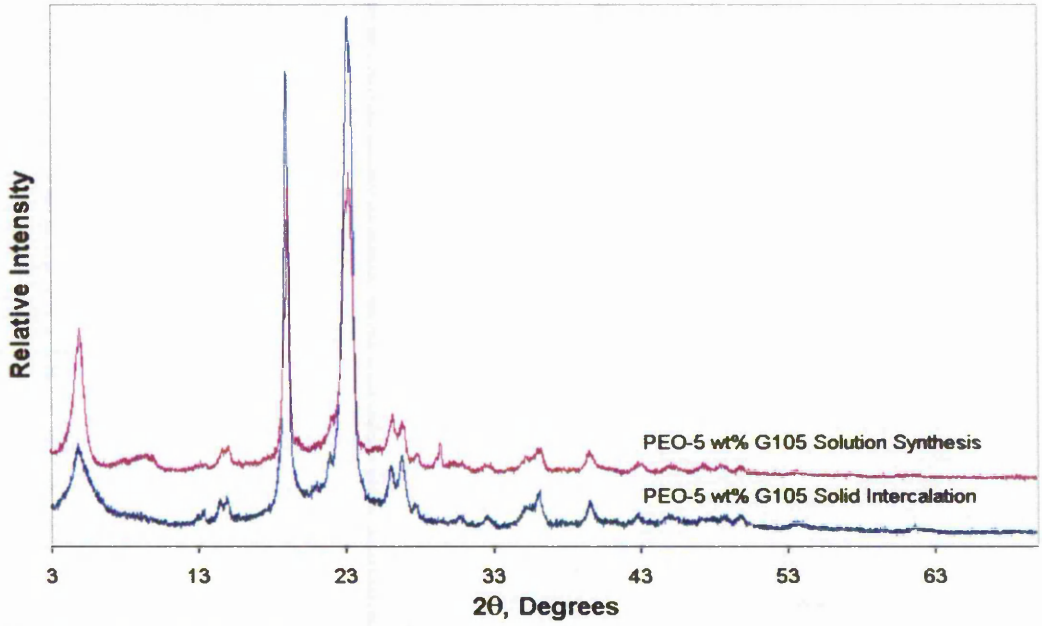

Figure 4-32 XRD patterns of PEO-5 wt% G105 composites produced by solid intercalation and solution synthesis, respectively.

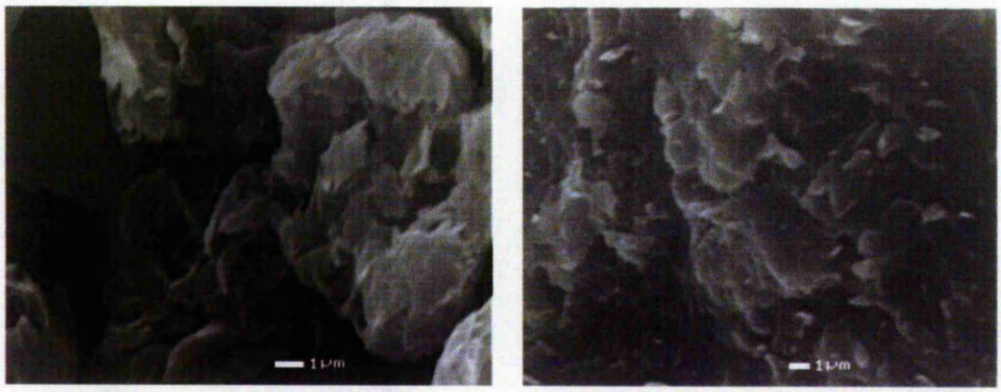

(a). Organoclay, I.28 (×18400) (b). PS-I.28 nanocomposite (×14800)

Figure 4-33 SEM micrographs of organoclay, I.28 and PS- I.28 composite produced using solid intercalation

Figure 4-34 Morphology of the burned residue from the pure PEO film

(a). The composite with 5 wt% clay

(b). The composite with 20 wt% clay

(c). The composite with 50 wt% clay

Figure 4-35 Morphology of the burned residue from PEO-G105 composites with different clay content produced using solution synthesis

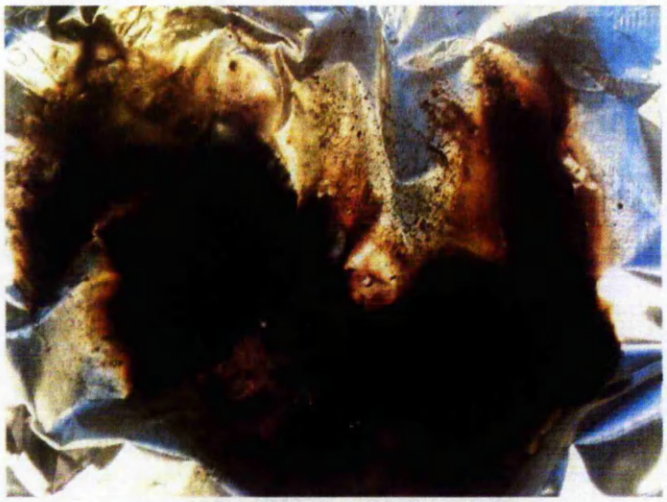

(a). The composite with 5 wt% clay

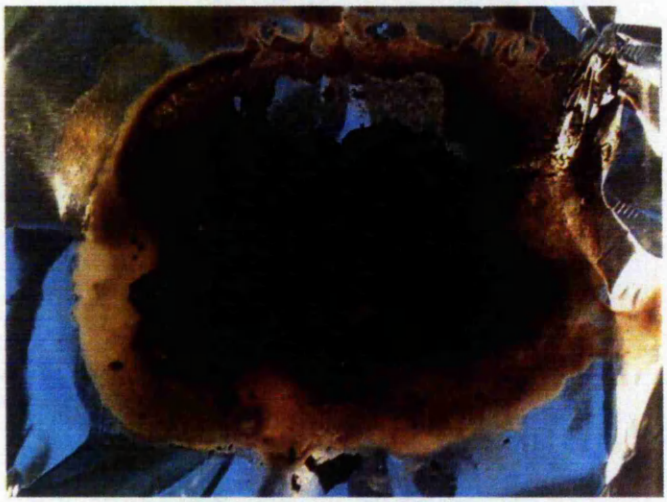

(b). The composite with 20 wt% clay

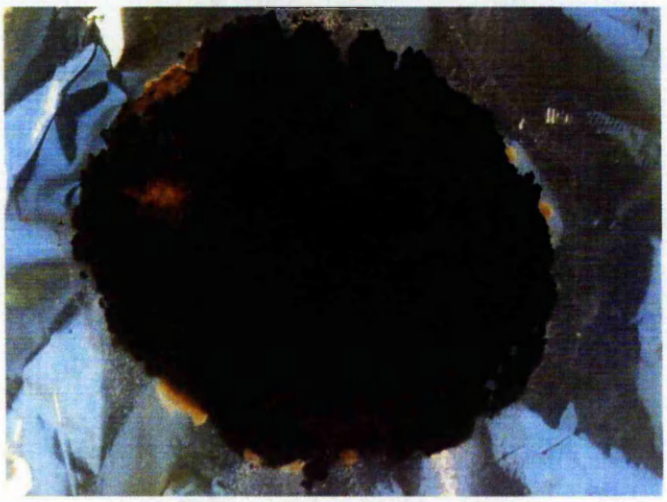

(c). The composite with 50 wt% clay

Figure 4-36 Morphology of the burned residues from the PEO-G105 composites produced using solid intercalation

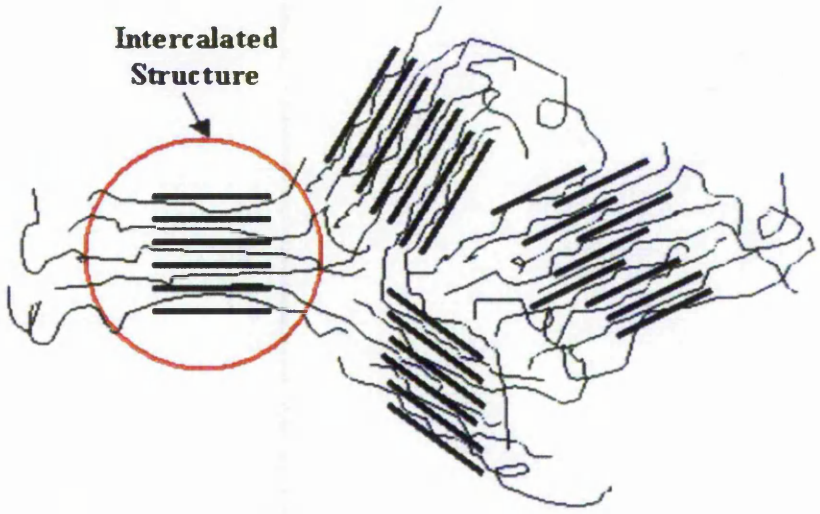

Figure 4-37 solution synthesis – all the polymer molecules took part in the intercalation

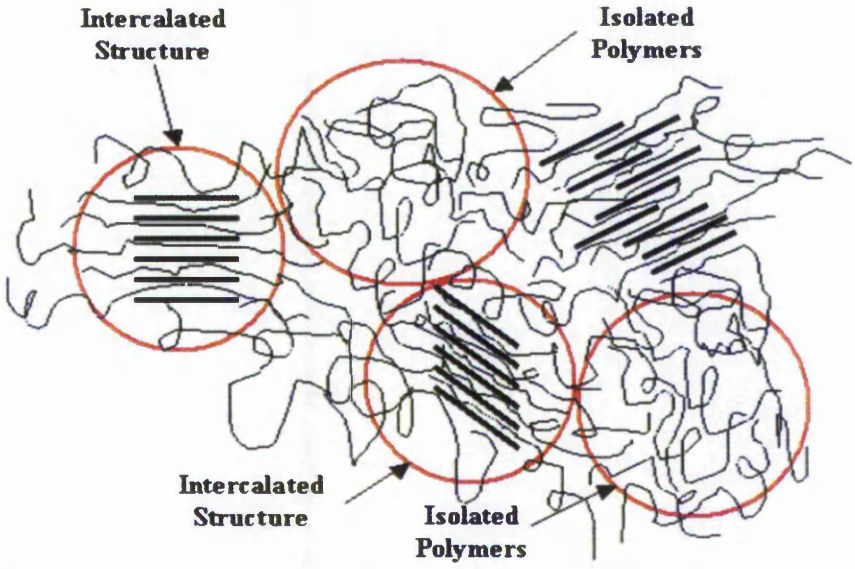

Figure 4-38 solid intercalation reaction – all the clay particles participated in the intercalation, while not all the polymer took part in intercalation

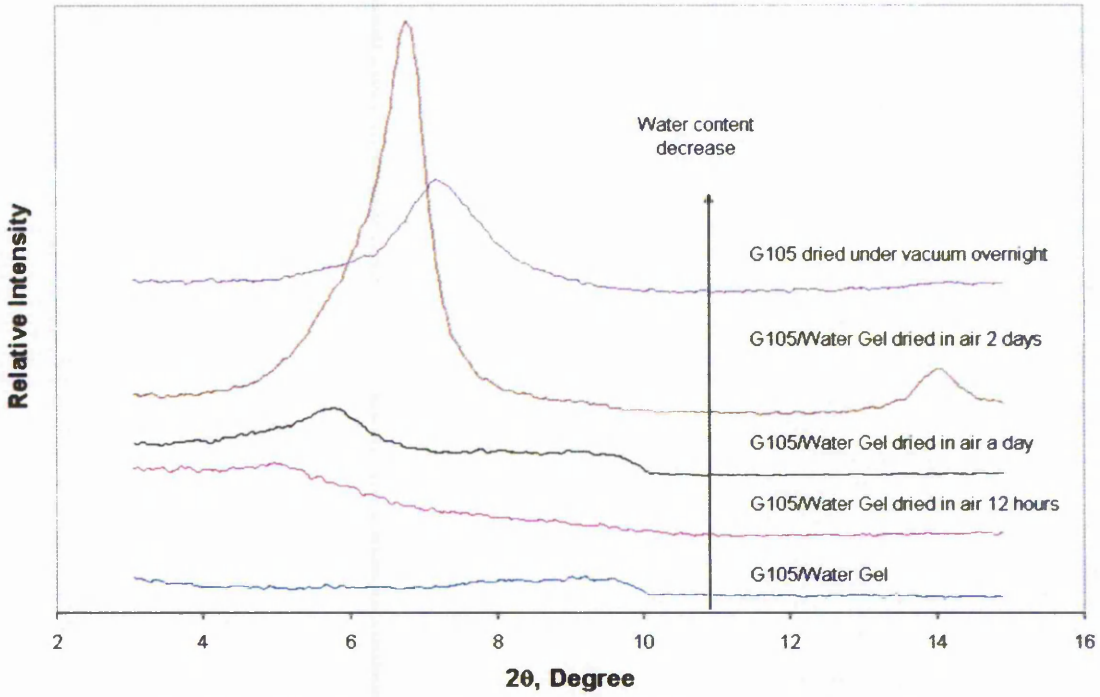

Figure 4-39 The effect of water content on the interlayer spacing of the hydrophilic clay, G105

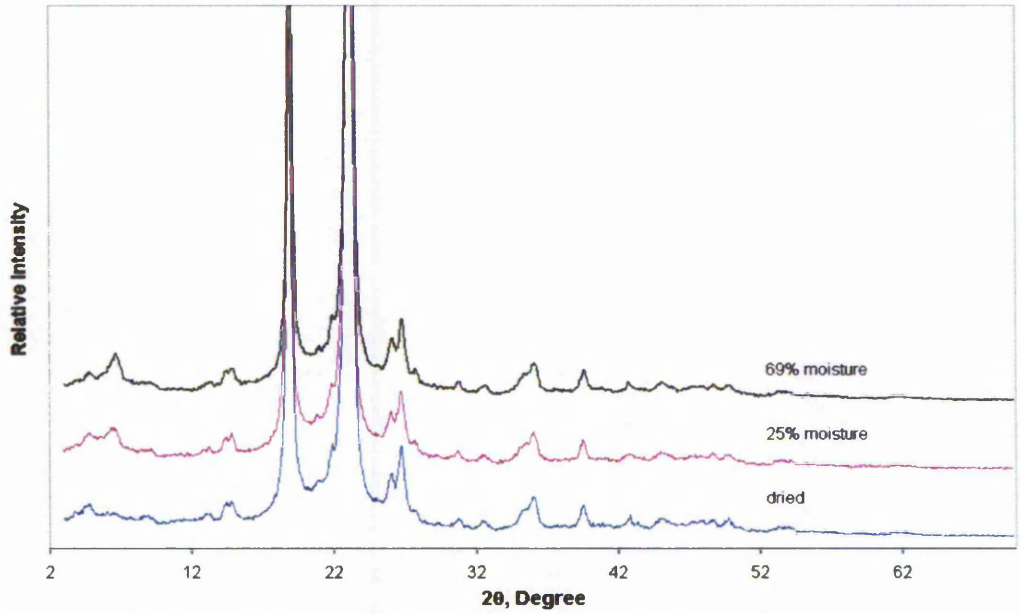

Figure 4-40 The effect of moisture on the extent of intercalation in solid synthesis based on the mixture of PEO with 5 wt% hydrophilic clay, G105

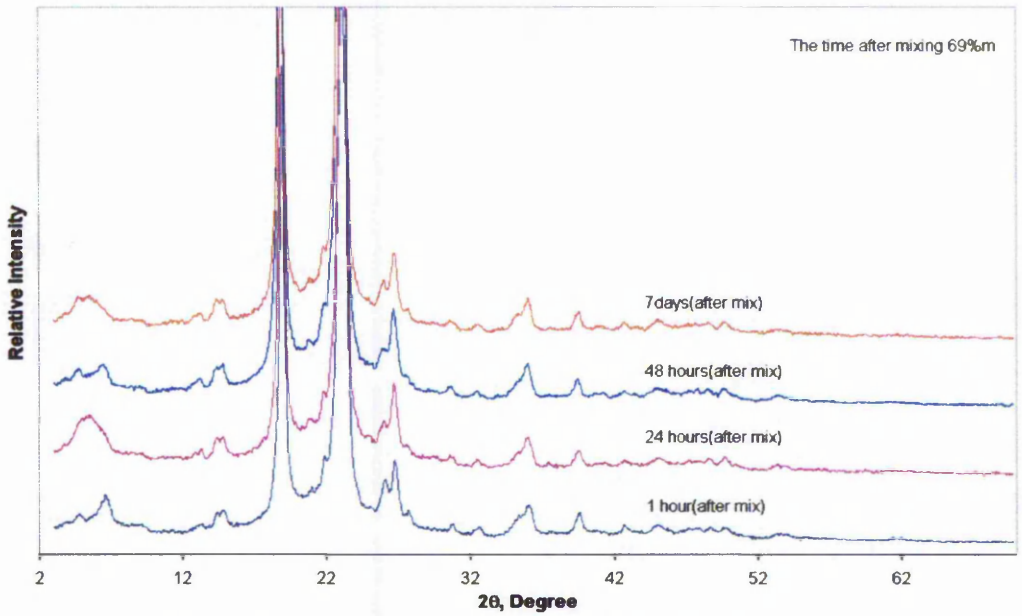

Figure 4-41 The effect of exposure time in 69% moisture on the extent of intercalation in solid synthesis based on the mixture of PEO with 5wt% clay G105

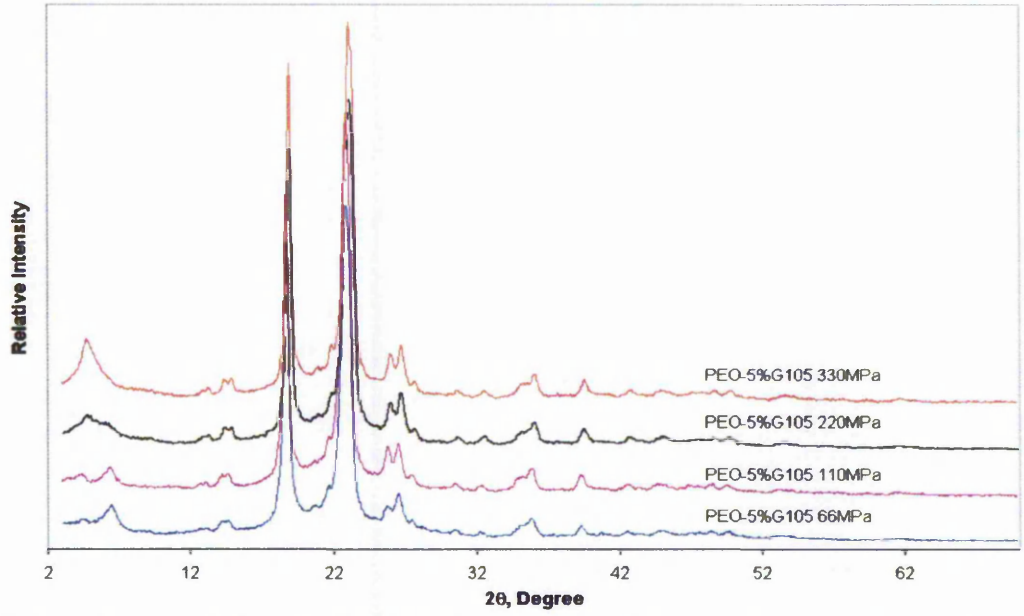

Figure 4-42 The effect of pressure on the extent of intercalation in solid synthesis based on the mixture of PEO with 5 wt% clay G105

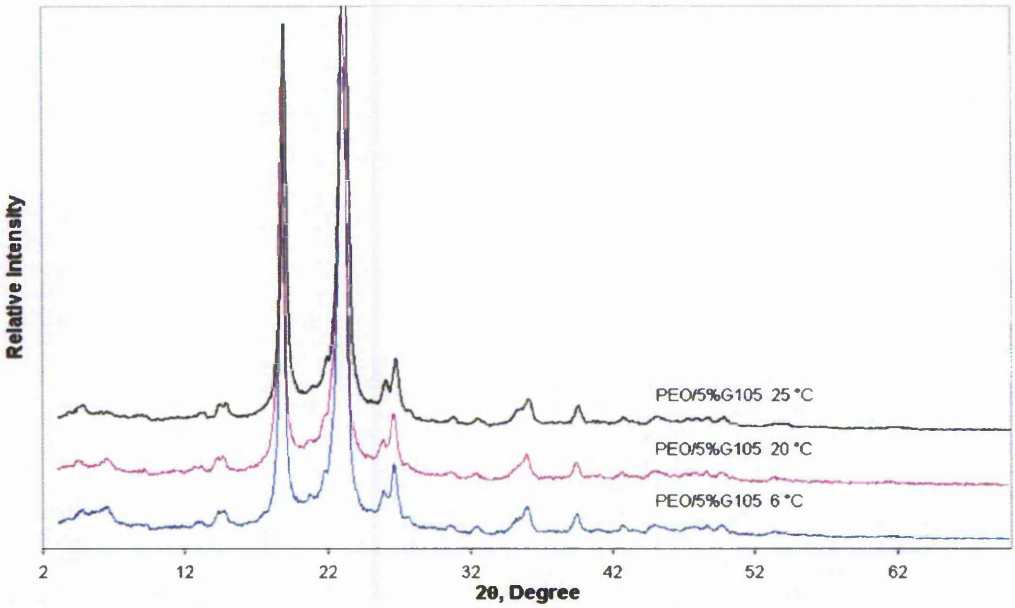

Figure 4-43 The effect of temperature on the extent of intercalation in solid synthesis based on the mixture of PEO with 5 wt% clay G105

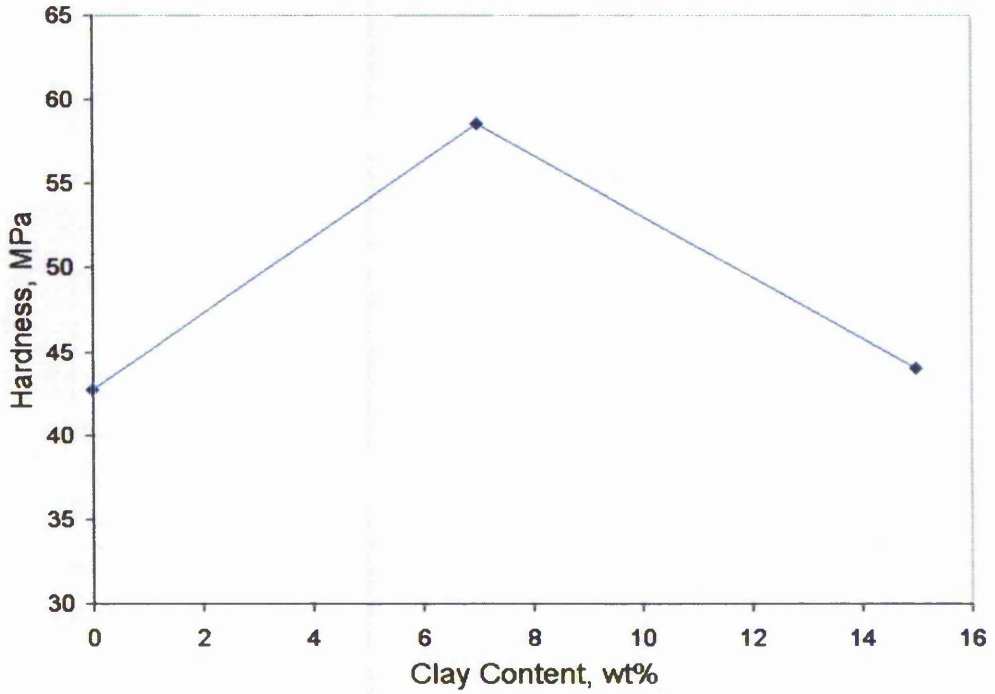

Figure 4-44 Hardness vs clay content of PEO-G105 composites produced using solid synthesis

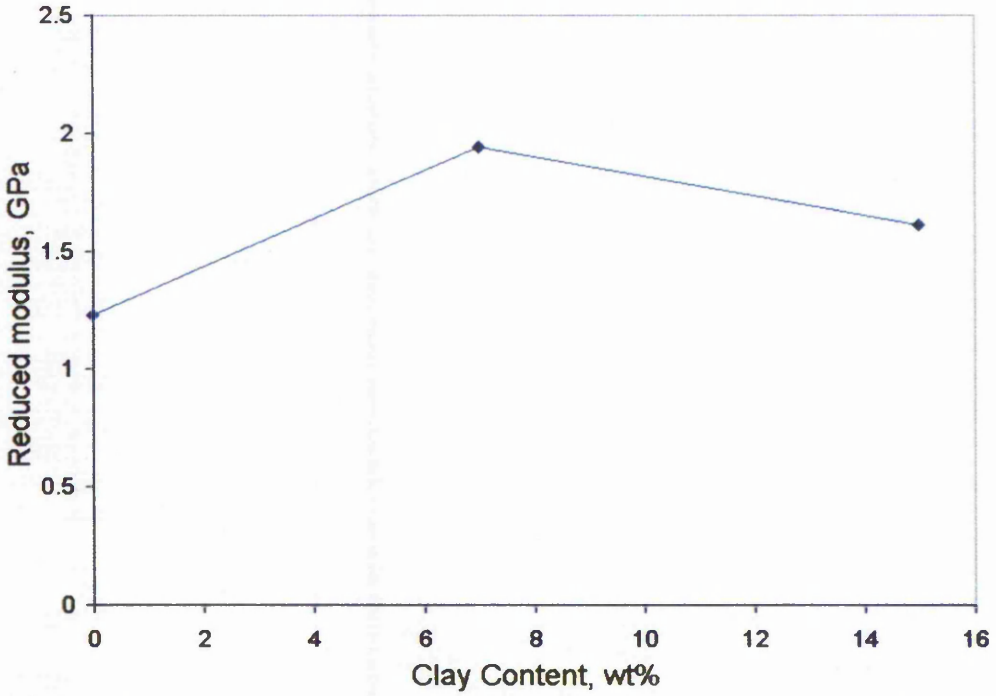

Figure 4-45 Reduced modulus vs clay content of PEO-G105 composites produced using solid synthesis

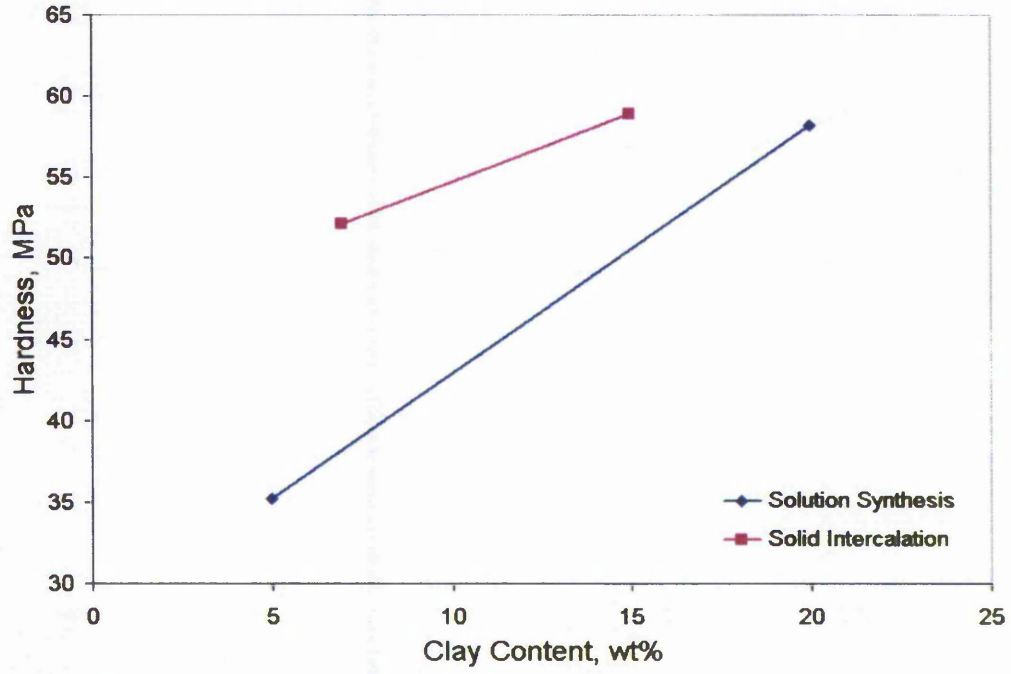

Figure 4-46 Hardness vs clay content of PEO-I.28 nanocomposites produced using solution and solid synthesis

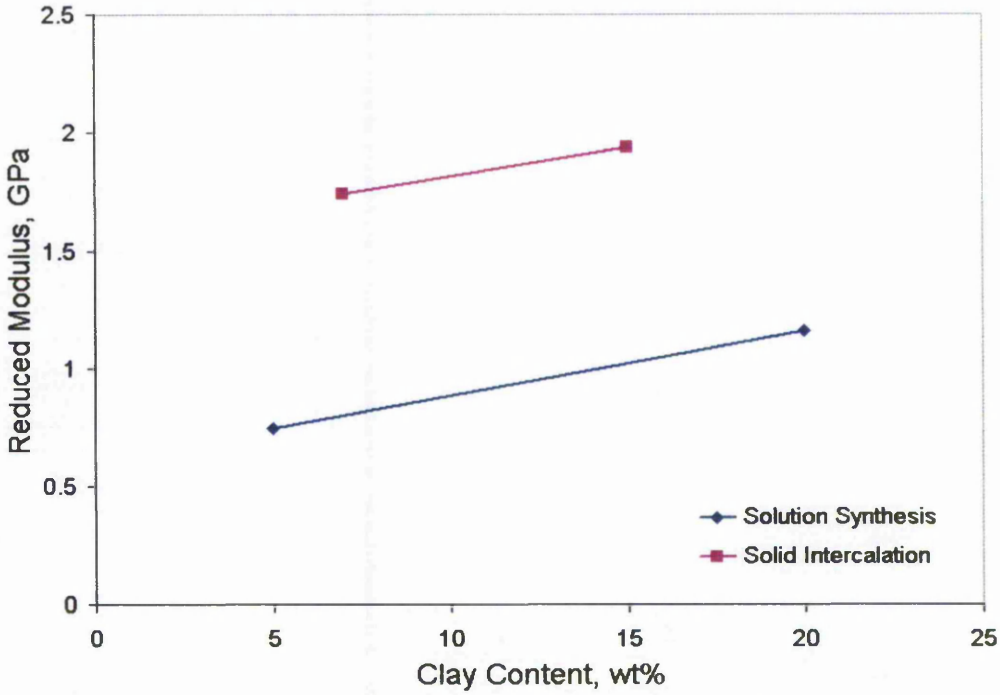

Figure 4-47 Reduced modulus (Er) vs clay content of PEO-I.28 nanocomposites produced using solution and solid synthesis

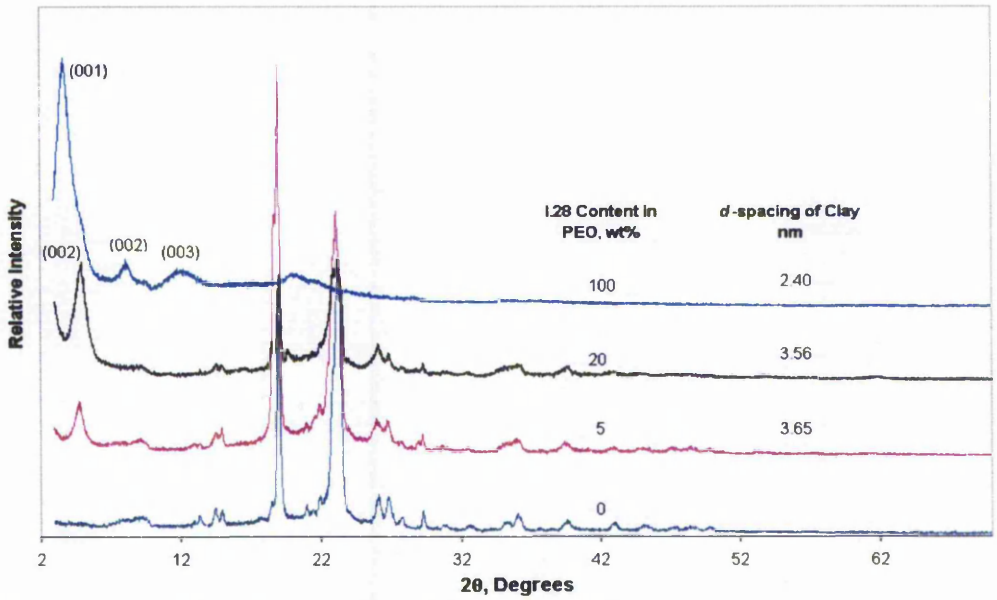

Figure 4-48 XRD patterns of PEO-I.28 composites from solution synthesis

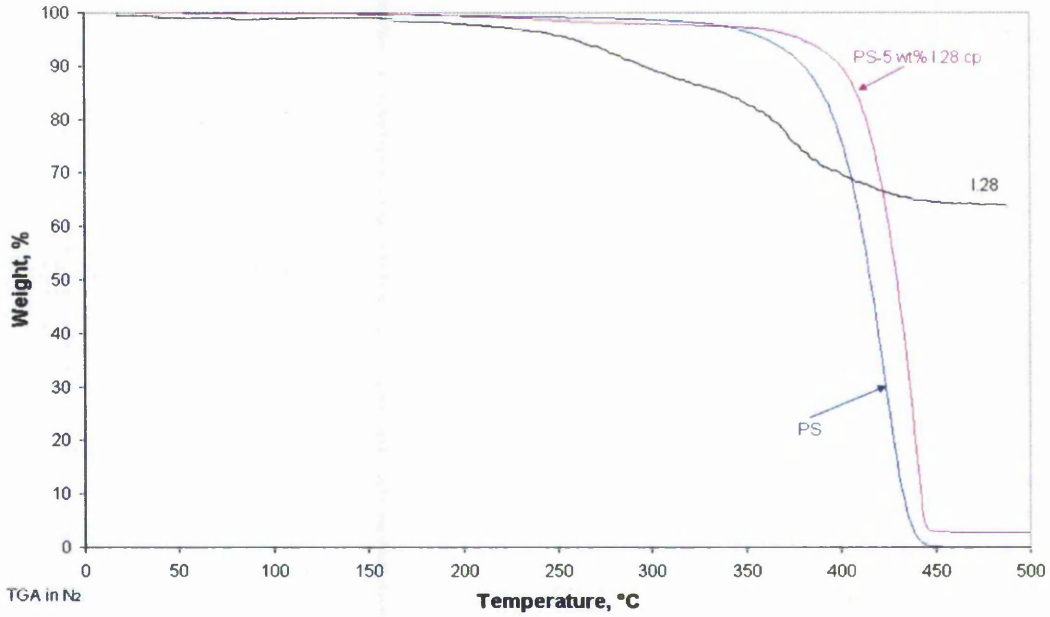

Figure 4-49 TGA diagrams of pure polystyrene, polystyrene/organoclay nanocomposites and I.28 in a nitrogen atmosphere

Tables for Chapter 4

Table 4-1 The apparent aspect ratio of clay tactoids

Clay Type	βa	2θa	βc	2θc	d(001), nm	(Lc/La)e
Nanomer ® G105	2	20.1	4.5	7.3	1.2	0.76
Cloisite ® NA+	1.5	19.66	6.9	7.46	1.18	0.44
Nanomer ® I.28	1.8	20.12	4.1	3.68	2.4	2.44
Nanomer ® I.30	2.2	20.28	3.7	3.68	2.4	3.11
Cloisite ® 93A	2.6	20.06	3.6	3.8	2.33	3.38
Cloisite ® 20A	3.2	20.22	5.5	3.76	2.35	2.72

Table 4-2 The residue yield of clays after the TGA test

	Residue yield	
Clay Type	In Nitrogen	In Air
Nanomer ® G105	93.6%	-
Cloisite ® NA+	92.3%	-
Nanomer ® I.28	64.2%	-
Nanomer ® I.30	64.2%	79.2%
Cloisite ® 93A	67.4%	78.4%
Cloisite ® 20A	64.7%	72.6%
Cloisite ® 15A	57.3%	69.2%

Table 4-3 The interlayer spacing of clays after the aging test

Clay Type	d(001) before aging test, nm	d(001) after aging test, nm
Nanomer ® I.28	2.4	1.37
Nanomer ® I.30	2.4	1.37
Cloisite ® 93A	2.33	1.31
Cloisite ® 20A	2.35	1.39
Cloisite ® 15A	3.66	1.35

Table 4-4 The ratio of the peak intensities between $2\theta = 4.98$ and $2\theta = 6.72$ related to the effect of the temperature on the intercalation

Temperature, °C	Ratio of the peak intensities
25	2:1
20	7:8
6	9:11

Chapter 5 CONCLUSIONS

The nano-structure, micro-structure and thermal stability of unmodified clays and organoclays from different manufacturers have been studied using XRD, SEM, TGA and a thermal aging test. Based on the data obtained, the problems of the current nanocomposite technology especially melt processing were examined and the clays used in this research were selected. The efficiency of the intercalation by melt processing is affected by the degradation of the organoclays, thus an organoclay I.28 was used to develop a new method to produce polymer/clay nanocomposites. A hydrophilic clay G105 was investigated to see if it is possible to be used directly to produce polymer/clay nanocomposites.

A fourth method, namely solid intercalation, to produce polymer/clay nanocomposites has been developed. Well-intercalated nanocomposite structures of polyethylene oxide and polystyrene with the hydrophilic clay, G105 and the organoclay, I.28 have been produced using this method. The clay layer expansion in the polymer/clay nanocomposites depends on the clay, the polymer and the interactions between the polymer and the clay. The mechanism of solid intercalation has been discussed based on the polymer/clay system used. For the polymer/clay system studied, organoclay I.28 can be well dispersed and expanded in both polymers with the clay content up to 80 wt%. Hydrophilic clay can be well dispersed and expanded in PEO at the clay content below 10 wt%.

A comparison between solid intercalation and an established method, solution method, was carried out for crystalline polymer PEO/clay system using SEM and the burning test. Polyethylene oxide was selected due to its solubility in water and its potential use in polymeric electrolytes for lithium batteries. The SEM and the burning test results indicate that melting of the PEO occurred during the solid intercalation process, but the polymer chain movement is limited to the region close to the clay layers in the PEO/clay system examined. The nanocomposites produced by solid intercalation are composed of isolated polymer, intercalated/exfoliated polymer/clay structures. During the solution synthesis of the PEO/clay system, the polymer dissolves; thus almost every polymer molecule participated in the intercalation reaction. However, there is a limit in producing exfoliated

nanocomposites with current clays using solution synthesis due to the clay layers' expansion being reduced during the release of the solvent. This problem can be avoided in the solid intercalation process.

Polystyrene was studied because it is a commonly used amorphous polymer and its glass transition temperature is more than 80 °C above the process temperature of solid intercalation. The effectiveness of solid intercalation in such a material has the potential to produce master-batch materials commercially. In the solid intercalation of this brittle amorphous polymer PS/clay system, the mechanism of the reaction is complicated. Scanning electron microscopy was used to observe the micro-structure of the PS/clay composite. The results showed the evidence of the formation of an intercalated structure. The intercalation is caused by the pre-inserted organic groups between the clay layers "dissolving" the PS under the high pressure. From this SEM and above XRD results, it can be concluded that a master-batch material can be produced based on PS/organoclay system with the clay content up to 80 wt%.

Studies of the processing conditions of solid intercalation of a water soluble polymer with a clay were carried out using PEO with 5 wt% G105 clay. The results show that the moisture level is critical in producing the composites by solid intercalation. There are two possible mechanisms for producing the composites. The first mechanism is by the melt and flow of polymer into the clay galleries. The second mechanism is that the polymer dissolves in any moisture present and the solution flows into the clay layers. At zero or low moisture levels, the first mechanism appears to occur, and very low moisture levels may even slow the intercalation of clay and polymer down. When the moisture levels increases above 69% in this case, the second mechanism takes over and there is considerable clay layer expansion. The results also show that high pressure and temperature improve the melt and flow of the polymer in solid intercalation which encourages more intercalation to take place.

The mechanical behaviour of PEO/clay nanocomposites produced using both solid intercalation and solution synthesis were studied through nanoindentation test. The hardness and reduced modulus of the nanocomposites produced using both methods are improved compared to the base polymer because of the formation of the nanostructure. The results show that the solid intercalated composites are harder and stiffer than solution-synthesised materials. The improved mechanical properties of

the solid intercalated composites offer a potential for applying solid intercalation directly in producing small components such as electrolytes in the future.

The thermal behaviour of a polystyrene/organoclay nanocomposite produced using solid intercalation has been studied using TGA. The results show that the solid intercalated composites have significantly improved thermal properties – the main weight loss temperature increased 16 °C. This indicates that both the organoclay and the polymer will be protected due to the formation of the nanostructure during the traditional processing temperature for the polymer. Using a master batch of this polymer/organoclay system offers the opportunity to use the existing available organoclays to produce high quality nanocomposites by using a combined approach involving both solid intercalation and melt processing.

The research shows that the solid intercalation technique is an effective method to produce polymer/clay nanocomposites. There is the potential to use this method in commercial application such as producing polymer electrolyte nanocomposites. Master batches can be produced which can then processed with conventional polymer processing equipment to produce polymer/clay nanocomposites.

Chapter 6 RECOMMENDATIONS FOR FURTHER WORK

The major work in the PhD project was focused on solid intercalation technique development. This technique can be directly used to produce polymer/clay nanocomposites or make a master batch material which can be processed in conventional polymer processing equipment to produce polymer/clay nanocomposites.

The following are some recommendations for future work based on the understanding in the research area of polymer/clay nanocomposites.

Further studies on the mechanism and structure of the nanocomposites, produced by solution and solid intercalation process, needs to be carried out using a transmission electron microscope so that a full comparison of the structures can be carried out. This would increase the understanding of the relationships between the different materials in the composites.

Organoclay I.28 is more promising in the formation of intercalated or exfoliated polymer/clay nanocomposites with high clay content than hydrophilic clay G105 according to the results. To investigate the Nanocor organoclay I.30, the Cloisite organoclays and other organoclays available in polymer/clay systems by solid intercalation will enhance the potential of commercially producing the polymer/clay nanocomposites directly and obtaining the master batch materials at any clay content without the degradation of the organoclays.

The research needs to be expanded from PEO and PS to other commercial polymers, for example, polypropylene, high density polyethylene, polyester, poly(methyl methacrylate) and polyurethane for the commercial production of nanocomposites. Each polymer system will have its own specific problems which will be related to its structure, for example polypropylene has a crystallinity of ~93%, while the polyethylenes have various degrees of crystallinity and poly(methyl methacrylate) is an amorphous polymer. There will be benefits if solid intercalation can improve the dispersion and expansion of the clay layers in these polymer matrices.

To gain a complete understanding of how organoclays being intercalated with thermoplastics, more extensive studies of the processing conditions in solid intercalation producing polymer/clay nanocomposites need to be done. In this case, pressure and temperature are probably more significant than moisture since most of the thermoplastics are not affected much by water and it is usual for commercial users to dry the polymer before use. There are other factors, which need to be considered, the granule size of the polymer, the time the polymer and clay are subjected to pressure and how to achieve a specific loading in a polymer to give the nanocomposite the required mechanical properties.

The laboratory experiments where done at 6 ° to 25 °C, for PEO, this was well below the melting point of the polymer. In the case of common thermoplastics, higher temperatures could be considered. What temperatures used would have to be determined by the degradation temperatures of the polymer and the organoclays. The glass transition temperatures may play an important role here, as there is a volume change at these temperatures, which may affect the solid intercalation process. The higher processing temperatures would also improve the mobility of the polymer chains.

The solid intercalation process has been shown to be pressure dependent. Experiments can be carried out to determine if there is a maximum pressure beyond which solid intercalation decreases. This may also relate to the time the pressure is applied and the granule size. In the polystyrene and PEO experiments a powder form of the polymer was used, there may be an optimum size of polymer granule where intercalation at a specific pressure will occur. Time and pressure are important in deciding how to commercially produce nanocomposite materials. In the laboratory a flat press was used to make the intercalated polymers, but commercially a roller mill may be an easier option, which is why, pressure, time and granule size are important and require investigating. Processing in this way would make master batches which could then be processed conventionally.

Different polymers will have different unique processing problems, therefore the processing conditions in producing polymer/clay nanocomposites by solid intercalation need to be investigated individually.

REFERENCES

[1] Kojima Y. et al, Mechanical-properties of nylon 6-clay hybrid, Journal of Materials Research, 8(5), 1185-1189, 1993

[2] Kojima Y. et al, Sorption of water in nylon-6 clay hybrid, Journal of Applied Polymer Science, 7, 1259-1264, 1993

[3] Gilman J.W., Flammability and thermal stability studies of polymer layered silicate (clay) nanocomposites, Applied Clay Science, 15, 31-49, 1999

[4] LeBaron P.C., Wang Z. and Pinnavaia T.J., Polymer-layered silicate nanocomposites: an overview, Applied Clay Science, 15, 11-29, 1999

[5] Lagaly G., Introduction: from clay mineral-polymer interactions to clay mineral-polymer nanocomposites, Applied Clay Science, 15, 1-9, 1999

[6] Carter L.W., Hendrichs J.G. and Bolley D.S., Elastomer reinforced with a modified clay, US 2,531,396, 1950

[7] Chem. Abs., 45, 1804d, 1951

[8] Greenland D.J., Adsorption of polyvinyl alcohols by montmorillonite, Journal of Colloid Science, 18, 647-664, 1963

[9] Blumstein A., Polymerization of adsorbed monolayers: II. Thermal degradation of the inserted polymers, Journal of Polymer Science, Part A: General Papers, 3 (7), 2665-2672, 1965

[10] Parfitt R.L. and Greenland D.J., Adsorption of poly(ethylene glycols) on montmorillonites, Clay Minerals, 8, 305-323, 1970

[11] Fujiwara S. and Sakamoto T., Method for manufacturing a clay-polyamide composite: Kokai Patent Application, no. SHO 51(1976)-109998, 1976

[12] Theng B., Clay-Polymer Interactions - Summary and Perspectives, Clays and Clay Minerals, 30, 1-10, 1982

[13] Lagaly G., Intercalation of alkylamines with different types of layered compounds, Solid State Ionics, 22, 43-51, 1986

[14] Yano K., Usuki A., Okada A., Kurauchi T. and Kamigaito O., Synthesis and properties of polyimide-clay hybrid, Journal of Polymer Science Part A: Polymer Chemistry, 31, 2493–2498, 1993

[15] Okada A. and Usuki A., The chemistry of polymer-clay hybrids, Materials Science and Engineering: C 3, 109-115, 1995

[16] Usuki A. et al., Synthesis and properties of acrylic resin clay hybrid, Kobunshi Ronbunshu 52 (11), 727-733, 1995

[17] Kojima Y., Usuki A., Kawasumi M., Okada A., Kurauchi T. and Kamigaito O., Synthesis of nylon-6-clay hybrid by montmorillonite intercalated with ε-

caprolactam, Journal of Polymer Science Part A: Polymer Chemistry, 4, 983-986, 1993

[18] Usuki A., Kawasumi M., Kojima Y., Okada A., Kurauchi T. and Kamigaito O., Swelling behavior of montmorillonite cation exchanged for ω-aminoacids by ε-caprolactam, Journal of Materials Research, 5, 1174-1178, 1993

[19] Usuki A., Kojima Y., Kawasumi M., Okada A., Fukushima Y., Kurauchi T. and Kamigaito O., Synthesis of nylon 6-clay hybrid, Journal of Materials Research, 5, 1179-1184, 1993

[20] Kojima Y., Usuki A., Kawasumi M., Okada A., Kurauchi T. and Kamigaito O., One-pot synthesis of nylon-6-clay hybrid, Journal of Polymer Science Part A: Polymer Chemistry, 31, 1755-1758, 1993

[21] Wu J. and Lerner M.M., Structural, thermal, and electrical characterization of layered nanocomposites derived from sodium-montmorillonite and polyethers, Chemistry of Materials, 5, 835-838, 1993

[22] Vaia R.A., Sauer B.B., Tse O.K. and Giannelis E.P., Relaxations of confined chains in polymer nanocomposites: Glass transition properties of poly(ethylene oxide) intercalated in montmorillonite, Journal of Polymer Science Part B: Polymer Physics, 1, 59-67, 1997

[23] Vaia R.A., Ishii H. and Giannelis E.P., Synthesis and properties of 2-dimensional nanostructures by direct intercalation of polymer melts in layered silicates, Chemistry of Materials, 5, 1694-1696, 1993

[24] Vaia R.A., Vasudevan S., Krawiec W., Scanlon L.G. and Giannelis E.P., New polymer electrolyte nanocomposites: melt intercalation of poly(ethylene oxide) in mica-type silicates, Advanced Materials, 2, 154-156, 1995

[25] Gao F., Han Z., Chen S. and Hull J.B., The current problems with the use of reactive melt processing to produce clay/polymer nanocomposites, in Proc. Organic-Inorganic Hybrids II, PRA, Guildford, 28-29, 2002

[26] Alexandre M. and Dubois P., Polymer-layered silicate nanocomposites: preparation, properties and uses of a new class of materials, Materials Science and Engineering, 28, 1-63, 2000

[27] Solomon D.H. and Hawthorne D.G., Chemistry of Pigments and Fillers, Publisher: Krieger Publishing Company, ISBN: 0894646206, 1983

[28] Jordan J.W., Organophilic bentonites, Journal of Physical and Colloid Chemistry, 53, 294-306, 1949

[29] Weiss A., Organic derivatives of mica-type layer silicates, Angewandte Chemie International Edition, 2, 134-143, 1963

[30] Feldkamp J.R. and White J.L., Developments in Sedimentology, 27, 187, 1979

[31] Chem. Abs., 90, 175345, 1979

[32] Lan T., Kaviratna P.D. and Pinnavaia T.J., Mechanism of clay tactoid exfoliation in epoxy-clay nanocomposites, Chemistry of Materials, 7, 2144-2150, 1995

[33] Wang Z. and Pinnavaia T.J., Hybrid organic-inorganic nanocomposites: exfoliation of magadiite nanolayers in an elastomeric epoxy polymer, Chemistry of Materials, 10, 1820-1826, 1998

[34] Vaia R.A., Teukolsky R.K. and Giannelis E.P., Interlayer Structure and Molecular Environment of Alkylammonium Layered Silicate, Chemistry of Materials, 6, 1017-1022, 1994

[35] Kornmann X., Berglund L.A., Sterte J. and Giannelis E.P., Nanocomposites Based on Montmorillonite and Unsaturated Polyester, Polymer Engineering & Science, 38, 1351-1358, 1998

[36] http://www.koreaplastic.org/pds/2002japan3.asp

[37] Gultek A., Seckin T., Onal Y. and Icduygu M.G., Poly(methacrylic) acid and γ-methacryloxypropyltrimethoxy silane/clay nanocomposites prepared by in-situ polymerization, Turkish Journal of Chemistry, 26 (6), 925-937, 2002

[38] Seckin T., Gultek A., Icduygu M.G. and Onal Y., Polymerization and characterization of acrylonitrile with γ-methacryloxypropyltrimethoxy-silane grafted bentonite clay, Journal of Applied Polymer Science, 84 (1), 164-171, 2002

[39] Song K. and Sandi G., Characterization of montmorillonite surfaces after modification by organosilane, Clays and Clay Minerals, 49 (2), 119-125, 2001

[40] Manias E., Touny A., Wu L., Strawhecker K., Lu B. and Chung T.C., Polypropylene/montmorillonite nanocomposites: review of the synthetic routes and materials properties, Chemistry of Materials, 13 (10), 3516-3523, 2001

[41] Laus M., Camerani M., Lelli M., Sparnacci K., Sandrolini F. and Francescangeli O., Hybrid nanocomposites based on polystyrene and a reactive organophilic clay, Journal of Materials Science, 33, 2883-2888, 1998

[42] Hoffmann B., Dietrich C., Thomann R., Friedrich* C. and Mülhaupt R., Morphology and rheology of polystyrene nanocomposites based upon organoclay, Macromolecular Rapid Communications, 21 (1), 57-61, 2000

[43] Weimer M.W., Chen H., Giannelis E.P. and Sogah D.T., Direct synthesis of dispersed nanocomposites by in-situ living free radical polymerisation using a silicate-anchored initiator, Journal of American Chemical Society, 121, 1615-1616, 1999

[44] Ogawa M. and Kuroda K., Preparation of inorganic-organic nanocomposites through intercalation of organoammonium ions into layered silicates, Bulletin of the Chemical Society of Japan, 70, 2593-2618, 1997

[45] Lim S.K., Kim J.W., Chin I., Kwon Y.K. and Choi H.J., Preparation and Interaction characteristics of organically modified montmorillonite nanocomposite with miscible polymer blend of poly(ethylene oxide) and poly(methyl methacrylate), Chemistry of Materials, 14, 1989-1994, 2002

[46] Chen W., Xu Q and Yuan R.Z., The influence of polymer state on the electrical properties of polymer/layered-silicate nanocomposites, Composites Science and Technology, 61, 935-939, 2001

[47] Salahuddin N. and Akelah A., Synthesis and characterization of poly(styrene-maleic anhydride)-montmorillonite nanocomposite, Polymers for Advanced Technologies, 13 (5), 339-345, 2002

[48] Ko M.B., Kim J. and Choe C.R., Effects of the interaction between intercalant and matrix polymer in preparation of clay-dispersed nanocomposite, Polymer Journal, 8 (3), 120-124, 2000

[49] Ko M.B., Effects of acrylonitrile content on the properties of clay-dispersed poly(styrene-co-acrylonitrile) copolymer nanocomposite, Polymer Bulletin, 45 (2), 183-190, 2000

[50] Lee S.S., Lee C.S., Kim M.H., Kwak S.Y., Park M., Lim S., Choe C.R. and Kim J.Y., Specific interaction governing the melt intercalation of clay with poly(styrene-co-acrylonitrile) copolymers, Journal of Polymer Science Part B: Polymer Physics, 39 (20), 2430-2435, 2001

[51] Jeon H.G., Jung H.T., Lee S.W. and Hudson S.D., Morphology of polymer silicate nanocomposites. High density polyethylene and a nitrile, Polymer Bulletin, 41, 107-113, 1998

[52] Chang J.H. and Park D.K., Nanocomposites of poly(ethylene terephthalate-co-ethylene naphthalate) with organoclay, Journal of Polymer Science Part B: Polymer Physics, 39 (21), 2581-2588, 2001

[53] Chung T.C., Lu H.L. and Jankivul W., A novel synthesis of PP-b-PMMA copolymers via metallocene catalysis and borane chemistry, Polymer, 38 (6), 1495-1502, 1997

[54] Limary R., Swinnea S., and Green P.F., Stability of diblock copolymer/layered silicate nanocomposite thin films, Macromolecules, 33, 5227-5234, 2000

[55] Ren J., Silva A.S., and Krishnamoorti R., Linear viscoelasticity of disordered polystyrene-polyisoprene block copolymer based layered-silicate nanocomposites, Macromolecules, 33, 3739-3746, 2000

[56] Ha Y.H. and Thomas E.L., Deformation behavior of a roll-cast layered-silicate/lamellar triblock copolymer nanocomposite, Macromolecules, 35, 4419-4428, 2002

[57] Laus M., Francesangeli O. and Sandrolini F., New hybrid nanocomposites based on an organophilic clay and poly(styrene-b-butadiene) copolymers, Journal of Materials Research, 12, 3134-3139, 1997

[58] Lim Y.T. and Park O.O., Microstructure and rheological behavior of block copolymer/clay nanocomposites, Korean Journal of Chemical Engineering, 18 (1), 21-25, 2001

[59] Chen Z. and Gong K., Preparation and dynamic mechanical properties of poly(styrene-b-butadiene)-modified clay nanocomposites, Journal of Applied Polymer Science, 84 (8), 1499-1503, 2002

[60] Reichert P., Nitz H., Klinke S., Brandsch R., Thomann R. and Mulhaupt R., Poly(propylene)/organoclay nanocomposite formation: Influence of compatibilizer functionality and organoclay modification, Macromolecular Materials and Engineering, 275 (2), 8-17, 2000

[61] Reichert P., Hoffmann B., Bock T., Thomann R., Mülhaupt R. and Friedrich C.*, Morphological stability of poly(propylene) nanocomposites, Macromolecular Rapid Communications, 22 (7), 519-523, 2001

[62] Kaempfer D., Thomann R. and Mülhaupt R., Melt compounding of syndiotactic polypropylene nanocomposites containing organophilic layered silicates and in situ formed core/shell nanoparticles, Polymer, 43, 2909-2916, 2002

[63] Wang K.H., Choi M.H., Koo C.M., Choi Y.S. and Chung I.J., Synthesis and characterization of maleated polyethylene/clay nanocomposites, Polymer, 42 (24), 9819-9826, 2001

[64] Li X.C. et al. Effect of blending sequence on the microstructure and properties of PBT/EVA-g-MAH/organoclay ternary nanocomposites, Polymer Engineering Science, 42 (11), 2156-2164, 2002

[65] Manias E. et al, Polypropylene/silicate nanocomposites, synthetic routes and materials properties, Polymeric Materials: Science & Engineering, 82, 282-283, 2000

[66] Davis R.D., Jarrett W.L. and Mathias L.J., Observation of alpha and gamma crystal forms and amorphous regions of nylon-6 clay nanocomposites using solid-state N-15 nuclear magnetic resonance, ABSTR PAP AM CHEM S 219: 202-PMSE Part 2, 2000

[67] VanderHart D.L., Asano A. and Gilman J.W., Solid-State NMR Investigation of Paramagnetic Nylon-6 Clay Nanocomposites. 1. Crystallinity, Morphology, and the Direct Influence of Fe3+ on Nuclear Spins, Chemistry of Materials, 13, 3781- 3795, 2001

[68] VanderHart D.L., Asano A. and Gilman J.W., Solid-state NMR investigation of paramagnetic nylon-6 clay nanocomposites 2. Measurement of clay dispersion, crystal stratification, and stability of organic modifiers, Chemistry of Materials, 13, 3796-3809, 2001

[69] Ganter M., Reichert P., Mulhaupt R. and Gronski W., Morphology, mechanical properties, and mechanism of reinforcement of rubber nanocomposites. Polymeric Materials: Science & Engineering, 82, 228, 2000

[70] Reichert P., Kressler J., Thomann R., Mulhaupt R. and Stoppelmann G., Nanocomposites based on a synthetic layer silicate and polyamide-12, Acta Polymerica, 49 (2-3): 116-123, 1998

[71] Messersmith P.B. and Giannelis E.P., Polymer-layered silicate nanocomposites: in situ intercalative polymerization of e-caprolactone in layered silicates, Chemistry of Materials, 5, 1064-1066, 1993

[72] Doh J.G. and Cho I., Synthesis and properties of polystyrene-organoammonium montmorillonite hybrid, Polymer Bulletin., 41, 511-517, 1998

[73] Akelah A. and Moet A., Polymer-clay nanocomposites: free-radical grafting of polystyrene on to organophilic montmorillonite interlayers, Journal of Materials Science, 31, 3589-3596, 1996

[74] Fu X. and Qutubuddin S., Synthesis of polystyrene-clay nanocomposites, Materials Letters, 42 (1-2), 12-15, 2000

[75] Zeng C. and Lee L.J., Poly(methyl methacrylate) and polystyrene/clay nanocomposites prepared by in-situ polymerization, Macromolecules, 34 (12), 4098-4103, 2001

[76] Yeh J.M., Liou S.J., Lin C.Y., Cheng C.Y. and Chang Y.W., Anticorrosively enhanced pmma-clay nanocomposite materials with quaternary alkylphosphonium salt as an intercalating agent, Chemistry of Materials, 14, 154-161, 2002

[77] Wu Z., Zhou C., Qi R. and Zhang H., Synthesis and characterization of nylon 1012/clay nanocomposite, Journal of Applied Polymer Science, 83 (11), 2403-2410, 2002

[78] Ke Y.C., Long C.F. and Qi Z.N., Crystallization, properties, and crystal and nanoscale morphology of PET-clay nanocomposites, Journal of Applied Polymer Science, 71, 1139-1146, 1999

[79] Zhou Q., Fan X., Xia C., Mays J. and R Advincula., Living anionic surface initiated polymerization (sip) of styrene from clay surfaces, Chemistry of Materials, 13 (8), 2465-2467, 2001

[80] Zhu J. and Wilkie C.A., Thermal and fire studies on polystyrene-clay nanocomposites, Polymer International, 49 (10), 1158-1163, 2000

[81] Zhu J., Morgan A.B., Lamelas F.J. and Wilkie C.A., Fire Properties of polystyrene-clay nanocomposites, Chemistry of Materials, 13 (10), 3774-3780, 2001

[82] Chen G., Ma Y. and Qi Z., Preparation and morphological study of an exfoliated polystyrene/montmorillonite nanocomposite, Scripta Materialia, 44 (1), 125-128, 2001

[83] Fan J., Liu S., Chen G. and Qi Z., SEM study of a polystyrene/clay nanocomposite, Journal of Applied Polymer Science, 83 (1), 66-69, 2002

[84] Chen G. and Qi Z., Shear-induced ordered structure in polystyrene/clay nanocomposite, Journal of Materials Research, 15, 351-356, 2000

[85] Kim T.H., Jang L.W., Lee D.C., Choi H.J. and Jhon M.S., Synthesis and rheology of intercalated polystyrene/Na+-montmorillonite nanocomposites, Macromolecular Rapid Communications, 23 (3), 191-195, 2002

[86] Kim J.W., Noh M.H., Choi H.J., Lee D.C. and Jhon M.S., Synthesis and electrorheological characteristics of SAN-clay composite suspensions, Polymer, 41, 1229-1231, 2000

[87] Huang X.Y. and Brittain W.J., Synthesis and Characterization of PMMA Nanocomposites by Suspension and Emulsion Polymerization, Macromolecules, 34 (10), 3255-3260, 2001

[88] Heinemann J., Reichert P., Thomann R. and Mülhaupt R., Polyolefin nanocomposites formed by melt compounding and transition metal catalyzed ethene homo- and copolymerization in the presence of layered silicates, Macromolecular Rapid Communications, 20, 423-430, 1999

[89] Rong J., Li H., Jing Z., Hong X. and Sheng M., Novel organic/inorganic nanocomposite of polyethylene. I. Preparation via in situ polymerization approach, Journal of Applied Polymer Science, 82 (8), 1829-1837, 2001

[90] Rong J., Jing Z., Li H. and Sheng M., A polyethylene nanocomposite prepared via in-situ polymerization, Macromolecular Rapid Communications, 22 (5), 329-334, 2001

[91] Wang J., Liu Z.Y., Guo C.Y., Chen Y.J. and Wang D., Preparation of a PE/MT composite by copolymerization of ethylene with in-situ produced ethylene oligomers under a dual functional catalyst system intercalated into MT layer, Macromolecular Rapid Communications, 22 (17), 1422-1426, 2001

[92] Jin Y.H., Park H.J., Im S.S., Kwak S.Y. and Kwak S., polyethylene/clay nanocomposite by in-situ exfoliation of montmorillonite during Ziegler-Natta polymerization of ethylene, Macromolecular Rapid Communications, 23 (2), 135-140, 2002

[93] Alexandre M., Dubois P., Sun T., Garces J.M. and Jérôme R., Polyethylene-layered silicate nanocomposites prepared by the polymerization-filling technique: synthesis and mechanical properties, Polymer, 43 (8), 2123-2132, 2002

[94] Tudor J., Willington L., O'Hare D. and Royan B., Intercalation of catalytically active metal complexes in phyllosilicates and their application as propene polymerization catalysts, Chemical Communications, 17, 2031-2032, 1996

[95] Ma J., Qi Z. and Hu Y., Synthesis and characterization of polypropylene/clay nanocomposites, Journal of Applied Polymer Science, 82 (14), 3611-3617, 2001

[96] Chen G.H., Chen X.Q., Lin Z.Y., Ye W. and Yao K.D., Preparation and properties of PMMA/clay nanocomposite, Journal of Materials Science Letters, 18 (21), 1761-1763, 1999

[97] Choi Y.S., Choi M.H., Wang K.H., Kim S.O., Kim Y.K. and Chung I.J., Synthesis of exfoliated PMMA/Na-MMT nanocomposites via soap-free emulsion polymerization, Macromolecules, 34 (26), 8978-8985, 2001

[98] Okamoto M., Morita S., Taguchi H., Kim Y.H., Kotaka T. and Tateyama H., Synthesis and structure of smectic clay/poly(methyl methacrylate) and

clay/polystyrene nanocomposites via in situ intercalative polymerization, Polymer, 41 (10), 3887-3890, 2000

[99] Lee D.C. and Jang L.W., Preparation and characterization of PMMA-clay hybrid composite by emulsion polymerization, Journal of Applied Polymer Science, 61 (7), 1117-1122, 1996

[100] Meneghetti P. and Qutubuddin S., Synthesis of poly(methyl methacrylate) - clay nanocomposites, Chemical Engineering Communications, 188, 81-89, 2001

[101] Tabtiang A., Lumlong S. and Venables R.A., The influence of preparation method upon the structure and relaxation characteristics of poly(methyl methacrylate)/clay composites, European Polymer Journal, 36 (12), 2559-2568, 2000

[102] Usuki A. et al, Composite material containing a layered silicate, US4,889,885, 1989

[103] Brown J.M., Curliss D. and Vaia R.A., thermoset-layered silicate nanocomposites: quaternary ammonium montmorillonite with primary diamine cured epoxies, Chemistry of Materials, 12 (11), 3376-3384, 2000

[104] Lee D.C. and Jang L.W., Characterization of epoxy-clay hybrid composite prepared by emulsion polymerization, Journal of Applied Polymer Science, 68, 1997-2005, 1998

[105] Kornmann X., Lindberg H. and Berglund L.A., Synthesis of epoxy-clay nanocomposites: influence of the nature of the clay on structure, Polymer, 42, 1303-1310, 2001

[106] Messersmith P.B. and Giannelis E.P., Synthesis and characterization of layered silicate-epoxy nanocomposites, Chemistry of Materials, 10, 1719-1725, 1994

[107] Chin I.J., Thurn-Albrecht T., Kim H.C., Russell T.P. and Wang J., On exfoliation of montmorillonite in epoxy, Polymer, 42 (13), 5947-5952, 2001

[108] Ke Y., Lü J., Yi X., Zhao J. and Qi Z., The effects of promoter and curing process on exfoliation behavior of epoxy/clay nanocomposites, Journal of Applied Polymer Science, 78, 808-815, 2000

[109] Lü J., Ke Y., Qi Z. and Yi X., Study on Intercalation and Exfoliation Behavior of Organoclays in Epoxy Resin, Journal of Polymer Science Part B: Polymer Physics, 39, 115-120, 2001

[110] Kornmann X., Lindberg H. and Berglund L.A., Synthesis of epoxy-clay nanocomposites: Influence of the nature of the curing agent on structure, Polymer, 42, 4493-4499, 2001

[111] Zilg C., Thomann R., Mülhaupt R., and Finter J., Polyurethane nanocomposites containing laminated anisotropic nanoparticles derived from organophilic layered silicates, Advanced Materials, 11 (1), 49-52, 1999

[112] Chen T.K., Tien Y.I. and Wei K.H., Synthesis and characterization of novel segmented polyurethane clay nanocomposite via poly(ε-caprolactone)/clay, Journal of Polymer Science Part A: Polymer Chemistry, 37 (13), 2225-2233, 1999

[113] Hu Y., Song L., Xu J., Yang L., Chen Z. and Fan W., Synthesis of polyurethane/clay intercalated nanocomposites, Colloid and Polymer Science, 279 (8), 819-822, 2001

[114] Ma J.S., Zhang S.F. and Qi Z.N., Synthesis and characterization of elastomeric polyurethane/clay nanocomposites, Journal of Applied Polymer Science, 82 (6), 1444-1448, 2001

[115] Yao K.J., Song M., Hourston D.J. and Luo D.Z., Polymer/layered clay nanocomposites: 2 polyurethane nanocomposites, Polymer, 43 (3), 1017-1020, 2002

[116] Tortora M. et al., Structural characterization and transport properties of organically modified montmorillonite/polyurethane nanocomposites, Polymer, 43 (23), 6147-6157, 2002

[117] Kim B.K., Seo J.W. and Jeong H.M., Morphology and properties of waterborne polyurethane/clay nanocomposites, European Polymer Journal, 39 (1), 85-91, 2003

[118] Kornmann X., Berglund L.A. and Sterte J., Nanocomposites based on montmorillonite and unsaturated polyester, Polymer Engineering and Science, 38 (8), 1351-1358, 1998

[119] Suh D.J., Lim Y.T. and Park O.O., The property and formation mechanism of unsaturated polyester-layered silicate nanocomposite depending on the fabrication methods, Polymer, 41 (24), 8557-8563, 2000

[120] Choi M.H., Chung I.J. and Lee J.D., Morphology and curing behaviors of phenolic resin-layered silicate nanocomposites prepared by melt intercalation, Chemistry of Materials, 12 (10), 2977-2983, 2000

[121] Xu W.B., Bao S.P., Shen S.J., Tang S.P. and He P.S., Studies on the preparation and curing reaction kinetics of phenolic resin/montmorellonite nanocomposite, Acta Polymerica Sinica, 4, 457-461, 2002

[122] Greenland D.J., Adsorption of polyvinylalcohols by montmorillonite, Journal of Colloid Science, 18, 647-664, 1963

[123] Parfitt R.L. and Greenland D.J., Adsorption of poly(ethylene glycols) on montmorillonites, Clay Minerals, 8, 305-323, 1970

[124] Ogata N., Kawakage S. and Ogihara T., Poly vinyl alcohol-clay and polyethylene oxide-clay blends prepared using water as solvent. Journal of Applied Polymer Science, 66, 573–581, 1997

[125] Levy R. and Francis C.W., Interlayer adsorption of polyvinylpyrrolidone on montmorillonite, Journal of Colloid and Interface Science, 50, 442-450, 1975

[126] Aranda P. and Ruiz-Hitzky E., Poly(ethylene oxide)/NH_4^+-smectite nanocomposites, Applied Clay Science, 15, 119–135, 1999

[127] Chen H.W. and Chang F.C., The novel polymer electrolyte nanocomposite composed of poly(ethylene oxide), lithium triflate and mineral clay, Polymer, 42 (24), 9763-9769, 2001

[128] Hyun Y.H., Lim S.T., Choi H.J. and Jhon M.S., Rheology of Poly(ethylene oxide)/Organoclay Nanocomposites, Macromolecules, 34 (23), 8084-8093, 2001

[129] Shen Z.Q., Simon G.P. and Cheng Y.B., Comparison of solution intercalation and melt intercalation of polymer-clay nanocomposites, Polymer, 43 (15), 4251-4260, 2002

[130] Billingham J., Breen C. and Yarwood J., Adsorption of polyamine, polyacrylic acid and polyethylene glycol on montmorillonite: an in situ study using ATR-FTIR, Vibrational Spectroscopy, 14, 19-34, 1997

[131] Ogata N., Jimenez G., Kawai H. and Ogihara T., Structure and thermal/mechanical properties of poly(L-lactide)-clay blend, Journal of Polymer Science Part B: Polymer Physics, 35, 389-396, 1997

[132] Jimenez G., Ogata N., Kawai H. and Ogihara T., Structure and thermal/mechanical properties of poly(ε-caprolactone)-clay blend, Journal of Applied Polymer Science, 64, 2211-2220, 1997

[133] Wu H.D., Tseng C.R. and Chang F.C., Chain conformation and crystallization behavior of the syndiotactic polystyrene nanocomposites studied using fourier transform infrared analysis, Macromolecules, 34, 2992-2999, 2001

[134] Tseng C.R., Wu J.Y., Lee H.Y. and Chang F.C., Preparation and crystallization behavior of syndiotactic polystyrene-clay nanocomposites, Polymer, 42, 10063-10070, 2001

[135] Hwu J.M., Jiang G.J., Gao Z.M., Xie W. and Pan W.P., The characterization of organic modified clay and clay-filled PMMA nanocomposite, Journal of Applied Polymer Science, 83, 1702-1710, 2002

[136] Gu A.J. and Chang F.C., A novel preparation of polyimide/clay hybrid films with low coefficient of thermal expansion, Journal of Applied Polymer Science, 79 (2), 289-294, 2001

[137] Magaraphan R., Lilayuthalert W., Sirivat A. and Schwank J.W., Preparation, structure, properties and thermal behaviour of rigid-rod polyimide/montmorillonite nanocomposites, Composites Science and Technology, 61, 1253–1264, 2001

[138] Chang J.H., Park K.M., Cho D.H., Yang H.S. and Ihn K.J., Preparation and characterization of polyimide nanocomposites with different organo-montmorillonites, Polymer Engineering and Science, 41 (9), 1514-1520, 2001

[139] Delozier D.M. et al, Preparation and characterization of polyimide/organoclay nanocomposites, Polymer, 43 (3), 813-822, 2002

[140] Chang J.H., Park D.K. and Ihn K.J., Polyimide nanocomposite with a hexadecylamine clay: synthesis and characterization, Journal of Applied Polymer Science, 84, 2294–2301, 2000

[141] Sur G.S., Sun H.L., Lyu S.G. and Mark J.E., Synthesis, structure, mechanical properties, and thermal stability of some polysulfone/organoclay nanocomposites, Polymer, 42 (24), 9783-9789, 2001

[142] Fornes T.D., Yoon P.J., Keskkula H. and Paul D.R., Nylon 6 nanocomposites: the effect of matrix molecular weight, Polymer, 42, 9929-9940, 2001

[143] Vaia R.A., Jandt K.D., Kramer E.J. and Giannelis E.P., Kinetics of polymer melt intercalation, Macromolecules, 24, 8080-8085, 1995

[144] Vaia R.A., Jandt K.D., Kramer E.J. and Giannelis E.P., Microstructural evolution of melt intercalated polymer-organically modified layered silicates nanocomposites, Chemistry of Materials, 11, 2628-2635, 1996

[145] Vaia R.A. and Giannelis E.P., Lattice model of polymer melt intercalation in organically-modified layered silicates, Macromolecules, 25, 7990-7999, 1997

[146] Vaia R.A. and Giannelis E.P., Polymer melt intercalation in organically-modified layered silicates: Model predictions and experiment, Macromolecules, 25, 8000-8009, 1997

[147] Liu L.M., Fang Q., Zhu X.G. and Qi Z.N., Preparation and properties of Nylon 6/montmorillonite nanocomposites by melt intercalation process, Acta Polymerica Sinica, 3, 304-310, 1998

[148] Gilman J.W., NMR measurements related to clay-dispersion quality and organic-modifier stability in nylon-6/clay nanocomposites, Macromolecules, 34, 3819-3822, 2001

[149] Cho J.W. and Paul D.R., Nylon 6 nanocomposites by melt compounding, Polymer, 42, 1083-1094, 2001

[150] Dennis H.R., Hunter D.L., Chang D., Kim S., White J.L., Cho J.W. and Paul D.R., Effect of melt processing conditions on the extent of exfoliation in organoclay-based nanocomposites, Polymer, 42, 9513-9522, 2001

[151] Lepoittevin B., Pantoustier N., Devalckenaere M., Alexandre M., Calberg C., Jérôme R., Henrist C., Rulmont A. and Dubois P., Polymer/layered silicate nanocomposites by combined intercalative polymerization and melt intercalation: a masterbatch process, Polymer, 44 (7), 2033-2040, 2003

[152] Wang S., Hu Y., Qu Z., Wang Z., Chen Z. and Fan W., Preparation and flammability properties of polyethylene/clay nanocomposites by melt intercalation method from Na+ montmorillonite, Materials Letters, 57 (18), 2675-2678, 2003

[153] Wang S., Hu Y., Wang Z., Tang Y., Chen Z. and Fan W., Synthesis and characterization of polycarbonate/ABS/montmorillonite nanocomposites, Polymer Degradation and Stability, 80 (1), 157-161, 2002

[154] Wang J., Du J., Zhu J. and Wilkie C.A., An XPS study of the thermal degradation and flame retardant mechanism of polystyrene-clay nanocomposites, Polymer Degradation and Stability, 77 (2), 249-252, 2002

[155] Wang S., Hu Y., Song L., Wang Z., Chen Z. and Fan W., Preparation and thermal properties of ABS/montmorillonite nanocomposite, Polymer Degradation and Stability, 77 (3), 423-426, 2002

[156] Tang Y., Hu Y., Wang S., Gui Z., Chen Z. and Fan W., Preparation and flammability of ethylene-vinyl acetate copolymer/montmorillonite nanocomposites, Polymer Degradation and Stability, 78 (3), 555-559, 2002

[157] Pantoustier N., Lepoittevin B., Alexandre M., Kubies D., Calberg C., Jérôme R. and Dubois P., Biodegradable Polyester Layered Silicate Nanocomposites Based on Poly(ε-Caprolactone), Polymer Engineering and Science, 42 (9): 1928-1937, 2002

[158] Pantoustier N. et al, Poly(e-caprolactone) layered silicate nanocomposites: effect of clay surface modifiers on the melt intercalation process, http://www.e-polymers.org, E-Polymers, 009, 2001

[159] Di Y., Iannace S., Maio E.D. and Nicolais L., Nanocomposites by melt intercalation based on polycaprolactone and organoclay, Journal of Polymer Science Part B: Polymer Physics, 41 (7), 670-678, 2003

[160] Li X. and Ha C.S., Nanostructure of EVA/organoclay nanocomposites: Effects of kinds of organoclays and grafting of maleic anhydride onto EVA, Journal of Applied Polymer Science, 87 (12), 1901-1909, 2003

[161] Nah C., Ryu H.J., Kim W.D. and Choi S.S., Barrier property of clay/Acrylonitrile-butadiene copolymer nanocomposite, Polymers for Advanced Technologies, 13 (9), 649-652, 2002

[162] Park J.H. and Jana S.C., The relationship between nano- and micro-structures and mechanical properties in PMMA-epoxy-nanoclay composites, Polymer, 44 (7), 2091-2100, 2003

[163] Wang D. and Wilkie C.A., In-situ reactive blending to prepare polystyrene–clay and polypropylene-clay nanocomposites, Polymer Degradation and Stability, 80 (1), 171-182, 2002

[164] Du J., Wang D., Wilkie C.A. and Wang J., An XPS investigation of thermal degradation and charring on poly(vinyl chloride)–clay nanocomposites, Polymer Degradation and Stability, 79 (2), 319-324, 2003

[165] Park C.I., Park O.O., Lim J.G. and Kim H.J., The fabrication of syndiotactic polystyrene/organophilic clay nanocomposites and their properties, Polymer, 42, 7465-7475, 2001

[166] Tseng C.R., Wu S.C., Wu J.J. and Chang F.C., Crystallization behavior of syndiotactic polystyrene nanocomposites for melt- and cold-crystallizations, Journal of Applied Polymer Science, 86 (10), 2492-2501, 2002

[167] Devaux E., Bourbigot S. and Achari A.E., Crystallization behavior of PA-6 clay nanocomposite hybrid, Journal of Applied Polymer Science, 86 (10), 2416-2423, 2002

[168] Davis C.H. et al., Effects of melt-processing conditions on the quality of poly(ethylene terephthalate) montmorillonite clay nanocomposites, Journal of Polymer Science Part B: Polymer Physics, 40 (23), 2661-2666, 2002

[169] Morgan A.B., Harris R.H. Jr., Kashiwagi T., Chyall L.J. and Gilman J.W., Flammability of polystyrene layered silicate (clay) nanocomposites: Carbonaceous char formation, Fire and Materials, 26 (6), 247-253, 2002

[170] Svoboda P., Zeng C., Wang H., Lee L.J. and Tomasko D.L., Morphology and mechanical properties of polypropylene/organoclay nanocomposites, Journal of Applied Polymer Science, 85 (7), 1562-1570, 2002

[171] Liu X., Wu Q., Berglund L.A. and Qi Z., Investigation on Unusual Crystallization Behavior in Polyamide 6/Montmorillonite Nanocomposites, Macromolecular Materials and Engineering, 287 (8), 515-522, 2002

[172] Liu T.X., Liu Z.H., Ma K.X., Shen L., Zeng K.Y. and He C.B., Morphology, thermal and mechanical behavior of polyamide 6/layered-silicate nanocomposites, Composites Science and Technology, 63 (3-4), 331-337, 2003

[173] Bafna A., Beaucage G., Mirabella F. and Mehta S., 3D Hierarchical orientation in polymer–clay nanocomposite films, Polymer, 44 (4), 1103-1115, 2003

[174] Gilman J.W. et al., Polymer/ Layered Silicate Nanocomposites from Thermally Stable Trialkylimidazolium-Treated Montmorillonite, Chemistry of Materials, 14 (9), 3776-3785, 2002

[175] Chisholm, B. J. et al., Nanocomposites Derived from Sulfonated Poly(butylene terephthalate), Macromolecules, 35 (14), 5508-5516, 2002

[176] Liu X., Wu Q., Berglund L.A., Lindberg H., Fan J. and Qi Z., Polyamide 6/clay nanocomposites using a cointercalation organophilic clay via melt compounding, Journal of Applied Polymer Science, 88 (4), 953-958, 2003

[177] Dortmans A. et al., Nanocomposite materials: from lab-scale experiments to prototypes, http://www.e-polymers.org, E-Polymers, 010, 2002,

[178] Liu X. and Wu Q., PP/clay nanocomposites prepared by grafting-melt intercalation, Polymer, 42, 10013-10019, 2001

[179] Liu X. and Wu Q., Polyamide 66/clay nanocomposites via melt intercalation, Macromolecular Materials and Engineering, 287, 180-186, 2002

[180] Kim S.W., Jo W.H., Lee M.S., Ko M.B. and Jho J.Y., Effects of shear on melt exfoliation of clay in preparation of nylon 6/organoclay nanocomposites, Polymer Journal, 34 (3), 103-111, 2002

[181] Lincoln D.M., Vaia R.A., Wang Z.G. and Hsiao B.S., Secondary structure and elevated temperature crystallite morphology of nylon-6/layered silicate nanocomposites, Polymer, 42, 1621-1631, 2001

[182] Kim G.M., Lee D.H., Hoffmann B., Kressler J. and Stoppelmann G., Influence of nanofillers on the deformation process in layered silicate/polyamide-12 nanocomposites, Polymer, 42 (3), 1095-1100, 2001

[183] Uribe-Arocha P., Mehler C., Puskas J.E. and Altstadt V., Effect of sample thickness on the mechanical properties of injection-molded polyamide-6 and polyamide-6 clay nanocomposites, Polymer, 44 (8), 2441-2446, 2003

[184] Murphy M.J., Martin D.J., Truss R., and Halley P., Improving Polyethylene Performance – The Use of Nanocomposites in Ziegler-Natta Polyethylene for Rotational Moulding, ANTEC 2000: Society of Plastics Engineers Technical Papers, Conference Proceedings, 612-616, 2000

[185] Cheremisinoff N.P., Polymer Characterization: Laboratory Techniques and Analysis, Noyes Publications, ISBN 0-8155-1403-4, 1996

[186] Hasegawa N., Kawasumi M., Kato M., Usuki A. and Okada A., Preparation and mechanical properties of polypropylene-clay hybrids using a maleic anhydride-modified polypropylene oligomer, Journal of Applied Polymer Science, 67, 87-92, 1992

[187] Oya A., Polypropylene-clay nanocomposites, in Polymer-Clay Nanocomposites, Eds. Pinnavaia T.J. & Beall G.W., John Wiley & Sons Ltd, ISBN 0-471-63700-9, 151-172, 2000

[188] Shi H., Lan T. and Pinnavaia T.J., Interfacial effects on the reinforcement properties of polymerorganoclay nanocomposites, Chemistry of Materials, 8, 1584-1587, 1996

[189] Shia D., Hui C.Y., Burnside S.D. and Giannelis E.P., An interface model for the prediction of Young's modulus of layered silicate-elastomer nanocomposites, Polymer Composites, 19, 608-617, 1998

[190] Usuki A., Koiwai A., Kojima Y., Kawasumi M., Okada A., Kurauchi T. and Kamigaito O., Interaction of nylon 6-clay surface and mechanical properties of nylon 6-clay hybrid, Journal of Applied Polymer Science, 55, 119-123, 1995

[191] Massam J. and Pinnavaia T.J., Clay nanolayer reinforcement of a glassy epoxy polymer, in Nanostructured Powders And Their Industrial Applications, Materials Research Society Symposium Proceedings 520, 223-232, 1998

[192] Wang Z., Massam J. and Pinnavaia T.J., Epoxy-clay nanocomposites in Polymer-clay nanocomposites Eds. T.J. Pinnavaia and G.W. Beall, John Wiley & Sons Ltd, ISBN 0-471-63700-9, 127-149, 2000

[193] Kornmann X., *Introduction* in Synthesis and characterisation of thermoset-clay nanocomposites, 2000

[194] Zerda A.S. and Lesser A.J., Intercalated clay nanocomposites: morphology, mechanics, and fracture behavior, Journal of Polymer Science Part B: Polymer Physics, 39, 1137–1146, 2001

[195] Masenelli-Varlot K., Reynaud E., Vigier G. and Varlet J., Mechanical properties of clay-reinforced polyamide, Journal of Polymer Science: Part B: Polymer Physics, 40, 272–283, 2002

[196] Wu S.H. et al., Mechanical, thermal and morphological properties of glass fiber and carbon fiber reinforced polyamide-6 and polyamide-6/clay nanocomposites, Materials Letters, 49, 327–333, 2001

[197] Ma C-C.M., Kuo C.T., Kuan H.C. and Chiang C.L., Effects of swelling agents on the crystallization behavior and mechanical properties of polyamide 6/clay nanocomposites, Journal of Applied Polymer Science, 88, 1686-1693, 2003

[198] Inceoglu A.B. and Yilmazer U., Synthesis and mechanical properties of unsaturated polyester based nanocomposites, Polymer Engineering and Science, 43 (3), 661-669, 2003

[199] Kacperski M., Polymer nanocomposites. Part II. Nanocomposites based on thermoplastic polymers and layered silicates, Polimery, 48 (2), 85-90, 2003

[200] Wan C.Y., Qiao X.Y., Zhang Y. and Zhang Y.X., Effect of different clay treatment on morphology and mechanical properties of PVC-clay nanocomposites, Polymer Testing, 22 (4), 453-461, 2003

[201] Liu X.H. and Wu Q.J., Polyamide 66/clay nanocomposites via melt intercalation, Macromolecular Materials and Engineering, 287 (3), 180-186, 2002

[202] Inceoglu A.B. and Yilmazer U., Synthesis and mechanical properties of unsaturated polyester based nanocomposites, Polymer Engineering and Science, 43 (3), 661-669, 2003

[203] Li X.C., Park H.M., Lee J.O. and Ha C.S., Effect of blending sequence on the microstructure and properties of PBT/EVA-g-MAH/organoclay ternary nanocomposites, Polymer Engineering and Science, 42 (11), 2156-2164, 2002

[204] Messersmith P.B. and Giannelis E.P., Synthesis and barrier properties of poly(ε-caprolactone)-layered silicate nanocomposites, Journal of Polymer Science: Part A: Polymer Chemistry, 33, 1047-1057, 1995

[205] Strawhecker K.E. and Manias E., Structure and properties of poly(vinyl alcohol)/Na^+ montmorillonite nanocomposites, Chemistry of Materials, 12, 2943-2949, 2000

[206] Yeh J.M. et al., Enhancement of corrosion protection effect of poly(*o*-ethoxyaniline) via the formation of poly(*o*-ethoxyaniline)-clay nanocomposite materials, Polymer, 43, 2729-2736, 2002

[207] Yano K., Usuki A. and Okada A., Synthesis and properties of polyimide-clay hybrid films, Journal of Polymer Science: Part A: Polymer Chemistry, 35, 2289-2294, 1997

[208] Gu A.J., Kuo S.W. and Chang F.C., Syntheses and properties of PI/clay hybrids, Journal of Applied Polymer Science, 79 (10), 1902-1910, 2001

[209] Jiang L.Y. and Wei K.H., Bulk and surface properties of layered silicates/fluorinated polyimide nanocomposites, Journal of Applied Physics, 92 (10), 6219-6223, 2002

[210] Tsai M.H. and Whang W.T., Low dielectric polyimide/poly(silsesquioxane)-like nanocomposite material, Polymer, 42 (9), 4197-4207, 2001

[211] Chen T.K., Tien Y.I. and Wei K.H., Synthesis and characterization of novel segmented polyurethane/clay nanocomposites, Polymer, 41 (4), 1345-1353, 2000

[212] Krook M., Albertsson A.C., Gedde U.W. and Hedenqvist M.S., Barrier and mechanical properties of montmorillonite/polyesterarnide nanocomposites, Polymer Engineering and Science, 42 (6), 1238-1246, 2002

[213] Shah A.P. et al., Moisture Diffusion through Vinyl Ester Nanocomposites Made with Montmorillonite Clay, Polymer Engineering and Science, 42, 1852-1863, 2002

[214] Drozdov A.D., Christiansen J.D., Gupta R.K. and Shah A.P., Model for anomalous moisture diffusion through a polymer-clay nanocomposite, Journal of Polymer Science Part B: Polymer Physics, 41 (5), 476-492, 2003

[215] Gorrasi G., Tortora M., Vittoria V., Galli G. and Chiellini E., Transport and mechanical properties of blends of poly(ε-caprolactone) and a modified montmorillonite-poly(ε-caprolactone) nanocomposite, Journal of Polymer Science Part B: Polymer Physics, 40, 1118–1124, 2002

[216] Xu R., Manias E., Snyder A.J., and Runt J., New biomedical poly(urethane urea)-layered silicate nanocomposites, Macromolecules, 34, 337-339, 2001

[217] Socci E.P., Akkapeddi M.K. and Worley D.C., New high barrier, oxygen scavenging polyamides for packaging applications, ANTEC 2001, Society of Plastics Engineers Technical Papers, Conference Proceedings, 476-480, 2001

[218] Yeh J.M. et al., Enhancement of corrosion protection effect in polyaniline via the formation of polyaniline-clay nanocomposite materials, Chemistry of Materials, 13, 1131-1136, 2001

[219] Pinnavaia T.J., Lan T., Kaviratna P.D. and Wang M.S., Clay-polymer nanocomposites: Polyether and polyamide systems, Materials Research Society Symposium Proceedings, 346, 81-88, 1994

[220] Lan T., Kaviratna P.D. and Pinnavaia T.J., On the nature of poly(imide)-clay hybrid composites, Chemistry of Materials, 6, 573-575, 1994

[221] LeBaron P.C. and Pinnavaia T.J., Clay nanolayer reinforcement of a silicone elastomer, Chemistry of Materials, 13, 3760-3765, 2001

[222] Chang Y.W., Yang Y., Ryu S. and Nah C., Preparation and properties of EPDM/organomontmorillonite hybrid nanocomposites, Polymer International, 51, 319-324, 2002

[223] Bharadwaj R.K. et al., Structure-property relationships in cross-linked polyester-clay nanocomposites, Polymer, 43, 3699-3705, 2002

[224] Scherer C., PA Film grade with improved barrier properties for flexible food packaging applications, in: Proceedings of the New Plastics'99, London, 2-4, 1999

[225] http://www.inmat.com/Principia-News-Release.htm

[226] Harcup J.P. and Yee A.F., Deformation and fracture of polymer silicate layer nanocomposites, ANTEC 1999, Society of Plastics Engineers Technical Papers, Conference Proceedings, 3396-3398, 1999

[227] Krishnamoorti R., Vaia R.A. and Giannelis E.P., Structure and dynamics of polymer-layered silicate nanocomposites, Chemistry of Materials, 8 (8): 1728-1734, 1996

[228] Giannelis E.P., Polymer layered silicate nanocomposites, Advanced Materials, 8, 29–35, 1996

[229] Kenig S., Ophir A., Shepelev O. and Weiner F., High barrier blow molded containers based on nano clay composites, ANTEC 2002, Society of Plastics Engineers Technical Papers, Conference Proceedings, Paper 406, 2002

[230] Burnside S.D. and Giannelis E.P., Nanostructure and properties of polysiloxane-layered silicate nanocomposites, Journal of Polymer Science Part B: Polymer Physics, 38 (12): 1595-1604, 2000

[231] http://www.azom.com/details.asp?ArticleID=921#_Areas_of_Application

[232] Zhu J., Start P., Mauritz K.A. and Wilkie C.A., Thermal stability and flame retardancy of poly(methyl methacrylate)-clay nanocomposites, Polymer Degradation and Stability, 77 (2), 253-258, 2002

[233] Kashiwagi T., Inaba A., Brown J.E., et al. Effects of weak linkages on the thermal and oxidative-degradation of poly(methyl methacrylates), Macromolecules, 19 (8), 2160-2168, 1986

[234] Blumstein A. and Billmeyer F.W., Polymerization of adsorbed monolayers. III. Preliminary structure studies in dilute solution of the insertion polymers, Journal of Polymer Science Part A-2: Polymer Physics, 4 (3), 465-474, 1966

[235] Kim T.H., Lim S.T., Lee C.H., Choi H.J. and Jhon M.S., preparation and rheological characterization of intercalated polystyrene/organophilic montmorillonite nanocomposite, Journal of Applied Polymer Science, 87, 2106–2112, 2003

[236] Alexandre M., Beyer G., Henrist C., Cloots R., Rulmont A., Jérôme J. and Dubois P., Preparation and Properties of Layered Silicate Nanocomposites Based on Ethylene Vinyl Acetate Copolymers, Macromolecular Rapid Communications, 22 (8), 643-646, 2001

[237] Lee J., Takekoshi T. and Giannelis E.P., Fire retardant polyetherimide nanocomposites, Materials Research Society Symposium Proceedings, 457, 513-518, 1997

[238] Lepoittevin B., Devalckenaere M., Pantoustier N., Alexandre M., Kubies D., Calberg C., Jérôme R. and Dubois P., Poly(ε-caprolactone)/clay nanocomposites prepared by melt intercalation: mechanical, thermal and rheological properties, Polymer, 43, 4017-4023, 2002

[239] Burnside S.D. and Giannelis E.P., Synthesis and properties of new poly(dimethylsiloxane) nanocomposites, Chemistry of Materials, 7, 1597-1600, 1995

[240] Kim B.H. et al., Nanocomposite of Polyaniline and Na+-Montmorillonite Clay, Macromolecules, 35, 1419-1423, 2002

[241] Takeichi T., Zeidam R. and Agag T., Polybenzoxazine/clay hybrid nanocomposites: influence of preparation method on the curing behavior and properties of polybenzoxazines, Polymer, 43 (1), 45-53, 2002

[242] Hsu S. L-C. and Chang K.C., Synthesis and properties of polybenzoxazole-clay nanocomposites, Polymer, 43 (15), 4097-4101, 2002

[243] Tong X., Zhao H., Tang T., Feng Z. and Huang B., Preparation and Characterization of Poly(ethyl acrylate)/Bentonite Nanocomposites by In Situ Emulsion Polymerization, Journal of Polymer Science Part A: Polymer Chemistry, 40, 1706-1711, 2002

[244] Petrovic X.S., Javni I., Waddong A. and Banhegyi G.J., Structure and properties of polyurethane-silica nanocomposites, Journal of Applied Polymer Science, 76 (2), 133-151, 2000

[245] Zhu Z.K., Yang Y., Yin J., et al., Preparation and properties of organosoluble montmorillonite polyimide hybrid materials, Journal of Applied Polymer Science, 73 (11), 2063-2068, 1999

[246] Gilman J.W., Kashiwagi T., and Lichtenhan J.D., Nanocomposites: A revolutionary new flame retardant approach, SAMPE Journal, 33, 40-46, 1997

[247] Gilman J.W. et al., Polymer layered-silicate nanocomposites: polyamide-6, polypropylene and polystyrene, New Advances in Flame Retardant Technology Proceedings, Fire Retardant Chemicals Association, October 24-27, 1999

[248] Dietsche F. and Mulhaupt R., Thermal properties and flammability of acrylic nanocomposites based upon organophilic layered silicates, Polymer Bulletin, 43, 395-402, 1999

[249] Gilman J.W. et al., Flammability studies of polymer layered silicate nanocomposites: polyolefin, epoxy, and vinyl ester resins, Chemistry and Technology of Polymer Additives. Chapter 14, 1999

[250] Gilman J.W. et al., flammability properties of polymer-layered-silicate nanocomposites. polypropylene and polystyrene nanocomposites, Chemistry of Materials, 12 (7), 1866-1873, 2000

[251] Wang Z. and Pinnavaia T.J., Nanolayer reinforcement of elastomeric polyurethane, Chemistry of Materials, 10, 3769-3771, 1998

[252] Chen K.H. and Yang S.M., synthesis of epoxy-montmorillonite nanocomposite, Journal of Applied Polymer Science, 86, 414-421, 2002

[253] Lee H.C., Lee T.W., Lim Y.T. and Park O.O., Improved environmental stability in poly(p-phenylene vinylene)/layered silicate nanocomposite, Applied Clay Science, 21, 287-293, 2002

[254] Singh A. and Haghighat R., High-temperature polymer/inorganic nanocomposites, US6,057,035, 2000

[255] Ellsworth M.W., Organoclay-polymer composites, US5,962,553, 1999

[256] Barbee R.B. et al, Process for preparing high barrier nanocomposites, US0,169,246, 2002

[257] Juan M.G. et al, Polymeric nanocomposites for automotive application, Advanced Materials, 12 (23), 1835-1839, 2000

[258] Pinnavaia T.J. and Beall G.W., Polymer-clay nanocomposites, John Wiley & Sons Ltd, ISBN 0-471-63700-9, 2000

[259] Debasis M., Thomas N.B. and Dwight W.S., Clay-polymer Nanocomposite Coatings for Imaging Application, in Proc. 1st World Congress in Nanocomposites, ECM, Chicago, 25-27 June, 2001

[260] http://composite.miningco.com/library/PR/2001/blgm1.htm

[261] http://www.nanoclay.com/data /Na.htm

[262] http://www.nanoclay.com/data/93A.htm

[263] http://www.nanoclay.com/data/20A.htm

[264] http://www.nanoclay.com/data/15A.htm

[265] Ruland W. and Tompa H., The influence of preferred Orientation on the line width and peak shift of (hk) interferences, Journal of Applied Crystallography, 5, 225-230, 1972

[266] Ruland W. and Tompa H., The effect of preferred orientation on the intensity distribution of (hk) interferences, Acta Crystallographica, A24, 93-99, 1968

[267] Xie W. et al, Thermal characterization of organically modified montmorillonite, Thermochimica Acta, 367-368, 339-350, 2001

[268] Beake B.D., Chen S., Hull J.B. and Gao F, Nanoindentation behaviour of clay/poly(ethylene oxide) nanocomposites, Journal of Nanoscience and Nanotechnology, 2, 73-79, 2002

[269] Beake B.D. and Leggett G.J., Nanoindentation and nanoscratch testing of uniaxially and biaxially drawn poly(ethylene terephthalate) film, Polymer, 43, 319-327, 2002

[270] Oliver W.C. and Pharr G.M., An improved technique for determining hardness and elastic-modulus using load and displacement sensing indentation experiments, Journal of Materials Research, 7(6), 1564-1583, 1992

APPENDIX 1

List of Publications

F. Gao, S. Chen, Z. Han and J.B. Hull, A Screening of the Microstructure of Major Commercial Clays for Nanocomposite Application, Nanocomposites 2003, ECM, San Francisco, California, 10-12 November 2003

F. Gao, Z. Han, S. Chen and J.B. Hull, The Current Problems with the Use of Reactive Melt Processing to Produce Clay/Polymer Nanocomposites, in Proc. Organic-Inorganic Hybrids II, PRA, Guildford, 28-29 May 2002

F. Gao, S. Chen and J.B. Hull, From Burning Behaviour to Understand the Mechanisms of Solution and Solid Intercalations in Clay/PEO Nanocomposites, in Proc. Organic-Inorganic Hybrids II, PRA, Guildford, 28-29 May 2002.

B.D. Beake, S. Chen, J.B. Hull and F Gao, Nanoindentation Behaviour of Clay/Poly(ethylene oxide) Nanocomposites, Journal of Nanoscience and Nanotechnology, 2, 73-79, 2002.

F. Gao, S. Chen and J.B. Hull, Layer Expansion of Layered Silicates in Solid Polymer Matrices by Compression, Journal of Materials Science Letters, 20, 1807-1810, 2001.

Fengge Gao, Shuaijin Chen and J Barry Hull, A Novel Approach to Produce Clay/Polymer Nanocomposites – Solid Intercalation, in Proc. 1st World Congress in Nanocomposites, ECM, Chicago, 25-27 June, 2001.